Characterization of Optimized Low Heat High Performance Concrete

NWMO-TR-2021-20 January 2022

Corina-Maria Aldea

Wood Environment & Infrastructure Solutions

nwmo

NUCLEAR WASTE MANAGEMENT ORGANIZATION

SOCIÉTÉ DE GESTION DES DÉCHETS NUCLÉAIRES

Nuclear Waste Management Organization
22 St. Clair Avenue East, 6th Floor
Toronto, Ontario
M4T 2S3
Canada

Tel: 416-934-9814
Web: www.nwmo.ca

Characterization of Optimized Low Heat High Performance Concrete

NWMO-TR-2021-20

January 2022

Corina-Maria Aldea
Wood Environment & Infrastructure Solutions

Document History

Title:	Characterization of Optimized Low Heat High Performance Concrete		
Report Number:			
Revision:	R000d	Date:	January 2022
Wood Environment & Infrastructure Solutions			
Authored by:	Corina-Maria Aldea		
Verified by:	Bruce J Cornelius		
Approved by:	Dudley R. Morgan		
Nuclear Waste Management Organization			
Reviewed by:	Chang Seok Kim		
Reviewed by:	Peter Keech		
Reviewed by:	Mihaela Ion		
Accepted by:	Paul Gierszewski		

Revision Summary		
Revision Number	**Date**	**Description of Changes/Improvements**
R000a	2021-09	Draft final report
R000b	2021-10	Address NWMO's comments dated September 27, 2021
R000c	2021-11	Address NWMO's comments dated October 29, 2021. Final report
R000d	2022-01	Include final hydraulic conductivity and creep results. Revised final report

ABSTRACT

Title: **Characterization of Optimized Low Heat High Performance Concrete**
Report No.: **NWMO-TR-2021-20**
Author(s): Corina-Maria Aldea
Company: Wood Environment & Infrastructure Solutions
Date: January 2022

Executive Summary
The shaft seals for a deep geological repository may include various materials (bentonite/sand, asphalt-based material, and concrete) with different functions. The Nuclear Waste Management Organization reference concrete is the Low Heat High Performance Concrete (LHHPC) originally developed by the Atomic Energy of Canada Limited (AECL). The LHHPC mix was optimized based on the original reference concrete mix design, using mix ingredients from local and sustainable sources.

The purpose of the current project was to obtain further characterization data to confirm the performance of the optimized LHHPC mix.

The study includes the following:

- Optimized mix ingredients sourcing;
- Reference water preparation and testing;
- Mix ingredients characterization;
- Trial batch qualification; and
- Test program.

The optimized mix ingredients selected, sourced and characterized are all suitable for LHHPC mixes. In particular, the free silicon content in the silica fume met the performance target for the study.

The reference waters prepared for the test program include a reference crystalline rock water (CR-10) and a reference sedimentary rock saline water (SR-270) for saturated hydraulic conductivity tests. Reference waters were prepared by Wood and their chemical composition was tested in a certified external laboratory. It is understood that another reference sedimentary rock saline water (SR-290) will be used for further testing.

Optimized LHHPC trial batches were prepared and the LHHPC specimens were cured in a moist environment at 100% relative humidity. The qualification tests were conducted, including bulk density and porosity at 30 days, pH in distilled water at 28 days, 7-day unconfined compressive strength (UCS) and slump and slump flow retention up to 2 hours from the time of mixing. All these test results met the qualification test requirements for the study.

The following properties were measured at the appropriate age for the optimized LHHPC mixture following test methods as described in the project test plan:

- Chemical and mineralogical composition to approximately the 1 wt% level;
- Bulk density;
- Porosity;
- Unconfined compressive strength and crack initiation;
- Split tensile strength;
- Creep;

- Triaxial compression;
- Saturated hydraulic conductivity;
- Maximum temperature rise at the center of cubic specimens;
- Shrinkage rate;
- pH;
- Slump and slump flow retention;
- Rheology of fresh concrete mix to obtain viscosity and yield stress; and
- Thermal conductivity.

The results indicate that the optimized LHHPC mix met the relevant performance requirements for up to 270-day project parameters.

Based on the slump and slump flow retention test results, along with the rheology test results, the following revisions to the performance targets for initial slump and slump flow are recommended to be made:

- Slump 220 +30/-20mm provided no bleeding and/or segregation
- Slump flow 400 – 650mm provided no bleeding and/or segregation.

Based on the trial batch qualification test results, it is recommended to add the temperature rise test to the existing LHHPC trial batch qualification tests.

This is the final report.

TABLE OF CONTENTS

LIST OF TABLES

Page

LIST OF FIGURES

Page

1. INTRODUCTION

The shaft seal for a deep geological repository (DGR) may include various materials (bentonite/sand, asphalt-based material, and concrete) with different functions. The Nuclear Waste Management Organization (NWMO) reference concrete is the Low Heat High Performance Concrete (LHHPC) originally developed by the Atomic Energy of Canada Limited (Gray and Shenton 1998). Measurements of the material properties of this reference LHHPC were conducted in support of Ontario Power Generation (OPG)'s proposed DGR for Low and Intermediate Level Radioactive Waste near the existing Western Waste Management Facility at the Bruce nuclear site. Low alkalinity concretes are favored for use in DGRs, as they will minimize the potential for adverse chemical interaction with bentonite also used in these repositories

The LHHPC mix was optimized based on the original reference concrete mix, using mix ingredients from local and sustainable sources (Aldea et al. 2016, 2019). Binary and ternary mixes were developed, tested and compared to the original reference mix design. Different types of water (distilled water, and CR-10 crystalline rock water, and SR-270 sedimentary rock water) were used for the curing and testing of various material properties such as density, porosity, compressive strength, hydraulic conductivity, slump, slump flow, pH. Free silicon content in silica fume was measured. Based on the test results, an optimized binary LHHPC mix was proposed with a mix design that was similar to the reference mix and met, or was expected to meet the performance targets, particularly on pH. The optimized mix development test program had further identified the need for performance measurements for the optimized binary mix (i.e., notably porosity, saturated hydraulic conductivity, maximum temperature rise and shrinkage rate). Although these properties were expected to be similar in the optimized binary mix compared to the original reference mix, these properties had not been measured in the optimized binary mix. In addition, the development program had also identified the need for the pumpability of the optimized binary mixture to be evaluated.

Therefore, the purpose of this study was to obtain further characterization data to confirm the performance of the optimized binary LHHPC mix.

Table 1 gives the mix design of the optimized LHHPC; and Table 2 shows the performance parameters and targets for the optimized LHHPC material.

This final report presents results, including characterization of the mix ingredients, details of the trial batches, as well as up to 270-day test results for the optimized LHHPC mix. The report also includes a summary of findings and some recommendations for revised performance parameters and targets.

Sections 2, 3 and 4 describe the optimized LHHPC mix ingredients sourcing, optimized LHHPC mix ingredients characterization, and reference water preparation and testing, respectively. Optimized LHHPC trial batch qualification is provided in Section 5 and optimized LHHPC test results are described in Section 6. Finally, the summary of the study findings and recommendations are provided in Section 7.

Table 1: Optimized LHHPC Mix Design

Mix Ingredients	Optimized LHHPC Mix Design (kg/m^3)	Ingredient Source
Cement	95.6	Type GU, St. Marys
Silica fume	95.6	Norchem USA
Silica flour	190.0	US Silica
Sand	911.1	Natural concrete sand from Lafarge, Cambridge, Ontario
Coarse aggregate	1060.9	Concrete stone from carbonate and crystalline pits, Lafarge, Cambridge, Ontario
Superplasticizer (dry mass)	6.7	MasterGlenium 7500, polycarboxylate-based BASF
Water	113.6	Tap water
Water-to-cementitious material ratio	0.6	-

Table 2: Performance of Optimized LHHPC Mixes

No.	Performance Parameters	Preliminary Performance Target	Performance of Original Reference Mix	Performance of Optimized Binary Mix
B1	Bulk Density	>2400 kg/m^3	Distilled Water 2442 kg/m^3 (180 days) SR-270 Water 2442 kg/m^3 (180 days)	SR-270 Water 2445 kg/m^3 (7 days)
B2	Porosity at 180 days	≤6%	Distilled Water 3.62% SR-270 Water 4.03%	NA
B3	Saturated Hydraulic Conductivity	<1 x 10^{-12} m/s	Distilled water Inflow 1.09x10^{-13} m/s Outflow 2.03x10^{-14} m/s SR-270 Water Inflow 2.45x10^{-13} m/s Outflow 2.7x10^{-15} m/s	NA
B4	Unconfined Compressive Strength (UCS)	>25 MPa (7 days) >60 MPa (90 days)	Distilled Water 34.7 MPa (7 days) 84.6 MPa (90 days) SR-270 Water 35.7 MPa (7 days) 83.0 MPa (90 days)	SR-270 Water 28.7 MPa (7 days) 73.0 MPa (90 days)

No.	Performance Parameters	Preliminary Performance Target	Performance of Original Reference Mix	Performance of Optimized Binary Mix
B5	Maximum temperature rise at the center of 300 mm-side cubical specimen*	≤15°C over 10 days	Peak of about 15°C over ~80 hours of monitoring	NM
B6	Shrinkage rate over 200 days	<1% (volume)	NM	NM
B7	pH at 90 days	≤11, preferably 9 – 10	Canadian Shield Saline Solution (58 g/L) 10.0 (7 days) 9.7 (28 days) 9.3 (90 days)	Distilled Water 10.1 (90 days) CR-10 Water 9.5 (90 days) Mont Terri Water 9.5 (90 days)
B8	Slump	200 +/-50 mm provided no bleeding and/or segregation	250 mm with no bleeding/segregation	225 mm with no bleeding/segregation
B9	Slump flow	300 – 650 mm provided no bleeding and/or segregation	530 mm with no bleeding/segregation	356 mm with no bleeding/segregation
B10	Slump and slump flow retention up to 2 hours from the time of mixing	≥75%	NM	Slump retention~78% static, ~111% remix Slump flow retention~79% static, 119% remix
B11	Free silicon (Si) content in silica fume	<0.075% (by mass)	0. 086%	0.042%

Notes:
NM means not measured.
*Concrete poured into an insulated box.

2. OPTIMIZED LHHPC MIX INGREDIENTS AND SOURCING

Table 3 lists the mix ingredients and sources used for the LHHPC trial batches and batches evaluated for the optimization tests and this study.

For optimization tests, the LHHPC mixtures used mix ingredients from existing local and sustainable sources except silica fume (SF). Alternatives to Canadian SF sources were also used. For the LHHPC optimization tests, Type HS cement in the original reference design was replaced by blending varying amounts of supplementary cementitious materials with general use Portland cement (Type GU), meeting the performance requirements of a high sulphate resistance and categorized as HSb cements in CSA A3000-13. Cement Type GU from St. Mary's (currently Votorantim Cimentos) met the temperature rise target in the optimization study and therefore it was recommended to be used for the optimized LHHPC mix. For this study, as Type GU cement is no longer available, general use limestone cement (GUL) was used for the LHHPC mixes. The GUL cement is slightly lower in total alkali due to the dilution with calcium carbonate, but otherwise very similar to the GU cement (Appendix A). Also results indicate that the optimized LHHPC using GUL meets the performance target in terms of temperature rise and the GUL is slightly lower in heat generation potential than the GU cement (see Section 6.2.8). Only aggregate classified as non-reactive, e.g., that conform to the requirements of CSA A23.1/2 for use in Portland cement concrete was considered and used for the project.

Table 3: Suppliers for Optimized LHHPC Mix and Reference Water Ingredients

Ingredient	Supplier Name	Address	Comments/ Revisions
General use limestone cement (Type GUL)	Votorantim Cimentos (formerly St. Mary's)	585 Water Street South, P. O. Box 1000, St. Marys, ON N4X 1B6	General use limestone cement (GUL), as GU is not produced any longer.
Silica fume	Norchem Inc.	Alloy Plant, West Virginia, U.S.A.	-
Silica flour	US Silica, Product SIL-CO-SIL® 53	701 Boyce Memorial Drive, Ottawa, IL 61350, U.S.A.	Supplier AGSCO CORP IL, 160 W Hintz Rd. Wheeling, IL 60090 U.S.A. Product silica flour #325/53u is similar to SIL-CO-SIL® 53.
Fine aggregate (natural concrete sand) and coarse aggregate (natural carbonate and crystalline pit coarse aggregate)	Lafarge	1773 Dumfries Cambridge, ON N0B 1E0	Availability from Cambridge will end in the next years, similar aggregate available from West Paris.
MasterGlenium 7500 poly-carboxylate-based superplasticizer	BASF	100 Milverton Drive, 5th Floor, Mississauga, ON L5R 4H1	-
SR-270 and CR-10 reference water ingredients	Alphachem	2485 Milltower Court Mississauga, ON L5N 5Z6	-

3. OPTIMIZED LHHPC MIX INGREDIENTS CHARACTERIZATION

3.1 MIX INGREDIENTS CHARACTERIZATION TESTS

The following characterization tests were conducted on the mix ingredients used for the prepared optimized LHHPC material:

- For the cementing materials in Table 3, including cement type GUL and SF, review of the mill-run certificates was conducted to understand the chemical composition of the binders. Additionally, chemical and mineralogical composition of the powders was conducted by chemical analysis and qualitative X-ray diffraction (XRD) following *ASTM C1365 Standard Test Method for Determination of the Proportion of Phases in Portland Cement and Portland Cement Clinker Using X-Ray Powder Diffraction Analysis*, respectively. Chemical composition of the binders was conducted by AGAT Laboratories. AGAT Laboratories is a Canadian-owned country-wide provider of laboratory services in a wide range of scientific fields. Major divisions include Environmental Testing, Mining Geochemistry, Air Quality Monitoring, Oil and Gas Chemistry, Rock Properties, Agri-Food, and Forensics. AGAT is accredited to ISO 17025:2005 for all services.

- For the SF determination of the tendency of silica fume to entrain air was conducted following *CSA A3004-A5 Rapid Test Method for Determining the Tendency of Silica Fume to Entrap Air in Mortar or Concrete*. Additionally, the potential for gas generation was evaluated following the method detailed in Zhang et al. (2000) to estimate the free Si content in silica fume. Evolution of hydrogen gas has raised concerns over possible explosion hazards; therefore, it was recommended to be determined for the SF used in LHHPC mixes for DGR applications. The test to determine the tendency of SF to entrain air and the potential for gas generation were conducted sequentially. The tendency to entrain air was tested first. If it passed (i.e., no visible entrapped air bubbles on the surface of the SF slurry; see Appendix B), the SF was tested for free silicon content. The SF must meet the performance target of <0.075% free Si content by mass prior to its use in the concrete fabrication.

- For the aggregate material in Table 3, including concrete sand, silica flour and coarse aggregate, physical, chemical and mineralogical characterization was conducted. Chemical analysis was conducted by X-ray fluorescence (XRF) and mineralogical composition was determined by XRD. Physical characterization included gradation, following ASTM C136 Standard Test Method for Sieve Analysis of Fine and Coarse Aggregate, and density, specific gravity and absorption, following *ASTM C128 Standard test Method for Density, Relative Density (Specific Gravity), and Absorption of Fine Aggregate* and *ASTM C127 Standard test Method for Density, Relative Density (Specific Gravity), and Absorption of Coarse Aggregate*. The aggregates used conform to the requirements of *CSA A23.1/2 for use in Portland cement concrete*. Chemical composition of the aggregates was conducted by AGAT Laboratories.

3.2 TEST RESULTS

The mix ingredient characterization test results are available in Appendices A - F as presented in Table 4. Based on the characterization test results, the mix ingredients evaluated to be used for optimized LHHPC mixes are all within typical property ranges. They are all suitable to be

used for concrete mixes and consequently for LHHPC mixes. In particular, the free silicon (Si) content in the SF met the performance target <0.075% (by mass) for the project.

Table 4: Summary of the Optimized LHHPC Mix Ingredient Characterization Test Results

Mix Ingredients	Supplier	Wood Log No.	Properties, Reports/ References	Test Method	Appendix
Cement Type GUL	Votorantim Cimentos (formerly St. Marys Cement)	S198-20	Votorantim Cimentos Cement Mill Test Report		Appendix A
			Chemical composition	Borate Fusion and X-ray Fluorescence Spectrometry	
			XRD pattern	ASTM C1365	
Silica Fume	Norchem Inc., Alloy Plant, U.S.A.	S070-20	Norchem Chemical and Physical Report		Appendix B
			Chemical composition	Borate Fusion and X-ray Fluorescence Spectrometry	
			XRD pattern	ASTM C1365	
			Tendency to entrap air	CSA A3004-A5	
			Potential for hydrogen generation	Zhang et al. 2000	
Silica Flour	AGSCO	C158-20	Ground Silica (#270/53u) Specifications		Appendix C
			Chemical composition	Borate Fusion and X-ray Fluorescence Spectrometry	
			XRD pattern	ASTM C1365	
Natural Concrete Sand	Lafarge, Cambridge, ON	S027-20	Absorption and specific gravity	ASTM C128	Appendix D
			Chemical composition	Borate Fusion and X-ray Fluorescence Spectrometry	
			Particle size distribution	ASTM C136	
			XRD pattern	ASTM C1365	

Mix Ingredients	Supplier	Wood Log No.	Properties, Reports/ References	Test Method	Appendix
Natural Carbonate and Crystalline Pit Coarse Aggregate	Lafarge, Cambridge, ON	S028-20 & S029-20	Absorption and specific gravity	ASTM C127	Appendix E
			Chemical composition	Borate Fusion and X-ray Fluorescence Spectrometry	
			Particle size distribution	ASTM C136	
			XRD pattern	ASTM C1365	
Poly-carboxylate-based Super Plasticizer	BASF	C115-20	BASF MasterGlenium ® 7500 full range water-reducing admixture technical data sheet	-	Appendix F

4. REFERENCE WATERS

The reference waters were prepared for saturated hydraulic conductivity tests and pH only:

- Reference crystalline rock water – CR-10
- Reference sedimentary rock water – SR-270.

NWMO is currently updating the sedimentary rock water from SR-270 to SR-290. It is understood that further similar testing will be conducted with SR-290.

4.1 REFERENCE WATER CHEMISTRY

Details of the chemical composition of the reference waters are available in Table 5 (Duro et al., 2010).

Table 5: Reference Water Chemical Composition

Parameter	CR-10 Crystalline Rock Water	SR-270 Sedimentary Rock Water
pH	7	5.8
TDS (mg/L)	11,300	275,000
Na (mg/L)	1,900	50,100
K (mg/L)	15	12,500
Ca (mg/L)	2,130	32,000
Mg (mg/L)	60	8,200
HCO_3 (mg/L)	70	110
SO_4 (mg/L)	1,000	440
Cl (mg/L)	6,100	168,500
Br	-	1,700
Sr	25	1,200

4.2 CHEMICAL COMPOSITION

The reference waters, which are used for hydraulic conductivity and pH testing, were prepared in the Wood Burlington laboratory and their chemical composition was verified by testing by a third-party accredited laboratory (Bureau Veritas). Table 5 presents the target compositions, with Tables 6 and 7 presenting the results of the chemical analyses of the laboratory prepared reference CR-10 and SR-270 waters with reportable detection limit (RDL), respectively. Extremely high concentration of the SR-270 brine made analyses by the third party laboratory very difficult, as they needed to significantly dilute the brine, in order for it to be measurable in their instruments which are typically calibrated for detections for drinking water. The results for the CR-10 water, which has only 4% the solids content of the SR-270 water, are much more reliable. The in-situ crystalline and sedimentary rock water samples represented by the compositions in Table 5 have measured pH values in equilibrium with the surrounding rock mass. The lab prepared water samples have the correct concentrations of dissolved ions but the pH measured is at equilibrium with air. A small amount of acid is added to bring the lab waters to the correct pH value prior to use in hydraulic conductivity or pH testing.

For the SR-270 water, the pH is adjusted from 6.75 to 5.8 prior to hydraulic conductivity or pH testing. This ensures proper pH in contact with the LHHPC samples. The amount of HCl needed to decrease the pH from 6.75 to 5.8 is 1.407×10^{-6} moles/L (0.0000511 g/L). A total of 0.1402 ml of 0.01 molar HCl solution is required to adjust 1 liter of SR-270 water from a pH of 6.75 to the target pH of 5.8. This represents a 0.04% increase in total chloride, which is approximately 1/40 of the reportable detection limit for chloride.

For the CR-10 water, the pH is adjusted from 7.57 to 7.0 prior to hydraulic conductivity or pH testing. This ensures proper pH in contact with the LHHPC samples. The amount of HCl needed to decrease the pH from 7.57 to 7.0 is 7.308×10^{-8} moles/L (0.00000266 g/L). A total of 0.0073 ml of 0.01 molar HCl solution is required to adjust 1 liter of CR-10 water from a pH of 7.57 to the target pH of 7.0. This represents a negligible increase in total chloride.

Table 6: Crystalline Rock Water CR-10 Chemical Composition Results

Parameter	Reference CR-10 Water	Analyzed CR-10 Water Sample	RDL
pH	7	7.57	NA
Na (mg/L)	1,900	1,900	0.500
K (mg/L)	15	49	1
Ca (mg/L)	2,130	2,100	2
Mg (mg/L)	60	68	0.250
HCO_3 (mg/L)	70	NA	NA
SO_4 (mg/L)	1,000	910	5.0
Cl (mg/L)	6,100	5,800	60
Sr (mg/L)	25	26	0.005
Li (mg/L)	-	0.048	0.025
F (mg/L)	-	0.69	0.10
B (mg/L)	-	0.480	0.050
Si (mg/L)	-	0.940	0.250
TDS (mg/L)	11,300	NA	NA

Notes:

- = Not reported

NA = Not available

RDL = Reportable Detection Limit.

Table 7: Sedimentary Rock SR-270 Water Chemical Composition Results

Parameter	Reference SR-270 Water	Analyzed SR-270 Water Sample	RDL	Analyzed SR-270 Water Repeat Sample	RDL
pH	5.8	6.75	NA	6.83	NA
Na (mg/L)	50,100	46,000	10	46,000	10
K (mg/L)	12,500	11,000	20	12,000	20
Ca (mg/L)	32,000	27,000	100	28,000	100
Mg (mg/L)	8,200	7,300	5	7,100	2.50
HCO_3 (mg/L)	110	NA	0.05	148	0.05
SO_4 (mg/L)	440	230	1	310	1
Cl (mg/L)	168,500	130,000	2,000	130,000	2,000
Br (mg/L)	1,700	NA	500	1,700	500
Sr (mg/L)	1,200	1,000	0.100	1,000	0.050
Li (mg/L)	-	5.30	0.500	7.1	0.250
F (mg/L)	-	0.13	0.10	<0.10	0.10
I (mg/L)	-	NA	NA	NA	NA
B (mg/L)	-	77	1	67	0.50
Si (mg/L)	-	7.80	5	<2.5	2.5
TDS (mg/L)	275,000	NA	20	246,000	20

Notes: Before sampling for analysis, pH was measured to be approximately 5.8.
- = Not reported
NA = Not available
RDL = Reportable Detection Limit; NA= not applicable

5. OPTIMIZED LHHPC TRIAL BATCH QUALIFICATION

After the free silicon content in SF test was passed, trial LHHPC batches were prepared to conduct trial batch qualification tests. Tap water was used for LHHPC preparation. LHHPC specimens were cured in a moist environment at 100% relative humidity (RH) for qualification tests discussed below.

5.1 QUALIFICATION TESTS

Table 8 lists trial batch qualification tests for the following material properties:

- Bulk density and porosity following *ASTM C642 Standard Test Method for Density, Absorption, and Voids in Hardened Concrete*. Bulk density and porosity were measured at 30 days.
- pH testing in distilled water following the methodology described in Alonso et al. (2012). pH was measured at 28 days.
- Unconfined compressive strength (UCS) following *ASTM C39 Standard Test Method for Compressive Strength of Cylindrical Concrete Specimens*. UCS was measured at 7 days.
- Slump and slump flow retention up to 2 hours from the time of mixing following *ASTM C143/C143M Standard Test Method for Slump of Hydraulic-Cement Concrete* and *ASTM C1611/C1611M Standard Test Method for Slump Flow of Self-Consolidating Concrete*, respectively, at the following ages, assuming that the LHHPC would be placed in the DGR within two hours (120 minutes).
    - 0 minutes (“time 0”, initial slump), 20 minutes, 40 minutes, 60 minutes, 90 minutes and 120 minutes after mixing, with no additional mixing after “time 0”, and
    - 0 minutes (“time 0”, initial slump), 20 minutes, 40 minutes, 60 minutes, 90 minutes and 120 minutes after mixing, with additional mixing at each interval after “time 0”. These slump and slump flow measurements are proposed due to the fact that it is known that additional mixing can maintain some of the plastic properties of concrete and increase slump retention over time compared to slump retention without further mixing after “time 0”. Therefore, additional mixing and higher slump retention can be beneficial for placement of LHHPC in the DGR.

Table 8: Optimized LHHPC Trial Batch Qualification Tests

Property	Qualification Test Requirements
Bulk density	>2400 kg/m^3
Porosity	<6% (30 days)
pH (testing in distilled water)	≤11 (28 days)
Unconfined compressive strength	>25 MPa (7 days)
Slump and slump flow retention up to 2 hours from the time of mixing	Slump 200 +/- 50 mm Slump flow: 300 – 650 mm (provided no bleeding and/or segregation) Slump and slump flow retention: ≥75%

5.2 QUALIFICATION TEST RESULTS

5.2.1 Bulk Density and Porosity

Table 9 presents 30-day bulk density and porosity results. Three (3) measurements were obtained to determine these properties. An additional set of three measurements were obtained for quality assurance, as verification tests. The trial batch optimized LHHPC mix bulk density and porosity results met the qualification test requirements in Table 8.

Table 9: Bulk Density and Porosity Trial Batch Qualification Test Results

Log No.	Age (days)	Density (Apparent density) (kg/m^3)					Porosity (Volume of permeable pore space (voids)) (%)				
		Target Bulk Density >2400 kg/m^3					Target Porosity at 30 days <6%				
		Test 1	Test 2	Test 3	Aver. **	St. Dev.+	Test 1	Test 2	Test 3	Aver.	St. Dev.
C736-20	30	2,516	2,521	2,516	2,518	2.89	4.36	4.22	4.15	4.24	0.107
C737-20*	30	2,513	2,505	2,508	2,509	4.04	4.28	4.23	4.16	4.22	0.060

Notes: * QA measurement for verification test

** Average

+ Standard deviation

5.2.2 pH in Distilled Water

Table 10 presents 28-day pH testing in distilled water results. Three (3) measurements were obtained to determine the pH. The trial batch optimized LHHPC mix pH in distilled water results met the qualification test requirements in Table 8.

Table 10: pH in Distilled Water Trial Batch Qualification Test Results

Sample Log No.	Test No.	Sample Age (days)	Buffer pH	Slurry pH	Filtered pH	Average Slurry pH	Average Filtered pH
Target pH (testing in distilled water) ≤11 (28 days)							
C736-20A	Test 1	28	10.04	10.98	10.77	10.96	10.83
C736-20B	Test 2	28	10.04	10.90	10.89		
C736-20C	Test 3	28	10.04	11.01	10.83		

5.2.3 Unconfined Compressive Strength

Table 11 presents 7-day UCS results. Three (3) measurements were obtained to determine UCS. Plastic and hardened density were determined by simple measurements based on volume (calculated based on length and diameter measurements) and mass as quality control. An additional set of three measurements was obtained for quality assurance, as verification tests. The trial batch optimized LHHPC mix UCS results met the qualification test requirements in Table 8.

Table 11: UCS Trial Batch Qualification Test Results

Log No.	UCS Tests				
	Cylinder Label	Age	Density		Strength
			Plastic	Hardened	Target UCS>25 MPa at 7 days
		(days)	(kg/m^3)	(kg/m^3)	(MPa)
C736-20	C736-20A	7	2,499	2,448	29.95
	C736-20B	7	2,509	2,458	29.59
	C736-20C	7	2,497	2,443	30.11
		Average	2,502	2,450	29.88
		St. Dev.	6.59	7.55	0.27
C737-20*	C737-20A	7	2,484	2,437	27.20
	C737-20B	7	2,487	2,438	27.23
	C737-20C	7	2,494	2,451	27.01
		Average	2,489	2,442	27.15
		St. Dev.	5.27	7.67	0.12

Note: *Verification tests

5.2.4 Slump and Slump Flow Retention

Slump, or slump flow retention, represents the slump, or slump flow respectively, measured at a certain time after “time 0” and expressed as a percentage of the initial slump. Table 12 and Figures 1 and 2 present slump and slump flow retentions up to 2 hours results. Six (6) measurements were obtained to determine slump and slump flow retention up to 2 hours. The trial batch optimized LHHPC mix slump and slump flow results met the qualification test requirements in Table 8.

Table 12: Slump and Slump Flow Retention Trial Batch Qualification Test Results

No.	Static or Remix	Age (min.)	Slump		Slump Retention	Slump Flow		Slump Flow Retention
	Log No.		(mm)	(in)	(%)	(mm)	(in)	(%)
Target performance			**150 - 250**	**~5.9 - 9.8**	**≥75%**	**300 - 650**	**~11.8 - 25.6**	**≥75%**
1	**Static (no Additional Mixing)** C736-20	0	222.3	8.75	100.00	380.0	14.96	100.00
2		20	228.6	9.00	102.86	380.0	14.96	100.00
3		40	228.6	9.00	102.86	380.0	14.96	100.00
4		60	235.0	9.25	105.71	380.0	14.96	100.00
5		90	241.3	9.50	108.57	399.5	15.73	105.13
6		120	235.0	9.25	105.71	380.0	14.96	100.00
1	**Remix (Additional Mixing, 1 min.)** C737-20	0	235.0	9.25	100.00	380.0	14.96	100.00
2		20	235.0	9.25	100.00	405.0	15.94	106.58
3		40	235.0	9.25	100.00	415.0	16.34	109.21
4		60	247.7	9.75	105.41	420.0	16.54	110.53
5		90	241.3	9.50	102.70	400.0	15.75	105.26
6		120	235.0	9.25	100.00	370.0	14.57	97.37

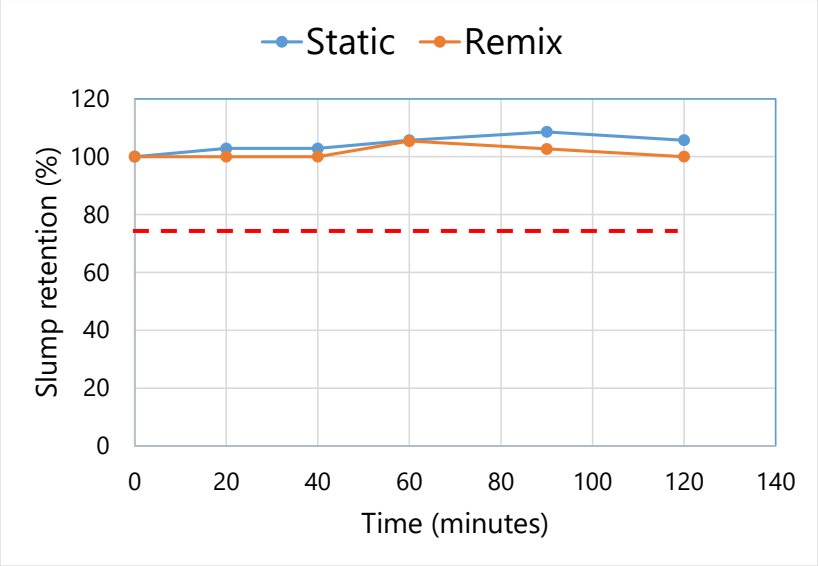

Figure 1: Slump Retention Trial Batch Qualification Test Results

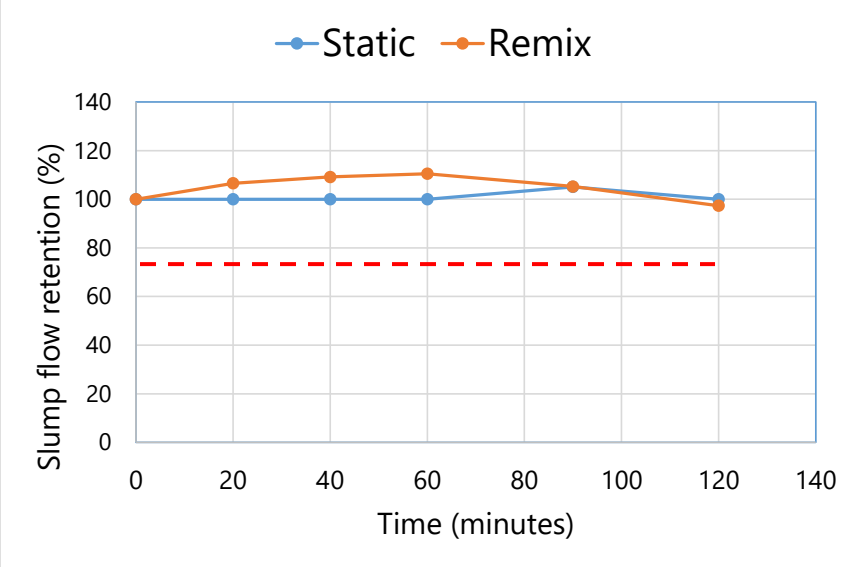

Figure 2: Slump Flow Retention Trial Batch Qualification Test Results

6. OPTIMIZED LHHPC TEST PROGRAM

6.1 TEST PROGRAM OPTIMIZED LHHPC

Production LHHPC batches were prepared to produce specimens for the optimized LHHPC mix. Ontario tap water was used for LHHPC preparation. The specimens were cured in a moist environment at room temperature (20 to 25ºC). The LHHPC specimens used for the previous studies were cured in two simulated reference water conditions: fresh water (distilled water) and highly saline water (SR-270). Overall, the test results were similar for LHPPC regardless of the type of curing water used in the previous study. Some differences in performance between the LHHPC cured in distilled water and SR-270 water were observed during the creep test.

The initial scope of work included the following properties measured at the appropriate age for the optimized LHHPC mixture following test methods as described in the Project Test Plan:

- Chemical and mineralogical composition to approximately the 1 wt% level, as detailed in Section 6.2.1.
- Bulk density, as detailed in Section 6.2.2;
- Porosity, as detailed in Section 6.2.2;
- Unconfined compressive strength and crack initiation, as detailed in Section 6.2.3;
- Split tensile strength, as detailed in Section 6.2.4;
- Creep, as detailed in Section 6.2.5;
- Triaxial compression, as detailed in Section 6.2.6;
- Saturated hydraulic conductivity, as detailed in Section 6.2.7;
- Maximum temperature rise at the center of cubic specimens, as detailed in Section 6.2.8;
- Shrinkage rate, as detailed in Section 6.2.8;
- pH, as detailed in Section 6.2.9;
- Slump and slump flow retention, as detailed in Section 6.2.10;
- Rheology of fresh concrete mix to obtain viscosity and yield stress, as detailed in section 6.2.11; and
- Thermal conductivity, as detailed in Section 6.2.12.

The additional scope of work included thermal conductivity measured at 28 days for the optimized LHHPC, normal strength concrete (NSC) and high performance concrete (HPC) mixtures following test methods as described in the Project Test Plan.

- Unconfined compressive strength, bulk density, porosity were measured along with thermal conductivity, as detailed in Section 6.2.13.

To meet quality assurance (QA) requirements as per the project test plan, additional tests were conducted, or samples were tested by a second professional for verification. Table 14, Table 15, Table 16 and Table 18 include bulk density, porosity, UCS and pH results obtained in verification tests.

Additional specimens were prepared to produce the remaining number of specimens required to conduct the test program detailed in the project test plan.

6.2 TEST RESULTS OPTIMIZED LHHPC

6.2.1 Chemical and Mineralogical Composition

Chemical composition and mineralogical composition of the LHHPC were determined on one sample cured in a moist environment at two (2) ages, 7 and 180 days. The objective of conducting these tests at two different ages was to understand changes in chemical and mineralogical composition of the LHHPC over time; however, both chemical and mineralogical composition are dominated by the aggregate fractions, which represent approximately 70% of the mix. It is the paste fraction (cement, silica fume, silica flour, water and admixtures) that is responsible for changes in the chemical and mineralogical composition of the LHHPC mix. Therefore, the chemical and mineralogical composition can be determined on the paste fraction of the LHHPC mix. For this purpose, specimens with a mix design identical to that of the paste fraction in LHHPC were prepared, cured in a moist environment to be used to determine the chemical and mineralogical composition at 7 and 180 days.

Chemical composition, conducted by AGAT Laboratories, was determined by chemical analysis including whole rock, carbon and sulphur. Mineralogical composition was determined by qualitative X-ray diffraction following *ASTM C1365 Standard Test Method for Determination of the Proportion of Phases in Portland Cement and Portland Cement Clinker Using X-Ray Powder Diffraction Analysis*. An as-fabricated LHHPC sample was crushed and pulverized prior to conducting these tests.

Table 13 presents 7-day and 180-day chemical composition results. The chemical composition of the 7-day paste fraction is typical and confirms the presence of the silica flour and silica fume (SiO_2) as well as hydration products (CaO, Al_2O_3), in the correct proportions. The 180-day results are the same chemically, but with a measurable change in both calcium hydroxide and silica fume.

Table 13: 7-day Chemical Composition Test Results

Age	7-day		180-day	
Sample	LHHPC paste	RDL*	LHHPC paste	RDL*
Element Oxide (%)	(%)	(%)	(%)	(%)
Total Carbon	1.79	0.01	1.87	0.01
Total Sulphur	0.273	0.005	0.336	0.005
Al_2O_3	1.15	0.01	1.08	0.01
BaO	0.04	0.01	<0.01	0.01
CaO	12.90	0.01	13.50	0.01
Cr_2O_3	<0.01	0.01	0.02	0.01
Fe_2O_3	0.56	0.01	0.56	0.01
K_2O	0.21	0.01	0.21	0.01
MgO	0.75	0.01	0.74	0.01
MnO	0.02	0.01	0.02	0.01
Na_2O	0.12	0.01	0.12	0.01
P_2O_5	0.05	0.01	0.05	0.01

Age Sample Element Oxide (%)	7-day		180-day	
	LHHPC paste (%)	RDL* (%)	LHHPC paste (%)	RDL* (%)
SiO_2	67.30	0.01	70.20	0.01
TiO_2	0.05	0.01	0.06	0.01
SrO	<0.01	0.01	<0.01	0.01
V_2O_5	<0.01	0.01	<0.01	0.01
LOI	16.70	0.01	13.20	0.01
Total	99.90	0.01	99.80	0.01
SO_3^{**}	0.68	-	0.84	-

Note: * Reported Detection Limit; ** Calculated

Figures 3 to 5 present XRD patterns for dry LHHPC paste powder, 7-day and 180-day LHHPC paste, respectively. The mineralogical composition results are in agreement with the chemical composition results in Table 13 and confirm the presence and changes of the hydration products (calcium hydroxide) over time.

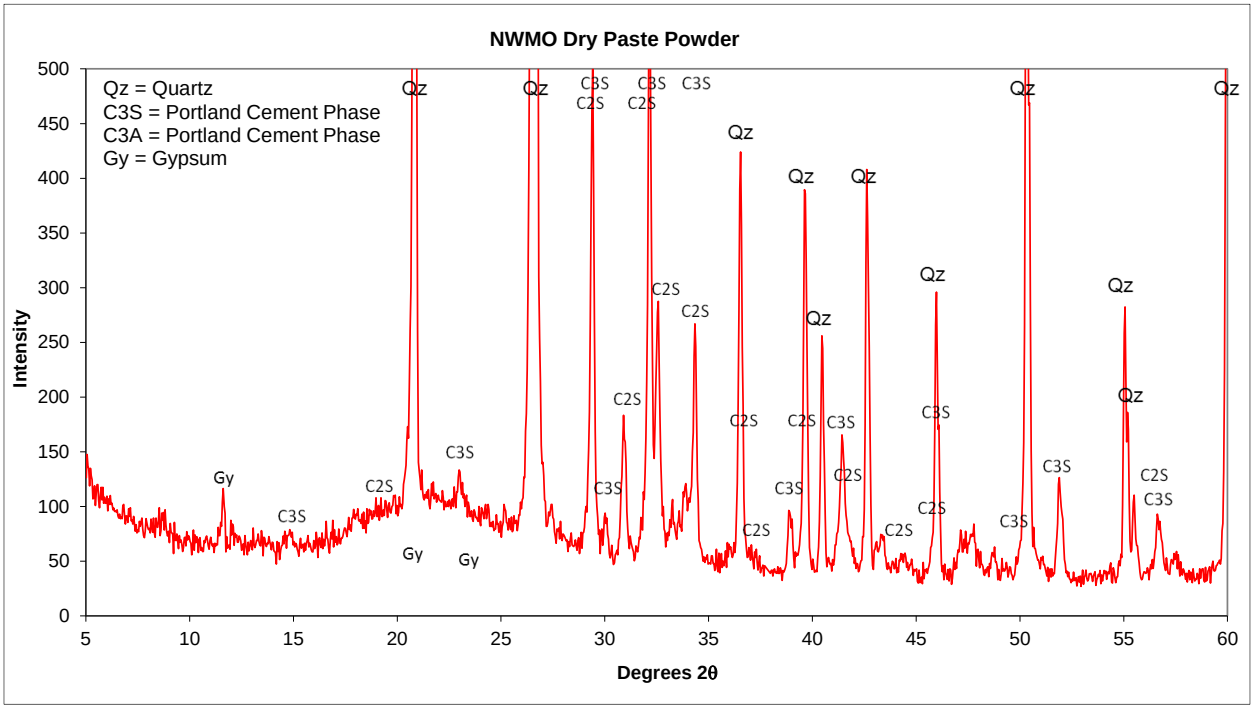

Figure 3: XRD pattern of dry LHHPC paste powder

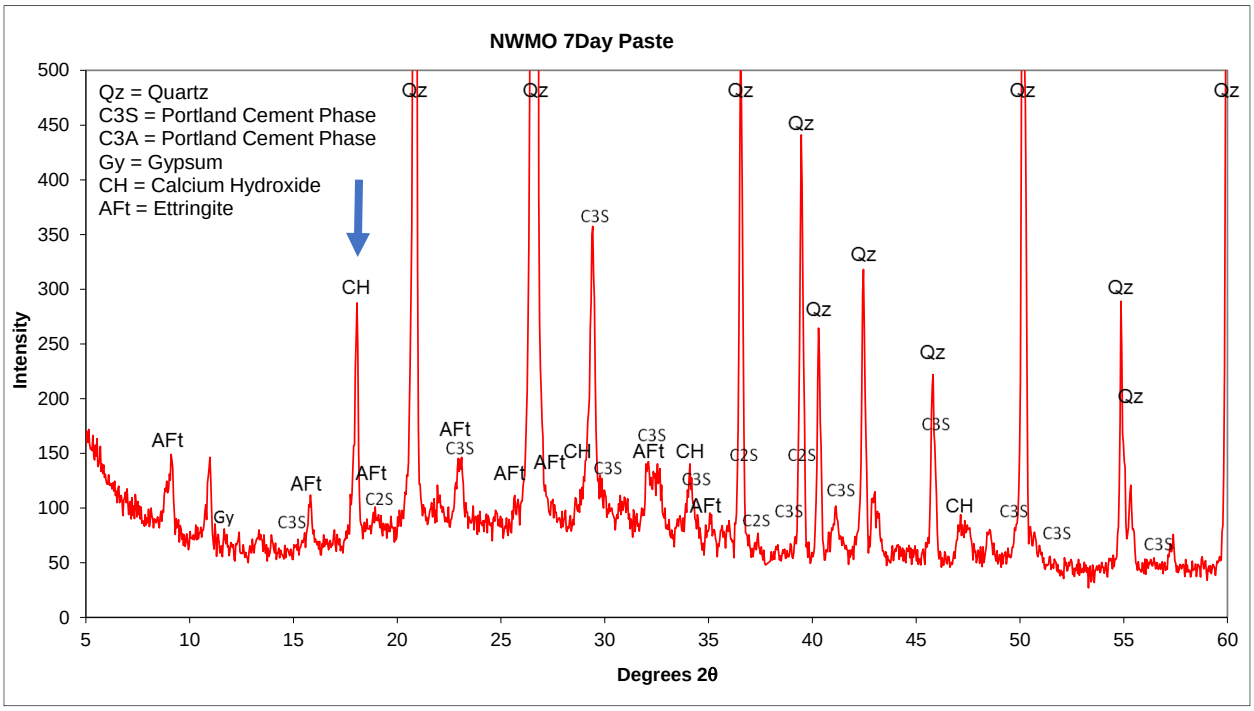

Figure 4: XRD pattern of 7-day LHHPC paste

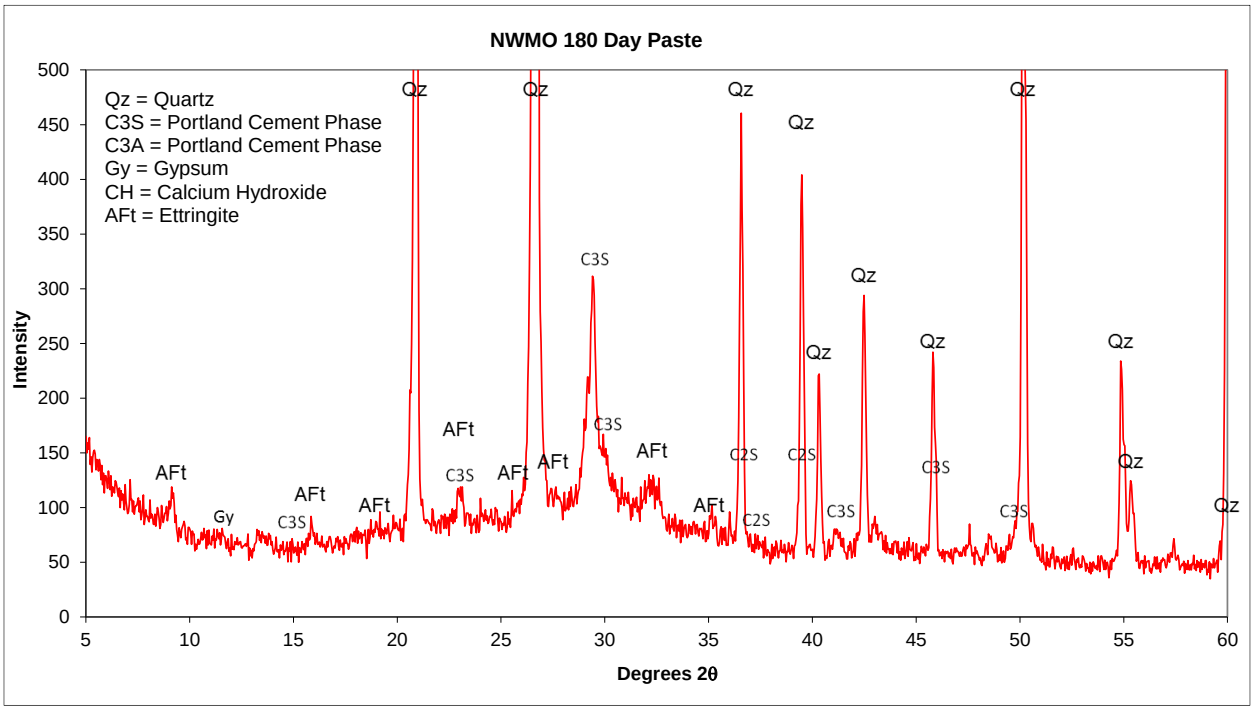

Figure 5: XRD pattern of 180-day LHHPC paste

6.2.2 Bulk Density and Porosity

Bulk density and porosity of as-fabricated LHHPC production mixes was determined following *ASTM C642 Standard Test Method for Density, Absorption, and Voids in Hardened Concrete*. According to this test method bulk density is determined based on mass of oven-dried sample at a temperature of 110 ± 5°C for not less than 24 hours in air, and apparent mass of sample in water after immersion and boiling. According to this test method porosity represents the volume of permeable pore space, or voids, and does not account for impermeable pores. LHHPC specimens were cured in a moist environment prior to measuring bulk density and porosity. Triplicate specimens are used to determine bulk density and porosity at two (2) ages: 7 and 180 days.

As part of the standard test procedure for compressive strength, the hardened density of the concrete was also determined by simple measurements based on volume (calculated based on length and diameter measurements) and mass. The additional density values for the LHHPC were measured as an additional quality control step to assess consistency.

Table 14 presents 7-day and 180-day bulk density test results. An additional set of three 7-day and 180-day measurements were obtained for quality assurance, as verification tests. 7-day and 180-day bulk density results meet the performance target in Table 2.

Table 15 presents 7-day and 180-day porosity test results. An additional set of three 7-day and 180-day measurements were obtained for quality assurance, as verification tests. 7-day and 180-day porosity results met the 180-day performance target in Table 2.

Table 14: Bulk Density Test Results

Tests	Density (kg/m^3)	Log No.	Age (days)	Target Bulk density ≥2,400 kg/m^3				
				Test 1	Test 2	Test 3	Average	St. Dev.
Test program	Bulk Density after Immersion and Boiling	C2000-20	7	2,460	2,466	2,466	2,464	3.46
	Apparent density		7	2,530	2,537	2,538	2,535	4.36
	Bulk Density after Immersion and Boiling	C1074-20	180	2,461	2.470	2.473	2,468	6.24
	Apparent density		180	2,536	2,541	2,538	2,538	2.52
Verification tests	Bulk Density after Immersion and Boiling	C1075-20	7	2,455	2,468	2,459	2,461	6.66
	Apparent density		7	2,525	2,539	2,526	2,530	7.81
	Bulk Density after Immersion and Boiling	C1075-20	180	2,456	2,457	2,466	2,459	5.51
	Apparent density		180	2,527	2,529	2,539	2,532	6.43

Table 15: Porosity Test Results

Tests	Log No.	Age (days)	Porosity (Volume of permeable pore space (voids)) (%) Target Porosity at 180 days ≤6%				
			Test 1	Test 2	Test 3	Average	St. Dev.
Test program	C2000-20	7	4.58	4.65	4.64	4.62	0.038
	C1074-20	180	4.90	4.61	4.24	4.58	0.331
Verification tests	C1075-20	7	4.59	4.59	4.41	4.53	0.105
	C1075-20	180	4.68	4.74	4.75	4.72	0.038

6.2.3 Unconfined compressive strength and crack initiation

Unconfined compressive strength (UCS) was determined following *ASTM C39 Standard Test Method for Compressive Strength of Cylindrical Concrete Specimens*. Three (3) cylindrical LHHPC 4" x 8" (100 mm x 200 mm) specimens were tested after 7, 28, 56, 90, 180 and 270 days curing in a moist environment. The same specimens were used to determine Young's modulus and Poisson's ratio following *ASTM C469/C469M Standard Test Method for Static Modulus of Elasticity and Poisson's Ratio of Concrete in Compression*. Crack initiation was determined using strain gauges in accordance with the Inverse Tangent Lateral Stiffness (ITLS) methodology summarized in Ghazvinian et al. (2012). According to this reference, ITLS is an indicator for crack initiation (CI) that is only dependent upon lateral strain (Figure 6). The equipment used to determine UCS, Young's modulus (e.g., the modulus of elasticity (MOE)) and crack initiation (CI) was a 4500 kN MTS 815 Rock Mechanics Test System with MTS 315.03S 4,500 kN Actuator/Load Frame. It includes a hydraulic pump, a hydraulic ram, a load frame, pressure transducers, or load cells and a data acquisition interface. UCS, Young's modulus, Poisson's ratio and crack initiation tests were conducted by CanmetMINING in Nepean, Ontario, Canada. Figure 7 presents a photograph of the specimen instrumented with strain gauges prior to the UCS test. Figure 8 presents a photograph of a UCS test in progress. Canmet MINING report summarizing the methodology and results of the mechanical test program conducted for this project is available in Appendix G. It includes sample preparation, measurement of intact physical properties, and determination of mechanical properties (strength, Young's modulus and crack initiation) of the cylinder specimens by uniaxial compression strength (UCS) tests, as well as summary tables, compression test data and CI interpretation.

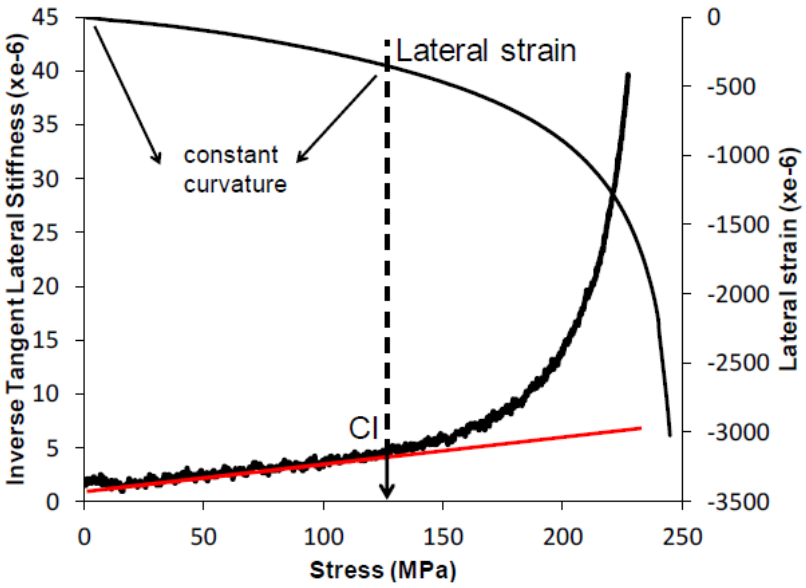

Figure 6: ITLS method for estimating CI by using lateral strain (Ghazvinian et al., 2012)

Table 16 presents up to 270-day UCS and MOE test results. An additional set of three measurements 7-day and 90-day UCS was obtained by Wood for quality assurance, as verification tests. UCS results met and exceed the performance targets in Table 2.

There is no standard test method to determine CI for concrete and the method proposed and used by Canmet was developed for rocks. Although the method using electric strain gauges described in the article by (Ghazvinian et al. 2012) is suitable for rocks it may not be suitable for concrete, or LHHPC due to the differences between rock and concrete, including porosity (concrete is more porous than rock), and homogeneity (concrete is a heterogeneous material, whereas rocks are typically more homogeneous). Therefore, CI for concrete is preceded by pore collapse/crushing, which is different from rocks. Crack initiation values in Table 16 have been calculated using the Inverse Tangent Lateral Stiffness (ITLS) method, as described in Ghazvinian et al. (2012). This method uses only the lateral strain data and is not dependent on the calculated value of Poisson's ratio, which is non-linear and thus dependent on the window selected for the calculation. The ITLS method amplifies the change in lateral strain to more readily identify the onset of rapid lateral strain increase, which is taken as the crack initiation point (i.e., axial cracking and dilation).

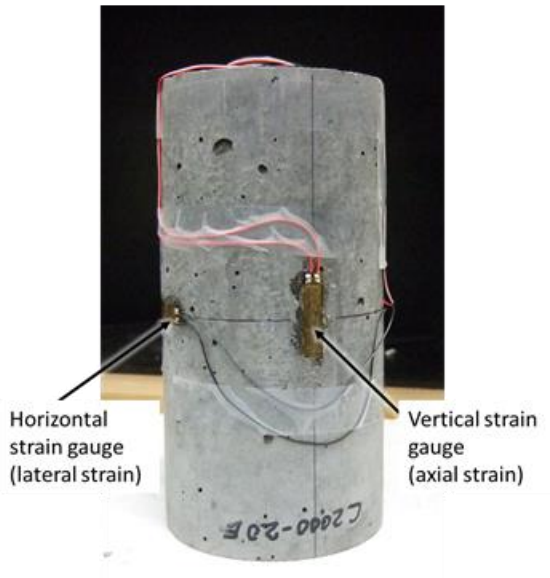

Figure 7: Specimen instrumented prior to UCS and CI test

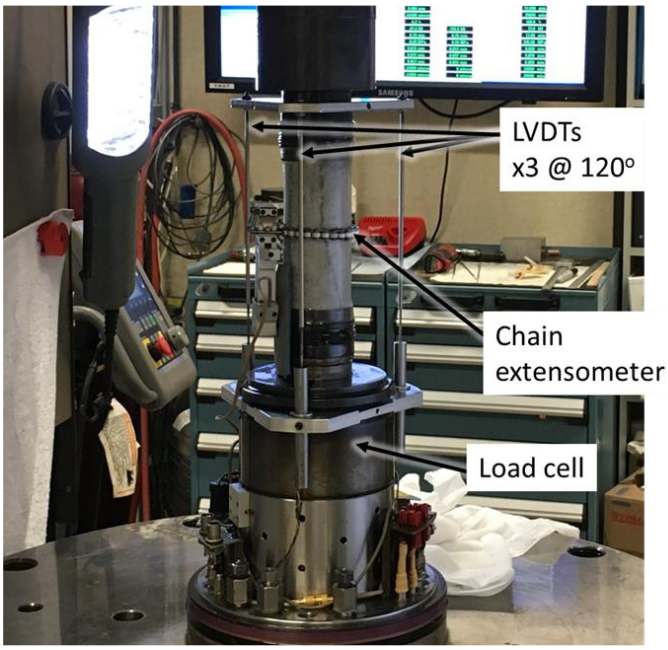

Figure 8: Test set up and UCS and CI test in progress

Table 16: UCS, Young's Modulus and Crack Initiation Test Results

Results		UCS results (MPa) Target UCS: >25 MPa @ 7 days, >60 MPa @ 90 days		Young's modulus (GPa)	Crack Initiation	
					CI (MPa)	% UCS
Age (days)	Laboratory	Canmet	Wood Verification	Canmet	Canmet	Canmet
7	Average	30.50	27.08	25.37	13.00	43%
	St. Dev.	0.14	0.173	0.32	0.44	
28	Average	62.99	54.10	31.40	29.07	46%
	St. Dev.	0.96	0.452	0.40	0.45	
56	Average	75.23		33.20	43.95	58%
	St. Dev.	1.25		1.73	0.21	
90	Average	71.40	68.92	32.50	36.60	51%
	St. Dev.	2.00	0.711	0.78	2.40	
180	Average	79.03		33.98	36.37	46%
	St. Dev.	0.93		0.59	1.07	
270	Average	78.98		33.67	39.20	50%
	St. Dev.	2.04		0.35	1.39	

6.2.4 Split Tensile Strength

Split tensile strength was determined following *ASTM C496/C496M Standard Test Method for Splitting Tensile Strength of Cylindrical Concrete Specimens* (CSA A23.2-13C). This test method consists of applying a diametral compressive force along the length of a cylindrical concrete specimen at a rate that is within a prescribed range until failure occurs. This loading induces tensile stresses on the plane containing the applied load and relatively high compressive stresses in the area immediately around the applied load. Tensile failure occurs rather than compressive failure. Figure 9 presents the split tensile test setup. Three (3) LHHPC samples were tested at the following ages: 28 and 270 days after curing in moist environment. Table 17 presents up to 28-day and 270-day split tensile strength results. There are empirical relationships between compressive and tensile strength and the concrete tensile strength is typically 10 – 15 times less than the compressive strength. The results obtained to date for the optimized LHHPC are within the expected range.

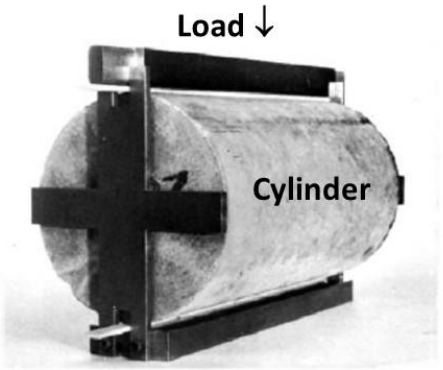

Figure 9: Split Tensile Test Setup

Table 17: Split Tensile Strength Results

No.	Sample Log No.	Age	Diameter	Length	Max. load	Split tensile strength	Curing	Defects	Type of Fracture
		(days)	(mm)	(mm)	(N)	(MPa)			
1	C2000-20Q	28	102	202	153.2	4.73	Moist	-	Split
2	C2000-20R	28	102	202	133.4	4.12	Moist	-	Split
3	C2000-20S	28	102	202	164.1	5.07	Moist	-	Split
4	C1074-20M	270	102	202	188.0	5.81	Moist	-	Split
5	C1074-20N	270	102	202	162.8	5.03	Moist	-	Split
6	C1074-20O	270	102	202	155.5	4.80	Moist	-	Split
	Average	28				4.64			
	St. Dev.	28				0.48			
	Average	270				5.21			
	St. Dev.	270				0.53			

6.2.5 Creep

Creep was determined following *ASTM C512/C512M Standard Test Method for Creep of Concrete in Compression*. This test method measures the load-induced time-dependent compressive strain at selected ages for concrete under a set of controlled environmental conditions. Molded concrete cylinders were subjected to sustained longitudinal compressive load representing no more than 40% of the compressive strength at the time of loading. Strain readings were taken prior to loading and after applying the load on a regular basis up to one year. Control samples without applied stress were stored in similar environmental conditions to permit correction of free strain per the test procedure. Six (6) LHHPC samples were cured for three (3) log cycles (72 days curing in a moist environment), with two (2) samples tested for creep, two (2) for control samples and two (2) for compressive strength test prior to loading. The age of the samples at the time of initiating creep testing was 72 days. The creep test was conducted for LHHPC specimens maintained in a moist condition (100% humidity, not immersed). A creep frame was used for the test and a load cell was used to maintain the compression load during the creep test, as shown in Figure 10. The specimens were fitted with bonded foil strain gauges to continuously monitor creep and specimen loading for the duration of the test. Figure 11 presents the optimized LHHPC corrected average creep test results up to one year, as per ASTM C 512 requirement.

The data presented in Figure 11 includes the average measured strain values for all strain gauges mounted on the two test specimen which are subject to the creep force. These values are labelled as “Test Average”, the average measured strain values for all strain gauges mounted on the two control specimen, which are subjected to the same ambient conditions (100% humidity in air), but with no applied force. The strain measurements for the control specimens, labelled as “Control Average”, show expansion, likely due to the uptake of free moisture. The strain measurements for the test specimens show compression deformation, both plastic and to some extent elastic, due to the applied axial force on the specimens.

Also shown in Figure 11 is the corrected creep strain labelled as “Test Average Corrected”, which is calculated by subtracting the control average strain from the test average strain. This

value shows the true deformation strain on the specimens due to the applied force, which must also overcome the expansion shown in the non-stressed control specimens.

When compared to the creep data reported in the previous LHHPC project, the overall trends in the data are similar. To be noted that there are differences between the previous work and the current work in terms of sample curing prior to initiating the creep test and the condition of the LHHPC samples during the creep test. In the previous work, the LHHPC samples were tested after 72 days curing in two (2) reference waters: distilled water and SR-270 water and the test samples were submerged in the appropriate curing solution for the duration of the creep test. In the current work the LHHPC samples were tested after 72 days moist curing and the test samples were maintained in a moist condition for the duration of the creep test. There are some notable differences between the creep test results for the optimized LHHPC samples available to date. In the early ages of the current project, the average corrected creep value is approximately -1350 microstrain (με), which is significantly higher than the -550 με previously reported at the same age. This is largely due to the much higher strain measurements in the control specimens that are factored into the corrected creep strain values. The data from 2014 shows approximately 400 με at approximately 40 days for the samples stored in distilled water, while the current samples stored in air at 100% humidity show approximately 1250 με. Interestingly, the measured strain in the distilled water control samples in 2014 also achieved approximately 1250 με, but this did not occur until approximately 100 days had elapsed. It may be too early to determine the cause of the differences in the rate at which expansion has occurred in the control samples in the two test programs. It could be due to the environment in which the control samples have been stored, submerged in distilled water vs stored in air at 100% humidity, or if it is a function or other factors inherent in the concrete. More data are required before drawing any conclusions. Despite the differences in the measured strain values for the control specimens, and the calculated corrected creep strain values, the actual measured creep strain at 40 days for the creep specimens from the two programs is very similar, approximately -100 με. This would indicate that the differences in the control strain data are not related to the mechanical properties of the concrete. The test average results obtained in the two programs are very similar. Additionally, the average corrected data obtained for this project has not significantly changed after 50-60 days. These measured creep strains are comparable with those obtained for the samples submerged in distilled water after 100 days.

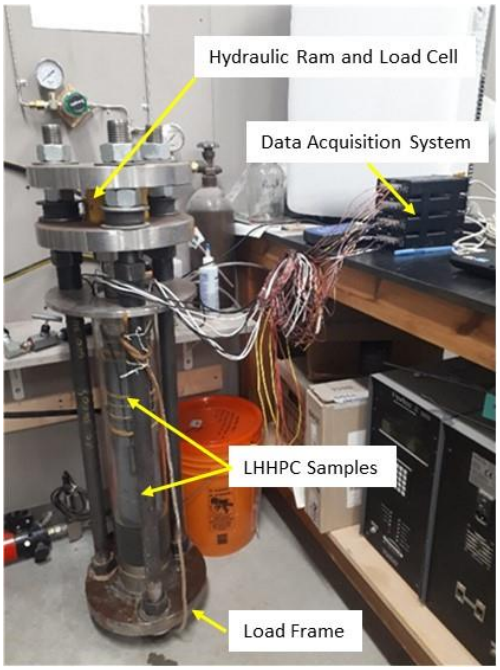

Figure 10: Creep Test Setup

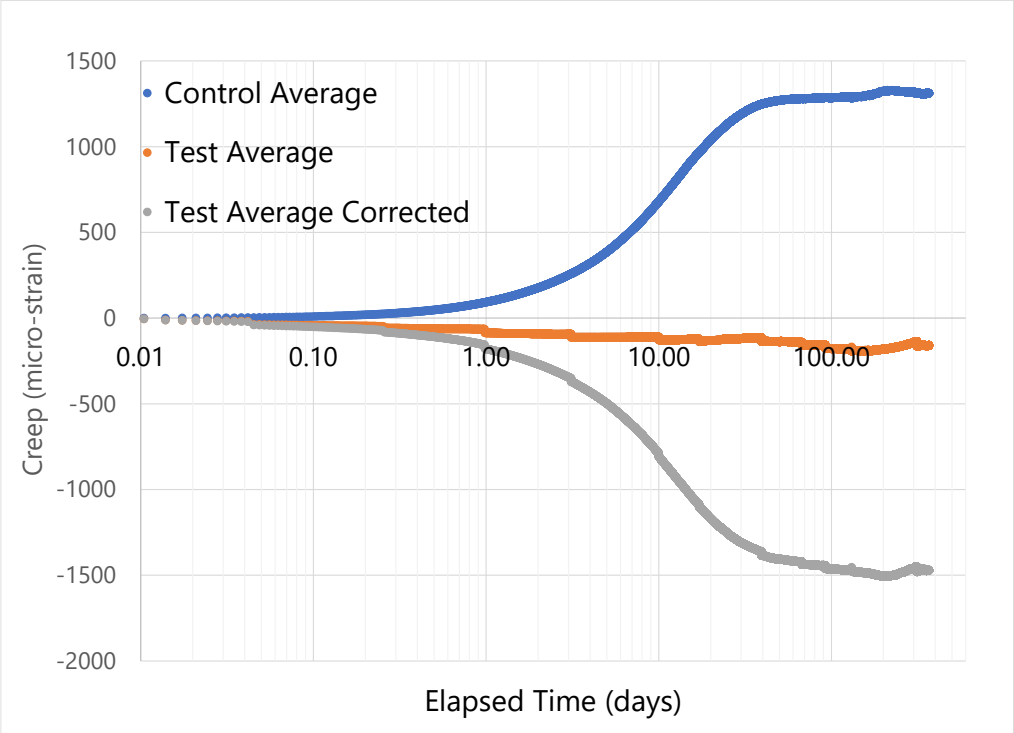

Figure 11: Corrected Average Creep Test Results

6.2.6 Triaxial Compression

Triaxial compression testing was conducted following *ASTM D7012 Compressive Strength and Elastic Modulus of Intact Rock Core Specimens under Varying States of Stress and Temperature* to determine friction angle and adhesion. The test method requires testing at three (3) confining pressures to determine the cohesion and friction angle. The Mohr-Coulomb failure criteria is represented by a linear locus of points on a shear stress versus normal stress plot, where the intercept represents the cohesive shear stress developed along a failure plane and the slope is the tangent of the internal friction angle of the material. Three (3) LHHPC samples were tested at each of four (4) confining pressures: 0 MPa (unconfined), 2 MPa, 7 MPa and 10 MPa, as recommended by NWMO, after 270 days curing in moist environment. Triaxial compression testing was conducted using a servo-hydraulic controlled load frame with 3,500 kN (800,000 lbs) capacity and triaxial pressure control. The test setup utilizes a Hoek bi-axial cell and servo-hydraulic pressurization system to provide confinement for the duration of each test (Figure 12). Table 18 presents the triaxial test results and includes the cohesion and apparent internal angle of friction values determined. Figure 13 presents the Mohr circles obtained from the triaxial tests. The results obtained for the optimized LHHPC are similar to those obtained by Wood for the previous LHHPC seal properties project.

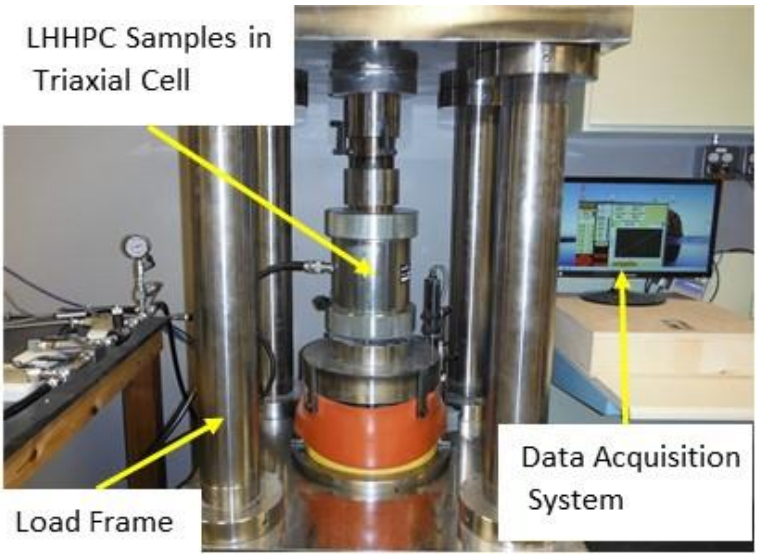

Figure 12: Triaxial Test Setup

Table 18: Triaxial Test Results

Test Age	No. of samples tested	Confining pressure, Sigma 3	Failure stress		Density		Intercept, apparent cohesion	Internal angle of friction
			Average	St. Dev.	Average	St. Dev.		
days		MPa	MPa	MPa	kg/m^3	kg/m^3	MPa	deg.
270	3	0	87.25	0.69	2,424	2.06	20	42.30
270	3	2	100.52	3.76	2,462	1.68		
270	3	7	126.32	3.43	2,463	5.80		
270	3	10	137.28	4.28	2,463	3.01		

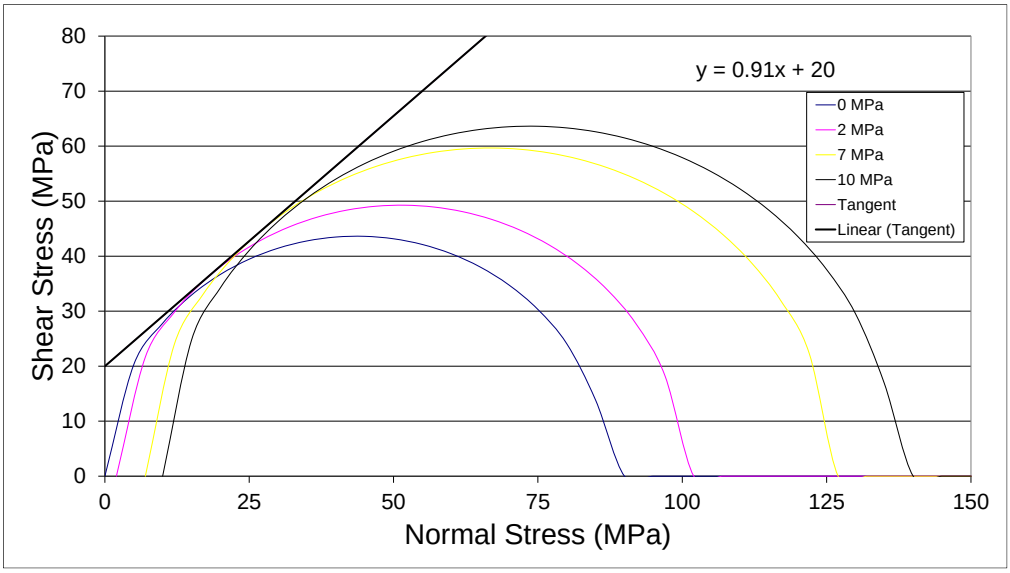

Figure 13: Mohr Circles Obtained From Triaxial Tests

6.2.7 Saturated Hydraulic Conductivity

Saturated hydraulic conductivity tests were conducted following a modified version of *ASTM D5856 Standard Test Method for Measurement of Hydraulic Conductivity of Porous Material Using a Rigid-Wall, Compaction-Mold Permeameter*. Three (3) LHHPC samples were tested after 180 days curing in a moist environment and using two (2) reference waters (CR-10 and SR-270 in Table 5). The general configuration of the hydraulic conductivity test cell was modified from the linear flow configuration to a radial flow configuration to address issues with leakage along the interface between the specimen and cell wall. Wood's permeameter utilizes radial flow through a hollow cylindrical specimen which is compressed and mechanically sealed on the ends with neoprene gaskets. The flow system can adjust the hydraulic gradient between 0 and 16,000 to provide adequate flow measurement with precision of 0.05 ml. The pressure applied for the LHHPC samples was up to ~380 psi (2.62 MPa) and created a hydraulic gradient of 4200. Figure 14 presents a photograph of the radial flow permeameter and hollow cylindrical

specimen, and Figure 15 presents a photograph of the hydraulic conductivity test setup. The hydraulic conductivity test setup described here was originally developed at AECL and successfully used for NWMO's previous LHHPC project work conducted by Wood. All testing equipment available in the Wood Burlington laboratory, which is required to measure the hydraulic conductivity for this project, is composed of materials compatible with the reference CR-10 and SR-270 NaCl water chemistries.

Hydraulic conductivity was determined on triplicate specimens for each reference water. Table 19 presents the test results.

Issues were encountered during testing in the form of spurious readings caused by unstable laboratory temperature. The instability was a result of ongoing building maintenance that resulted in frequent temperature change the laboratory. Changes in laboratory temperature caused small but proportionally significant fluctuation in the volume of the hydraulic conductivity cells when compared to the volume of flow being measured. This volume change in the cell resulted in readings that could not for certain be attributed to flow into or through the test specimens. The flow measuring systems were bypassed during this time to prevent damage. The pressure and flow were maintained but not measured. The issue has not been fully resolved, but the effect has been partially mitigated by increasing the gradient to increase water flow and to make the effect of volume change less significant.

Hydraulic conductivity was normally determined once steady state flow has been achieved in the test specimen, i.e., outflow rate is approximately equal to the inflow rate. However, with cementitious materials, and especially materials containing high proportions of supplementary cementing materials, steady state flow can be difficult to achieve due to continued hydration of cement as water is forced into the concrete. This condition was observed in previous work with the original reference LHHPC mix design and continued with this testing. In every case, the hydraulic conductivity determined by inflow volume was typically higher than that determined by outflow volume. In addition, hydraulic conductivity decreased throughout the test from start to finish, again, often by one or more orders of magnitude. Another property of high performance concrete is that flow on the downstream side of the specimen is often negative, meaning that the concrete is taking on water. This occurs for a period of time, dependant of the hydraulic conductivity and imposed gradient, until the specimen becomes fully saturated, at which time through flow can be achieved. This was observed with the current samples, and previous work on LHHPC and other concrete formulations, even under hydraulic gradients of more than 5000 across the 62.5 mm wall of the hollow cylindrical specimen. In this series of tests, each test specimen gained mass ranging between 6 and 24 grams during the test, showing storage or consumption of water. The samples from the third set tested, where the pressure applied for the LHHPC samples was 380 psi (2.62 MPa) presented the higher mass gain.

This phenomenon complicates presentation of the hydraulic conductivity (k) data. Typically, only positive values of k would be presented. However, this may not truly reflect the properties of the materials. Table 19 shows inflow and outflow k values where flow was positive. However, also presented is the average k value for the entire duration of each test. In the second case, the outflow k values are lower. This indicates that the hydraulic gradients applied during the test were insufficient to pass water through the system. At some locations in the wall of the samples, flow was not occurring.

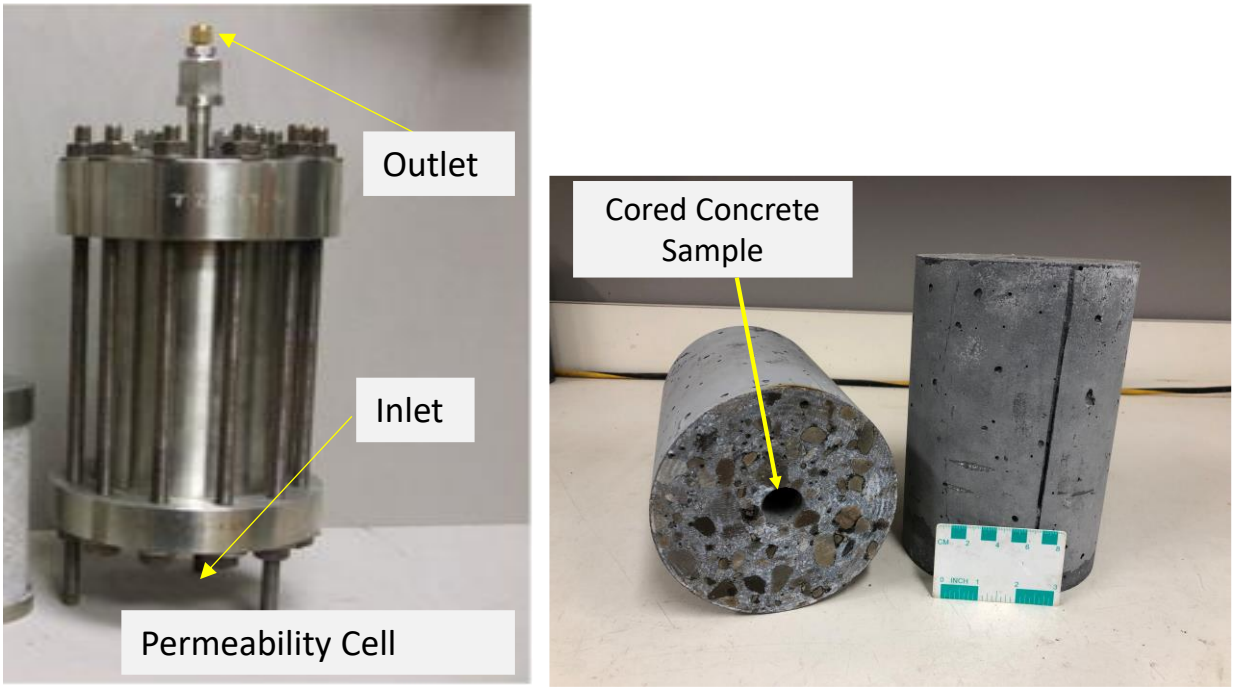

Figure 14: Radial Flow Permeameter and LHHPC Sample

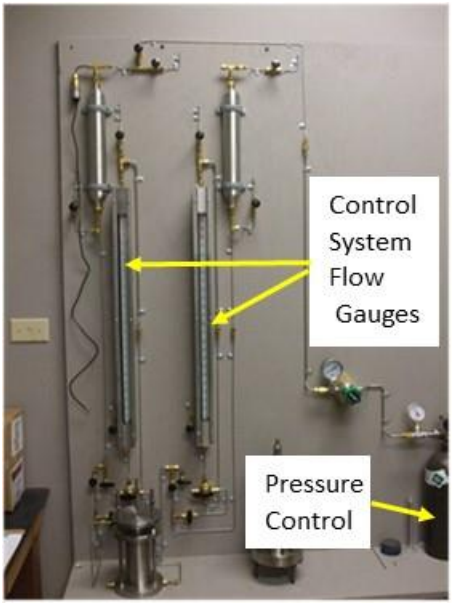

Figure 15: Hydraulic Conductivity Test Setup

Table 19: Hydraulic Conductivity Results in m/s

		Permeability coefficient k (m/s)				
		Target <1 x 10^{-12} m/s				
No.	**Sample Log No.**	**Reference water**	**Inflow k positive values only**	**Outflow k positive values only**	**Inflow k all values**	**Outflow k all values**
1	C1264-20A	CR-10	1.55 x 10^{-13}	7.68 x 10^{-15}	1.46 x 10^{-13}	7.68 x 10^{-16}
2	C249-21B	CR-10	7.99 x 10^{-14}	3.30 x 10^{-16}	7.99 x 10^{-14}	-6.68 x 10^{-15}
3	C249-21A	CR-10	5.89 x 10^{-14}	5.87 x 10^{-16}	5.89 x 10^{-14}	-1.59 x 10^{-15}
	Average	CR-10	7.79 x 10^{-14}	2.87 x 10^{-15}	9.49 x 10^{-14}	-2.50 x 10^{-15}
	St. Dev.	CR-10	5.05 x 10^{-14}	4.17 x 10^{-15}	5.55 x 10^{-14}	-1.59 x 10^{-15}
4	C1264-20B	SR-270	6.81 x 10^{-14}	7.87 x 10^{-15}	3.27 x 10^{-13}	6.20 x 10^{-15}
5	C249-21D	SR-270	4.25 x 10^{-14}	1.32 x 10^{-15}	4.01 x 10^{-14}	2.50 x 10^{-15}
6	C249-21C	SR-270	4.93 x 10^{-14}	2.01 x 10^{-15}	4.44 x 10^{-14}	1.49 x 10^{-15}
	Average	SR-270	5.33 x 10^{-14}	3.73 x 10^{-15}	1.37 x 10^{-14}	1.73 x 10^{-15}
	St. Dev.	SR-270	1.33 x 10^{-14}	3.60 x 10^{-15}	1.64 x 10^{-14}	4.36 x 10^{-15}

6.2.8 Maximum Temperature Rise (Heat of Hydration) and Shrinkage Rate

Although standard test methods exist to measure the heat of hydration in concrete by monitoring the maximum temperature rise (for example *CSA A23.1-10C Accelerating the curing of concrete cylinders and determining their compressive strength*), experience has shown that the standard methods are not representative for mass concrete, as in the case of the application for a DGR. Also, USACOE's test method *CRD-C 38-73 Method of Test for Temperature Rise in Concrete* is dated 1973 and it has not been revised since to account for more suitable insulating materials, temperature measurement devices, etc. To simulate actual in-situ conditions more closely, the heat of hydration and strain measurement is conducted in proven semi-adiabatic curing boxes that closely replicate the curing regimes present in mass concrete structures. This non-standard test method has proven to be superior to *ASTM C1698 Standard Test Method for Autogenous Strain of Cement Paste and Mortar* during research conducted at AECL in 1996 - 1997 as the increased mass of the sample (68 kg vs. 14 kg for C1698) and additional thickness of insulation (300 mm as opposed to 50 mm for C1698) more closely replicates the heat energy profiles of mass concrete.

The curing box for this study encloses one cubic foot (0.03 cubic meters) of concrete with one foot (0.3 meters) of high-density foam insulation on all sides. This arrangement retains the heat generated by the cement hydration to simulate the conditions of a mass structure. This test set up allows measuring both temperature and shrinkage for LHHPC. Strain and temperature are monitored by vibrating wire strain gauges fitted with integral thermistor temperature sensors. One (1) 30-liter sample is used for heat of hydration and strain measurement. This test method has been successfully used for the previous LHHPC studies. Two (2) one cubic foot specimens were used to measure both temperature rise and shrinkage rate for LHHPC. Temperature rise was measured up to 7 days. It should be noted that the maximum temperature rise is an early age property occurring typically within the first 72 hours from mixing. Beyond this point, there is a continual decrease in temperature to ambient, which is dependent on the insulation properties of the curing environment. The maximum temperature is likely reached within seven (7) days of casting. Therefore, it is not recommended to monitor the temperature beyond 7 to 14 days.

The temperature monitoring is stopped when the samples show no increase in temperature for 48 hours and/or have cooled to within 5°C of ambient.

Figures 16 and 17 show photographs of the steel box instrumented with strain gauges, which was used for temperature rise and shrinkage measurements, before placing LHHPC and after filling the box with LHHPC, respectively. As shown in Figure 18, the optimized LHPPC maximum temperature rise is 9.9 to 10.2°C and optimized LHPPC samples met the maximum temperature rise performance target in Table 2.

Figure 19 presents the linear strain change values for the optimizes LHHPC. The figure shows that strain initially followed the heat of hydration, and once the concrete had cooled, it followed the ambient temperature of the laboratory. Strain reached as high as 55 microstrain (55 με = 0.0055%) at peak hydration temperature, but it returned to below 100 microstrain (100 με=0.01%). The final shrinkage results at 345 days meet the performance target in Table 2. The maximum expansion strain (within the first 7 days) of 55 με corresponds to a total volumetric increase of 0.017%, and the maximum shrinkage strain at 345 days at ambient temperatures (-160 με and -211 με) corresponds to a total volumetric decrease of 0.048% and 0.063%, respectively.

Figure 16: Temperature Rise and Shrinkage Box before Placing LHHPC, Showing Vibrating Wire Strain Gauge and Temperature Thermistor (yellow)

Figure 17: Temperature Rise and Shrinkage Box after Placing LHHPC Test Setup (30 cm Concrete Cube (Dark) Surrounded by 30 cm Insulation on All Sides (Pink)

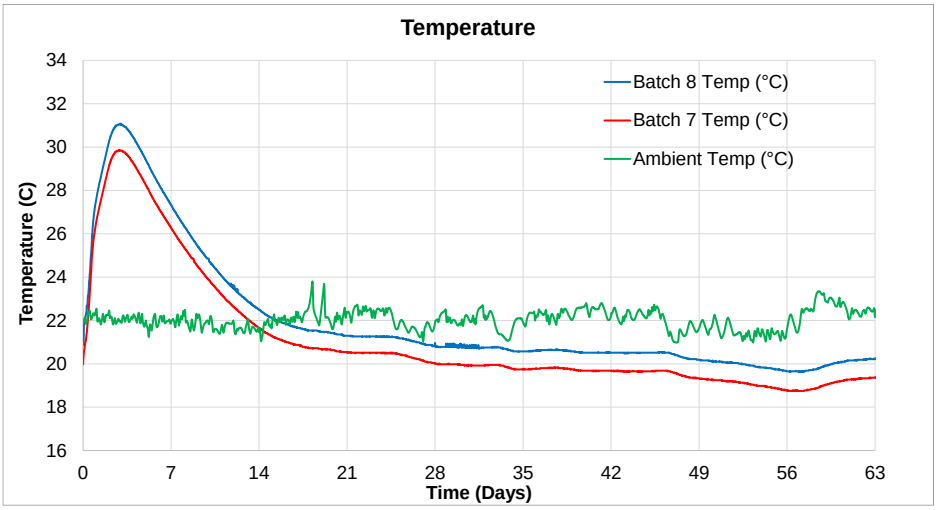

Figure 18: Temperature Rise over Time

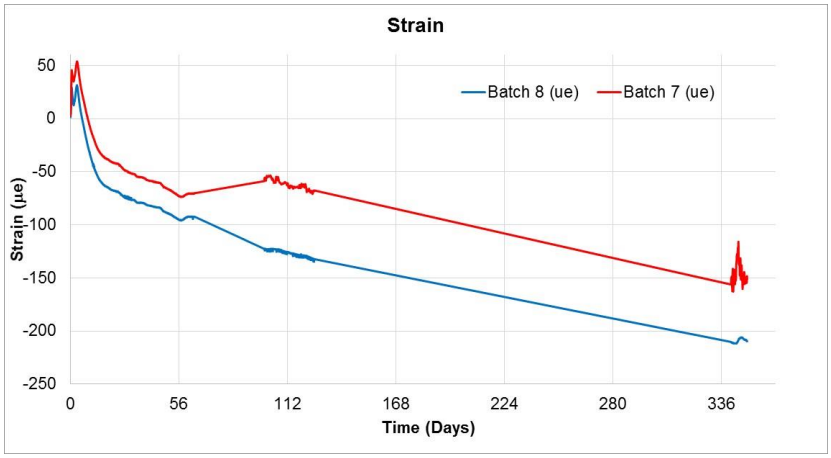

Figure 19: Shrinkage Strain Data

6.2.9 pH

pH of the LHHPC mixtures for this project was measured using the ex-situ leaching protocol as defined in Alonso et al. (2012). The ex-situ leaching method consists of grinding a sample of the LHHPC material to a fine powder and mixing it with CO_2 free deionized water at a mass ratio of 1:1. The suspension is protected from atmospheric CO_2 for the duration of the mixing and pH measurements. The pH measurements are made in the suspension and in the filtered water recovered from the suspension, with both values reported. The "Buffer pH" is the recorded measurement of the standard pH 10 buffer used to confirm calibration of the equipment prior to measuring the solutions. The standard pH 10 buffer should measure 10.05 at 21 °C. pH is measured for three (3) optimized LHHPC samples after curing in moist environment at 7, 28, 56, 90, 180 and 270 days. pH testing is conducted using three (3) types of water: distilled water and two (2) reference waters CR-10 and SR-270 (prepared as detailed in Section 5).

Figures 20 and 21 show up to 270-day average slurry pH and average filtered pH test results. An additional set of three 90-day pH measurements were obtained by Wood for quality assurance, as verification tests. Table 20 presents 90-day test results, including the verification test results. 90-day pH results met the performance target in Table 2.

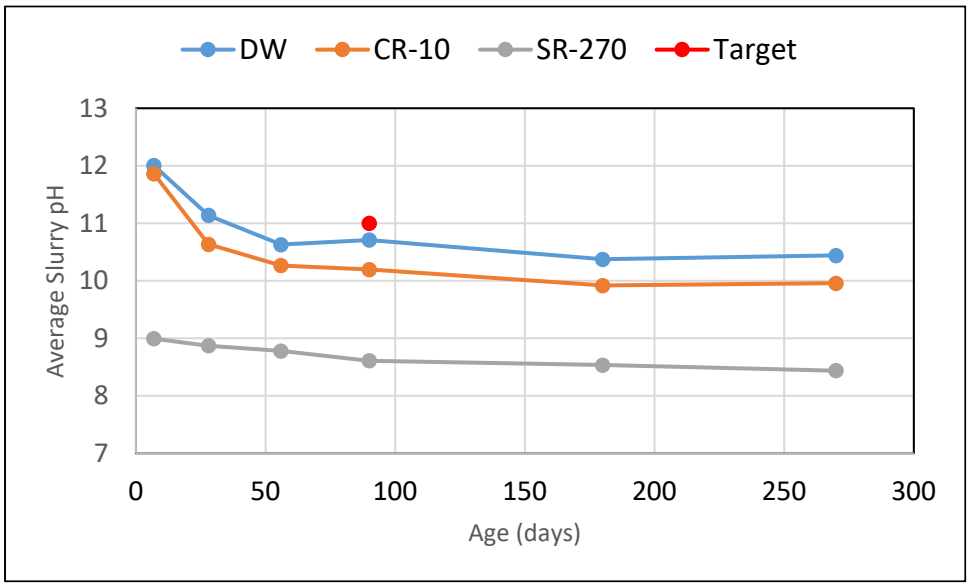

Figure 20: Average Slurry pH Results

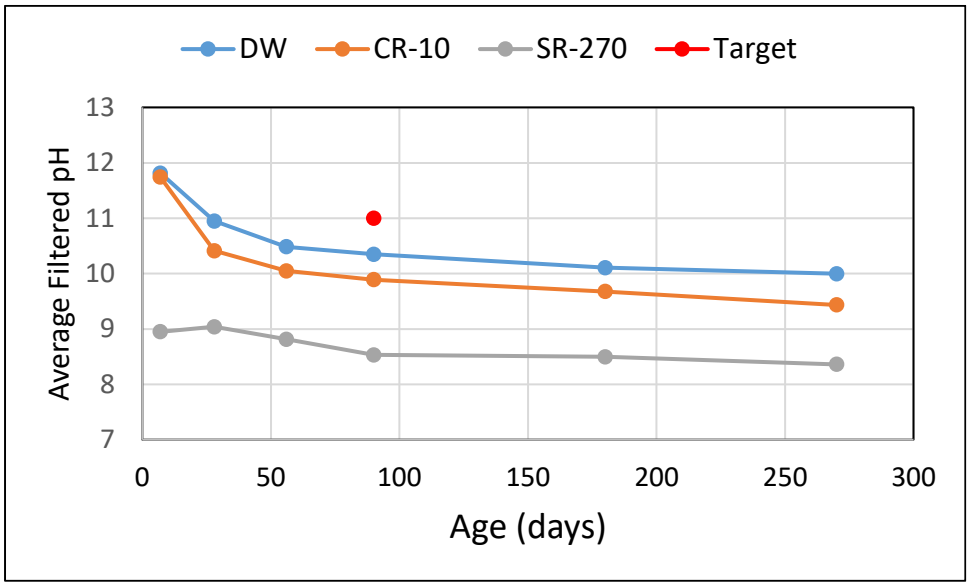

Figure 21: Average Filtered pH Results

Table 20: 90-day pH Test Results

Type of water	Deaerated Distilled Water		CR-10 Water		SR-270 Water	
	Target pH at 90 days ≤11 (preferably 9-10)					
	Average Slurry pH	Average Filtered pH	Average Slurry pH	Average Filtered pH	Average Slurry pH	Average Filtered pH
Test Program	10.71	10.35	10.20	9.89	8.61	8.53
Verification	10.61	10.44	10.21	9.99	8.66	8.63

It is noted that the pH values for the CR-10 and SR-270 waters are consistently lower than that measured using deaerated distilled water. This is likely because the various salts present in the CR-10 and SR-270 waters act to buffer the solution, in effect resisting the rise in pH values. In addition, the magnesium present in both the CR-10 and SR-270 waters reacts with the hydroxide from the LHHPC (both alkali hydroxides and calcium hydroxide) to form brucite ($Mg(OH)_2$), which has a very low solubility. Precipitation of brucite depletes the solution of hydroxyl ions. As the SR-270 water has significantly more salts and contains much more magnesium than the CR-10 water, the buffering and brucite precipitation are expected to be more pronounced.

6.2.10 Slump and Slump Flow Retention

Slump and slump flow were measured following ASTM C143/C143M *Standard Test Method for Slump of Hydraulic-Cement Concrete* and ASTM C1611/C1611M *Standard Test Method for Slump Flow of Self-Consolidating Concrete*, respectively, at the following ages, assuming that the LHHPC would be placed in the DGR within two (2) hours (120 minutes):

- 0 minutes (“time 0”, initial slump), 20 minutes, 40 minutes, 60 minutes, 90 minutes and 120 minutes after mixing, with no additional mixing after “time 0”, or “static”.
- 0 minutes (“time 0”, initial slump), 20 minutes, 40 minutes, 60 minutes, 90 minutes and 120 minutes after mixing, with additional mixing at each interval after “time 0”, or “remixed”. These slump and slump flow measurements were proposed due to the fact that it is known that additional mixing can maintain some of the plastic properties of concrete and increase slump retention over time compared to slump retention without further mixing after “time 0”. Therefore, additional mixing and higher slump retention can be beneficial for placement of LHHPC in the DGR.

According to ASTM C143 to measure slump, a sample of freshly mixed concrete is placed and compacted by rodding in a mold shaped as the frustum of a cone. The mold is raised, and the concrete allowed to subside. The vertical distance between the original and displaced position of the center of the top surface of the concrete is measured and reported as the slump of the concrete (Figure 22).

According to ASTM C1611 to measure slump flow, a sample of freshly mixed concrete is placed in a mold either in the upright or inverted position. The concrete is placed in one lift without tamping or vibration. The mold is raised, and the concrete is allowed to spread. After spreading

ceases, two diameters of the concrete mass are measured in approximately orthogonal directions. Slump flow is the average of the two diameters (Figure 23).

Figure 22: Slump Measurement

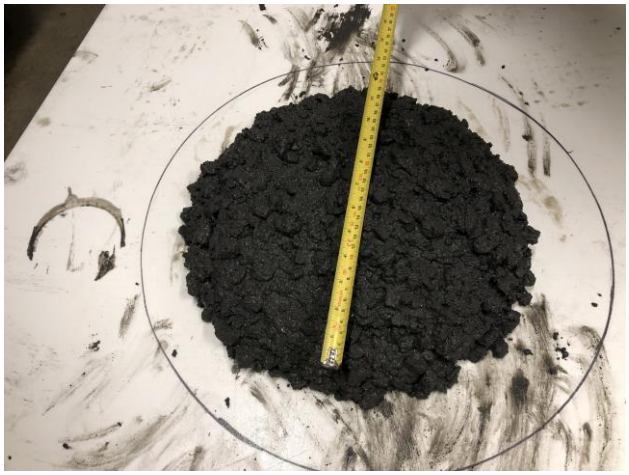

Figure 23: Slump Flow Measurement

Slump, or slump flow retention, represents the slump, or slump flow respectively, measured at a certain time after “time 0” and expressed as a percentage of the initial slump. Rheology tests as discussed in the following section were also conducted for the mixes used for slump and slump flow retention tests.

Table 21, Figures 24 and 25 present slump and slump flow test results, respectively. Since the “static” slump and slump flow retention results obtained after 120 minutes did not meet the performance requirements in Table 2 an additional batch was prepared to repeat the “static” tests, named “static repeat”. Although the initial slump and slump flow of the mix used for the “static” slump and slump flow reported in Table 21 met the performance target for slump and slump flow in Table 2 measurements, a LHHPC batch with a higher initial slump (10 in) was

prepared and used for “static repeat” tests. This LHHPC mix met the slump and slump flow retention targets. After taking the 120-minutes measurements, additional slump and slump flow measurements were taken after remixing for 1 minute. Remixing after 120-minutes had a beneficial effect on both slump and slump flow retention, as shown in Table 21 and Figures 24 and 25.

Table 21: Slump and Slump Flow Retention Results

No.	Static (no additional mixing)	Remix (additional mixing, 1 min.)	Age	Slump		Slump retention	Slump flow		Slump flow retention
	Log No.		min	(mm)	(in)	(%)	(mm)	(in)	(%)
Target performance				150 - 250	~5.9 - 9.8	≥75%	300 - 650	~11.8 - 25.6	≥75%
1	C1160-20		0	222.3	8.75	100.00	355.00	13.98	100.00
2			20	222.3	8.75	100.00	320.00	12.60	90.14
3			40	165.1	6.50	74.29	275.00	10.83	77.46
4			60	171.5	6.75	77.14	305.00	12.01	85.92
5			90	158.8	6.25	71.43	290.00	11.42	81.69
6			120	114.3	4.50	51.43	240.00	9.45	67.61
1	C1227-20		0	254.0	10.00	100.00	405.00	15.94	100.00
2			20	235.0	9.25	92.50	385.00	15.16	95.06
3			40	222.3	8.75	87.50	370.00	14.57	91.36
4			60	222.3	8.75	87.50	370.00	14.57	91.36
5			90	215.9	8.50	85.00	360.00	14.17	88.89
6			120	209.6	8.25	82.50	365.00	14.37	90.12
7	C1227-20	C1227-20	120	241.3	9.50	95.00	380.00	14.96	93.83
1		C1141-20	0	241.3	9.50	100.00	410.00	16.14	100.00
2			20	241.3	9.50	100.00	430.00	16.93	104.88
3			40	247.7	9.75	102.63	475.00	18.70	115.85
4			60	260.4	10.25	107.89	465.00	18.31	113.41
5			90	254.0	10.00	105.26	455.00	17.91	110.98
6			120	260.4	10.25	107.89	440.00	17.32	107.32

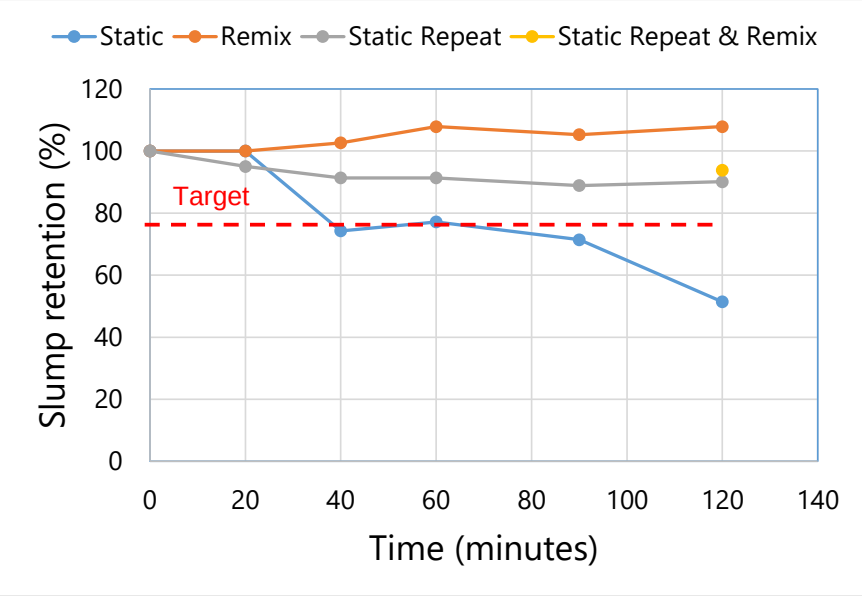

Figure 24: Slump Retention Results

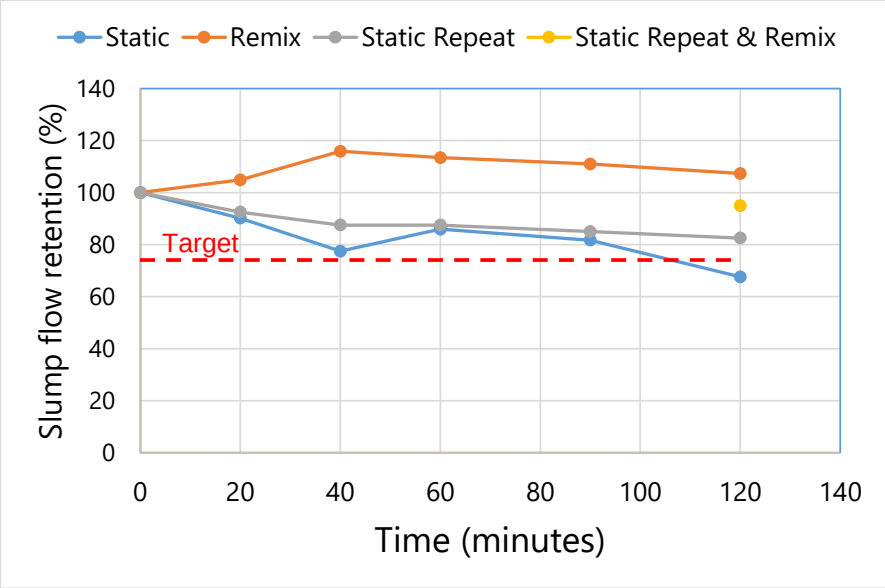

Figure 25: Slump Flow Retention Results

6.2.11 Rheology

Rheological properties, such as yield stress and viscosity, are indicative of the pumpability of the LHHPC mix when placed in a DGR.

Fresh concrete can be considered as a fluid, which means that it will flow under the action of shear stresses (Ferraris 1999). The flow behavior of concrete can be represented by the following two-parameter relationship $\tau=\tau_0 + \mu\dot{\gamma}$, which is known as the Bingham model (Figure 23). The parameter τ_0 is the yield stress, and it represents the shear stress required to initiate flow. The slope of the line is the plastic viscosity, μ, and it affects the resistance to flow after the

yield stress has been surpassed. These two parameters, which define the flow curve, provide a complete description of the flow behavior of a concrete mixture.

Concrete, however, is not a simple fluid because it displays thixotropic behavior. This behavior means that the shear stress required to initiate flow is high when the concrete has been in an "at rest" condition, but a lower shear stress is needed to maintain flow once it has begun. This type of behavior is summarized in the schematic plot shown in Figure 27, which shows the variation in shear stress with time for the case of a slowly applied shear strain. At the start, the shear stress increases gradually with time but there is no flow. When the stress reaches the static yield stress, the concrete begins to flow, and the stress required to maintain flow is reduced to the dynamic yield stress (Figure 27). If the applied shear strain is removed and the concrete is allowed to rest, inter-particle forces create a weak framework that restores the static yield stress. With time, the static and dynamic yield stresses increase as the effectiveness of water-reducing admixtures diminish and hydration proceeds, which is commonly referred to as "slump loss." A high static yield stress is desirable because it reduces formwork pressure and increases the resistance to segregation. But for ease of pumping, placement, and self-consolidation, a low dynamic yield stress is necessary.

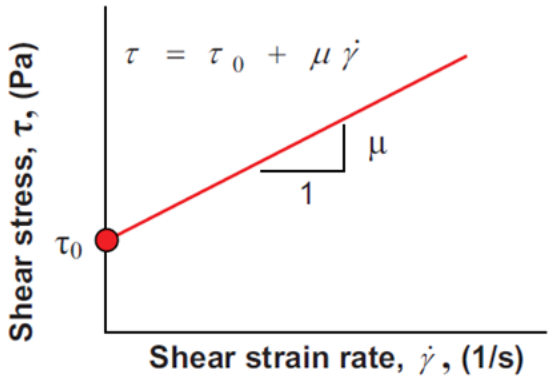

Figure 26: Bingham Model

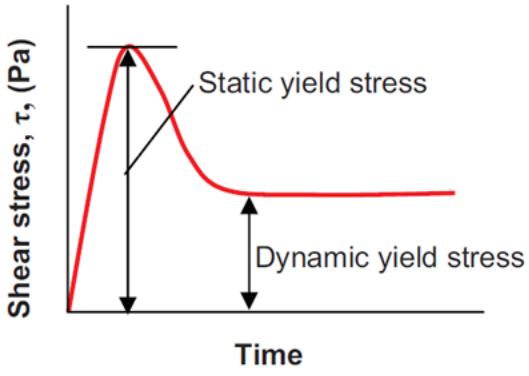

Figure 27: Thixotropic Behavior

Rheology tests were conducted for the plastic optimized LHHPC mixes used for slump and slump flow retention tests. ICAR rheometer, which is a concrete rheometer with a vane and a container suitable for the maximum size of the coarse aggregate used in LHHPC, was used to conduct rheology tests. Figure 28 presents the rheometer with LHHPC tests in progress. Rheology shear stress versus shear rate curve was obtained during the tests and recorded. The rheological properties were obtained from the corresponding shear stress – shear rate plots. Figure 29 presents typical curves generated during the rheology tests.

There are no standard or industry requirements in terms of yield stress required for pumpable concrete. Although no specific standard is available, cemented paste used for backfilling underground stopes in the mining industry is considered to be pumpable for yield stress values of ~250 - 800 Pa and lower yield stress is preferred for pumpability (Boger et al. 2015). In addition to slump and slump flow the yield stress, along with concrete density and details of the mix design, provides useful information for mechanical engineers who specialize in pump design and the selection of suitable pumps for a project. However, it is known that there is a relationship between slump and yield stress, as well as between slump flow and yield stress. Figures 30 and 31 present the relationship between the Bingham yield stress and slump, or slump flow for the optimized LHHPC mixes, respectively. The Bingham yield stress and slump, or slump flow are inversely proportional. For example, the yield stress is higher for lower slump and slump flow measurements. These results agree with the industry experience (Ferraris et al. 2001). The results in Figures 30 and 31 suggest that for yield stress values of 250 – 800 Pa the corresponding slump and slump flow ranges are ~175 – 250 mm and 300 – 400 mm, respectively.

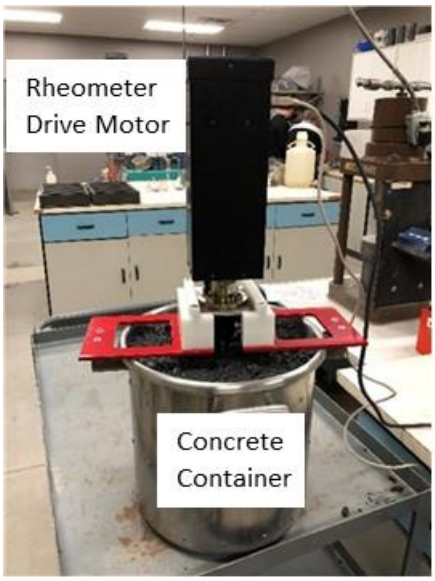

Figure 28: Rheometer and LHHPC Rheology Test in Progress

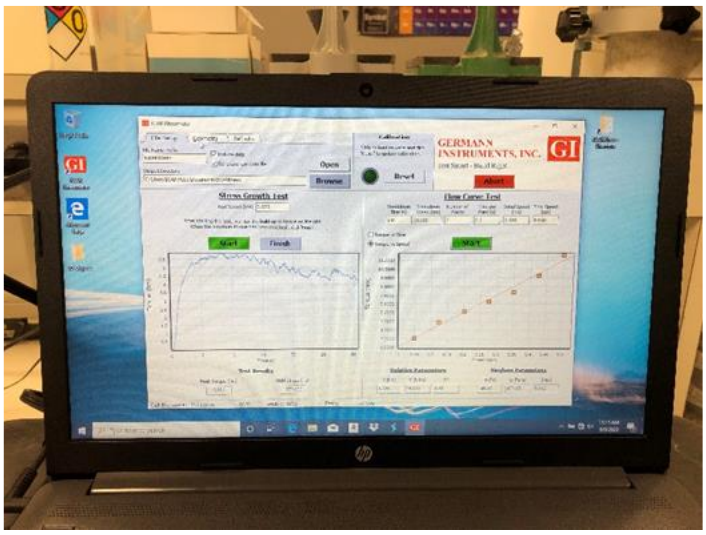

Figure 29: Typical Graphs Generated during the Rheology Tests

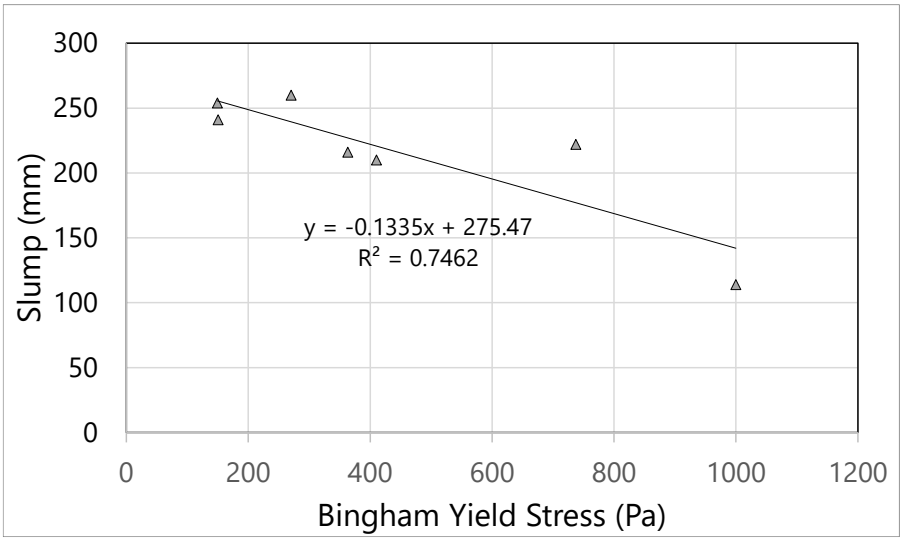

Figure 30: Typical Graphs Generated during the Rheology Tests

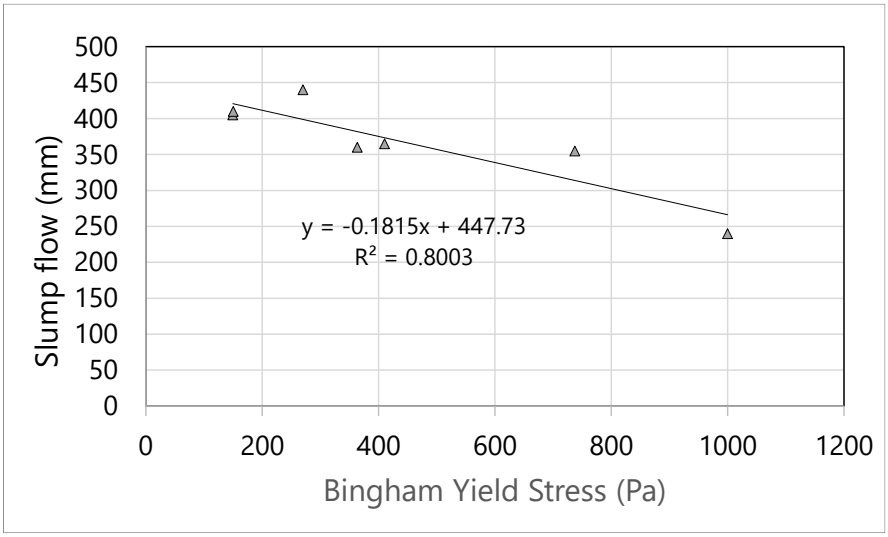

Figure 31: Typical Graphs Generated during the Rheology Tests

6.2.12 Thermal Conductivity

Thermal conductivity testing follows *ASTM WK49591 New Test Method for Determining Thermal Conductivity and Thermal Diffusivity Using the Transient Plane Source or Hot Disc Method*. Along with thermal conductivity, thermal diffusivity and specific heat are also determined with this test method, although not specifically required for the project. Thermal conductivity testing was performed by RESPEC in Rapid City, South Dakota, USA. Three (3) specimens with ground ends and with 3 in (~76 mm) diameter and lengths between 1.5 in and 2 in (~38 mm and 51 mm) are used to measure thermal conductivity at 7, 28, 56, 90, 180 and 270 days after curing in moist environment. Tests were conducted at five (5) temperatures starting at 26ºC and up to 100ºC: 26ºC, 40ºC, 60ºC, 80ºC and 100ºC. This temperature range is relevant for the concrete for the project application, as confirmed by NWMO. As the outside temperature of the used fuel container will not exceed 100ºC, the concrete used in the placement room floor may reach up to 100ºC. Thermal conductivity is determined using a hot disk thermal analyzer connected to a computer with Hot Disk Thermal Analyzing software installed, an oven capable of heating up to 300°C with the option of using computer control or manual control with adjustable ramp rate and transient plane source (TPS) disks of suitable size for samples being tested (Figure 32). Figure 33 presents details of the sample prior to being tested.

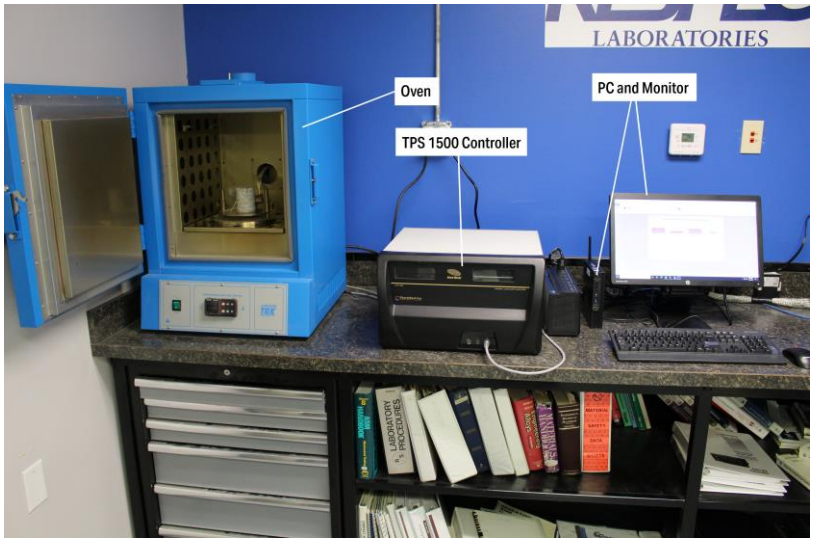

Figure 32: Hot Disk Test Setup

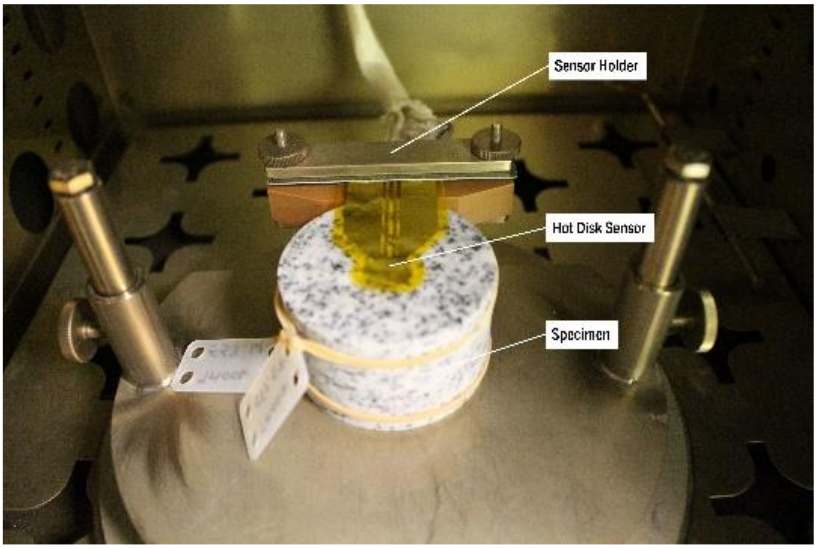

Figure 33: Sample Prior to the Hot Disk Test

Figures 34 and 35 present up to 270-day thermal conductivity test results. The test results suggest that thermal conductivity increases over time regardless of the measuring temperature. While the test results obtained for the lower temperatures show similar trends, the results obtained at 100°C are different from the rest; this is likely due to evaporation and/or boiling of the water in concrete at 100°C. Therefore, one should be cautious about the validity of the test results at 100°C.

The thermal conductivity results obtained to date range between ~3.0W/mK and ~3.4W/mK. Thermal properties identified in the literature and measured at 25°C range between 0.1 – 0.3 W/mK for lightweight concrete (~1400 – 1800 kg/m^3) and 1.0 – 1.8 W/mK for dense concrete (> 3000 kg/m^3) from https://www.engineeringtoolbox.com/thermal-conductivity-d_429.html. ACI

207.2R includes a list of normal density concrete (2360-2552 kg/m^3) structures using various types of coarse aggregates, where thermal conductivity results cover a broad range between 1.63 W/mK and 3.68 W/mK.

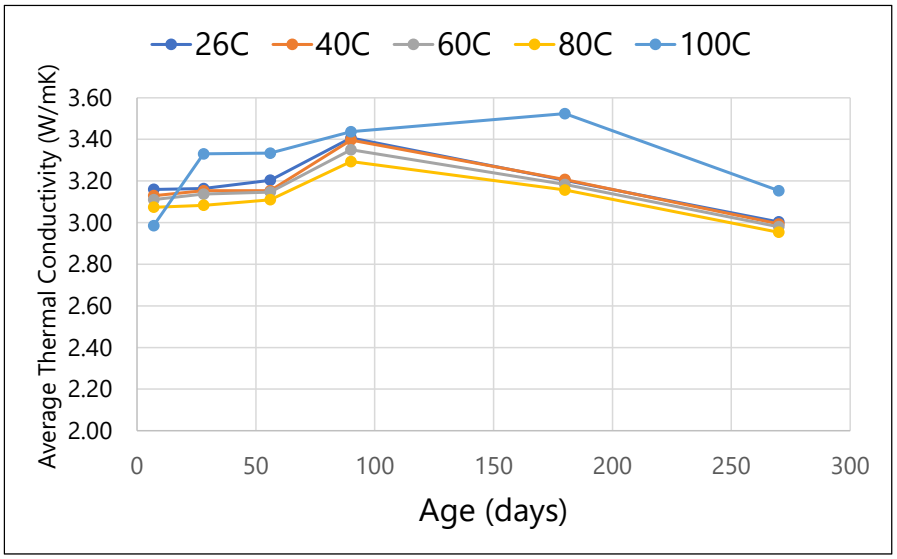

Figure 34: Thermal Conductivity Results over Time as a Function of Temperature

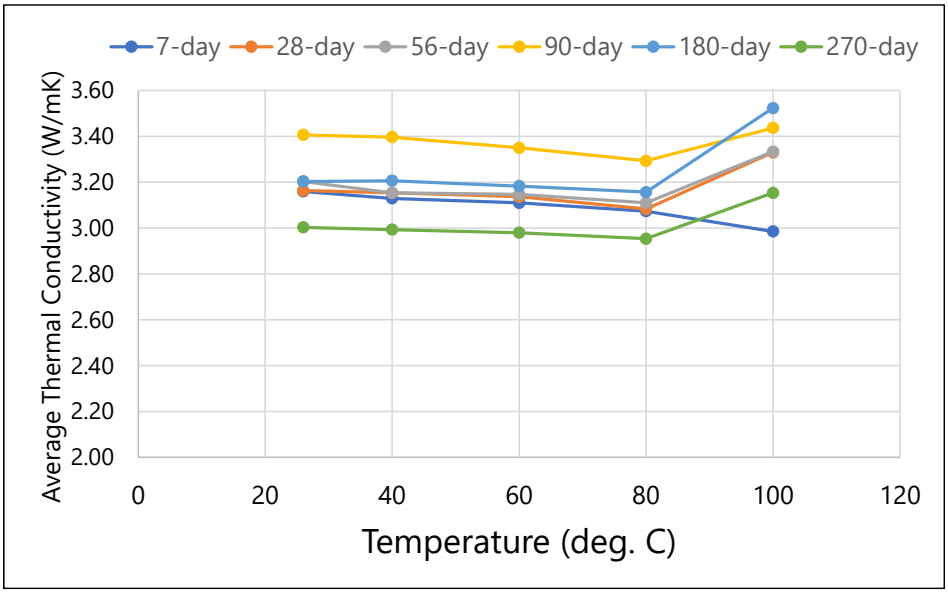

Figure 35: Thermal Conductivity Results per Temperature as a Function of Time

6.2.13 Additional Thermal Conductivity Tests

Additional thermal conductivity testing was initiated upon completion of 90-day thermal conductivity tests due to limited information available regarding the thermal conductivity of concrete in general, and particularly no information available regarding LHHPC. The objectives of the additional thermal conductivity tests were the following:

- To verify the LHHPC thermal conductivity tests available to date.
- To understand the repeatability of the LHHPC tests.
- To compare the LHHPC thermal conductivity with that of other more common types of concrete, such as normal strength concrete (NSC) and high performance concrete (HPC).

Three materials were prepared in the laboratory for the test program: optimized LHHPC, NSC and HPC, Table 22 presents the mix designs for LHHPC, NSC and HPC. In order to limit the number of variables, the mix ingredients used for these materials were the same as those used for the LHHPC and the mixes were appropriately designed for the NSC and HPC. Therefore, the same type and sources of cement, fine and coarse aggregate were used for NSC, HPC and LHHPC. HPC used silica fume from the same source selected for the optimized LHHPC.

Table 22: LHHPC, NSC and HPC Mix Designs and Plastic Properties

Mix Ingredients	Optimized LHHPC Mix Design (kg/m^3)	NSC Mix Design (kg/m^3)	HPC Mix Design (kg/m^3)	Ingredient Source
Cement	95.6	320	425	Type GUL, St. Marys
Silica fume	95.6	-	75	Norchem USA
Silica flour	190.0	-	-	US Silica
Sand	911.1	912	760	Natural concrete sand from Lafarge, Cambridge, Ontario
Coarse aggregate	1060.9	1015	980.7	Concrete stone from carbonate and crystalline pits, Lafarge, Cambridge, Ontario
Superplasticizer (dry mass)	6.7	0.008	0.613	MasterGlenium 7500, polycarboxylate-based BASF
Water	113.6	160	160	Tap water
Water-to-cementitious material ratio	0.6	0.5	0.32	-
Plastic air (%)	1.7	1.8	2.2	-
Slump (mm)	210	76.2	76.2	-
Slump flow (mm)	330	-	-	-
Plastic density (kg/m^3)	2,463	2,423	2,418	

NSC, HPC and LHHPC were prepared in laboratory size batches, including triplicate specimens for each of the following tests: 3” x 6” (75mm x 150mm) cylinder specimens for thermal expansion, 4” x 8” (100mm x 200mm) cylinder specimens for 28-day compressive strength and

4” x 8” (100mm x 200mm) cylinder specimens for bulk density and porosity tests. For each mix plastic properties were measured, as part of the standard procedure, such as plastic air following *ASTM C173 Standard Test Method for Air Content of Freshly Mixed Concrete by the Volumetric Method*, slump following *ASTM C143/C143M Standard Test Method for Slump of Hydraulic-Cement Concrete* and slump flow following *ASTM C1611/C1611M Standard Test Method for Slump Flow of Self-Consolidating Concrete,* and plastic density determined based on mass and volume measurements (Table 22).

Moist curing is representative for the project application, e.g. the seal materials in the DGR. Therefore, the samples were cured in a moist environment (100% relative humidity (RH)) until prior to the testing age, similar to the optimized LHHPC samples used for the rest of the test program.

28-day UCS, which is a characteristic concrete property was determined following *ASTM C39/C39M Standard Test Method for Compressive Strength of Cylindrical Concrete Specimens*. Table 23 presents UCS results.

Table 23: LHHPC, NSC and HPC UCS

Material Type	UCS (MPa)	
	Average	St. Dev.
LHHPC	69.76	0.53
NSC	48.18	0.80
HPC	98.62	3.19

Bulk density and porosity of hardened, as-fabricated materials were determined following *ASTM C642 Standard Test Method for Density, Absorption, and Voids in Hardened Concrete*. There is data in the literature suggesting that there is a relationship between concrete density and porosity and thermal conductivity (Tinker and Cabrera, 1992) and (Bhattacharjee and Krishnamoorthy, 2004). Therefore, these properties have been included in the test program to compare the results with those in the literature. To be noted that data reported by both (Tinker and Cabrera, 1992) and (Bhattacharjee and Krishnamoorthy, 2004) refers to concrete materials with lower densities and significantly higher porosities than LHHPC. Prior to the UCS tests the cylinder specimens were used for hardened density measurements based on volume (calculated based on length and diameter measurements) and mass. Table 24 presents bulk density, porosity and hardened density results.

Table 24: LHHPC, NSC and HPC Density and Porosity

Material Type	Hardened Density (kg/m^3)		Bulk Density after Immersion & Boiling (kg/m^3)		Apparent Density (kg/m^3)		Porosity (%)	
	Average	St. Dev.	Average	St. Dev.	Average	St. Dev.	Average	St. Dev.
LHHPC	2,440	18	2,475	9.27	2,531	9.97	3.67	0.07
NSC	2,417	11	2,461	2.55	2,461	4.54	9.59	0.23
HPC	2,421	3	2,453	1.53	2,453	2.57	5.11	0.10

Thermal conductivity testing of the LHHPC, NSC and HPC samples prepared for the additional thermal conductivity tests was conducted by RESPEC and followed *ASTM WK49591 New Test Method for Determining Thermal Conductivity and Thermal Diffusivity Using the Transient Plane Source or Hot Disc Method*. Triplicate specimens were tested per material type at 28 days. Figure 33 and Table 25 present thermal conductivity results, where the LHHPC results obtained in the first round of 28-day tests are labeled LHHPC_R. The test results show similar trends for all the materials tested, with similar NSC and LHHPC results and lower HPC results regardless of the temperature. The additional thermal conductivity test results obtained for the LHHPC samples are in agreement with those obtained in the first round of tests; they confirm the repeatability of the tests, except for those tests conducted at 100°C. As previously pointed out one should be cautious about the validity of the test results at 100°C.

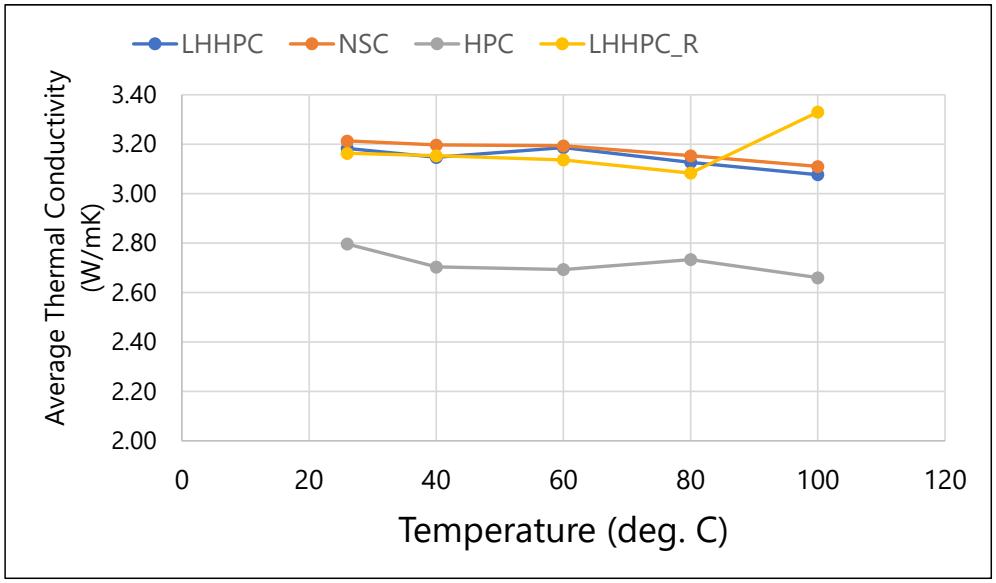

Figure 36: LHHPC, NSC and HPC 28-day Thermal Conductivity Results per Temperature as a Function of Temperature

Table 25: LHHPC, NSC and HPC 28-day Average Thermal Conductivity

		Material Type			
		LHHPC_R	**LHHPC**	**NSC**	**HPC**
Temperature (°C)		**Average Thermal Conductivity (W/mK)**			
26	Average	3.16	3.18	3.21	2.80
	St. Dev.	0.119	0.225	0.221	0.312
40	Average	3.15	3.15	3.20	2.70
	St. Dev.	0.119	0.255	0.180	0.287
60	Average	3.14	3.19	3.19	2.69
	St. Dev.	0.121	0.185	0.160	0.240
80	Average	3.08	3.13	3.15	2.73
	St. Dev.	0.176	0.176	0.162	0.249

		Material Type			
		LHHPC_R	LHHPC	NSC	HPC
Temperature (°C)		Average Thermal Conductivity (W/mK)			
100	Average	3.33	3.08	3.11	2.66
	St. Dev.	0.359	0.191	0.087	0.252

7. SUMMARY OF FINDINGS AND RECOMMENDATIONS

Table 25 presents a summary of the results available to date, which suggest that the optimized LHHPC mix met the relevant performance requirements for up to 270-day parameters in Table 2.

Table 26: Performance of Optimized LHHPC Mixes

No.	Performance Parameters	Performance Target	Performance of Original Reference Mix	Performance of Optimized LHHPC (This Study)
B1	Bulk Density	>2400 kg/m^3	Distilled Water 2442 kg/m^3 (180 days) SR-270 Water 2442 kg/m^3 (180 days)	2535 kg/m^3 (7 days) 2538 kg/m^3 (180 days)
B2	Porosity at 180 days	≤6%	Distilled Water 3.62% SR-270 Water 4.03%	4.62% (7 days) 4.58% (180 days)
B3	Saturated Hydraulic Conductivity	<1 x 10^{-12} m/s	Distilled water Inflow 1.09x10^{-13} m/s Outflow 2.03x10^{-14} m/s SR-270 Water Inflow 2.45x10^{-13} m/s Outflow 2.7x10^{-15} m/s	SR-270 Water Inflow 5.33x10^{-14} m/s Outflow 3.73x10^{-15} m/s CR-10 Water Inflow 9.79x10^{-14} m/s Outflow 2.87x10^{-15} m/s
B4	Unconfined Compressive Strength (UCS)	>25 MPa (7 days) >60 MPa (90 days)	Distilled Water 34.7 MPa (7 days) 84.6 MPa (90 days) SR-270 Water 35.7 MPa (7 days) 83.0 MPa (90 days)	30.5 MPa (7 days) 71.4 MPa (90 days)
B5	Maximum temperature rise at the center of 300-mm-side cubical specimen*	≤15°C over 10 days	Peak of about 15°C over ~80 hours of monitoring	9.9 ºC and 10.2 ºC over 10 days

No.	Performance Parameters	Performance Target	Performance of Original Reference Mix	Performance of Optimized LHHPC (This Study)
B6	Shrinkage rate over 200 days	<1% (volume)	NM	0.048%, 0.063% Average 0.056%
B7	pH at 90 days	≤11, preferably 9 – 10	Canadian Shield Saline Solution (58 g/L) 10.0 (7 days) 9.7 (28 days) 9.3 (90 days)	Distilled Water 10.35 (90 days) CR-10 Water 9.89 (90 days) SR-270 Water 8.53 (90 days)
B8	Slump	200 +/-50 mm provided no bleeding and/or segregation	250 mm with no bleeding/segregation	248 mm with no bleeding/segregation
B9	Slump flow	300 – 650 mm provided no bleeding and/or segregation	530 mm with no bleeding/segregation	408 mm with no bleeding/segregation
B10	Slump and slump flow retention up to 2 hours from the time of mixing	≥75%	NM	Slump retention~83% static, ~108% remix Slump flow retention~90% static, ~107% remix
B11	Free silicon (Si) content in silica fume	<0.075% (by mass)	0. 086%	0.042%

Notes:
NM means “not measured".
*Concrete poured into an insulated box.

Based on the slump and slump flow retention test results, along with the rheology test results (Section 6.2.11), the following revisions to the performance targets for initial slump and slump flow are recommended to be made:

- Slump 220 +30/-20mm provided no bleeding and/or segregation
- Slump flow 400 – 650mm provided no bleeding and/or segregation

Based on the trial batch qualification test results, it is recommended to add the temperature rise test to the existing LHHPC trial batch qualification tests, as maximum temperature rise is one of the key short-term performance parameters.

REFERENCES

REFERENCED STANDARDS

CRD-C 38-73. Method of Test for Temperature Rise in Concrete. U.S. Army Corps of Engineers.

American Society for Testing and Materials Standards (ASTM):

ASTM C39 / C39M-20 Standard. Test Method for Compressive Strength of Cylindrical Concrete Specimens. West Conshohocken, U.S.A.

ASTM C127-15 Standard. Test Method for Density, Relative Density (Specific Gravity), and Absorption of Coarse Aggregate. West Conshohocken, U.S.A.

ASTM C128-15 Standard. Test Method for Density, Relative Density (Specific Gravity), and Absorption of Fine Aggregate. West Conshohocken, U.S.A.

ASTM C136-19 Standard. Test Method for Sieve Analysis of Fine and Coarse Aggregate. West Conshohocken, U.S.A.

ASTM C138/C138M-17a Standard. Test Method for Density (Unit Weight), Yield, and Air Content (Gravimetric) of Concrete. West Conshohocken, U.S.A.

ASTM C143 / C143M-20 Standard. Test Method for Slump of Hydraulic-Cement Concrete. West Conshohocken, U.S.A.

ASTM C469/C469M-14 Standard. Test Method for Static Modulus of Elasticity and Poisson's Ratio of Concrete in Compression. West Conshohocken, U.S.A.

ASTM C512/C512M-15 Standard. Test Method for Creep of Concrete in Compression. West Conshohocken, U.S.A.

ASTM C642-13 Standard Test Method for Density, Absorption, and Voids in Hardened Concrete. West Conshohocken, U.S.A.

ASTM C1365-18 Standard Test. Method for Determination of the Proportion of Phases in Portland Cement and Portland Cement Clinker Using X-Ray Powder Diffraction Analysis. West Conshohocken, U.S.A.

ASTM C1611/C1611M-18 Standard. Test Method for Slump Flow of Self-Consolidating Concrete. West Conshohocken, U.S.A.

ASTM C1698-19 Standard. Test Method for Autogenous Strain of Cement Paste and Mortar. West Conshohocken, U.S.A.

ASTM D5856-15 Standard. Test Method for Measurement of Hydraulic Conductivity of Porous Material Using a Rigid-Wall, Compaction-Mold Permeameter. West Conshohocken, U.S.A.

ASTM D7012-14e1 Standard. Compressive Strength and Elastic Modulus of Intact Rock Core Specimens under Varying States of Stress and Temperature to Determine Friction Angle and Adhesion. West Conshohocken, U.S.A.

ASTM WK49591 Standard. New Test Method for Determining Thermal Conductivity and Thermal Diffusivity Using the Transient Plane Source or Hot Disc Method. West Conshohocken, U.S.A.

Canadian Standards Association (CSA):

CSA A23.1/23.2-19 Standard. Concrete Materials and Methods of Concrete Construction, Test Methods and Standard Practices. Toronto, Canada.

CSA A23.1-10C-19 Standard. Accelerating the Curing of Concrete Cylinders and Determining Their Compressive Strength. Toronto, Canada.

CSA A3004-A5-18 Standard. Rapid Test Method for Determining the Tendency of Silica Fume to Entrap Air in Mortar or Concrete. Toronto, Canada.

OTHER REFERENCES:

ACI 207.2R-07, Report on Thermal and Volume Change Effects on Cracking of Mass Concrete, American Concrete Institute, Farmington Hills, U.S.A., 2007.

Aldea C.-M., B. Shenton, B.J. Cornelius, and H. Leung. 2016. Optimized Low Heat High Performance Concrete Mixes for DGR shaft sealing, Proceedings 3rd Canadian Conference on Nuclear Waste Management, Decommissioning and Environmental Restoration, Ottawa, Ontario, Canada, 11 – 14 September 2016.

Aldea C.-M., B.J. Cornelius, and H. Leung. 2019. Optimization of Low Heat High Performance Concrete Mixes for DGR shaft sealing, Proceedings 4th Canadian Conference on Nuclear Waste Management, Decommissioning and Environmental Restoration, Ottawa, Ontario, Canada, 8 – 11 September 2019.

Alonso, M. C. and J.L. García Calvo (The Spanish National Research Council (CSIC)); Walker C. and M. Naito (Japan Atomic Energy Agency (JAEA)); Pettersson, S., I. Puigdomenech, Svensk, A.B. Kärnbränslehantering, and M.A. Cuñado (Empresa Nacional de Residuos Radiactivos (ENRESA)); Vuorio M. (Posiva); Weber, H. (Nationale Genossenschaft für die Lagerung radioaktiver Abfälle (NAGRA)); Ueda, H. and K. Fujisaki (Nuclear Waste Management Organization of Japan (NUMO)). 2012. Development of An Accurate pH Measurement Methodology for the Pore Fluids of Low pH Cementitious Materials. SKB report R-12-02. August 2012. Stockholm, Sweden.

Bhattacharjee, B. and S. Krishnamoorthy. 2004. Permeable Porosity and Thermal Conductivity of Construction Materials. 2004. ASCE Journal of Materials in Civil Engineering, July/August, pp. 322-330.

Boger D., P. Scales, and F. Sofra. 2015. Rheological Concepts. Edited by Jewell, R.J., and AB. Fourie. 3 edition. Australian Centre for Geomechanics. pp. 21-43. Perth, Australia.

Duro, L., V. Montoya, E. Colàs and D. García. 2010. Groundwater equilibration and radionuclide solubility calculations. Nuclear Waste Management Organization Technical Report NWMO TR-2010-02. Toronto, Canada.

Ferraris C. 1999. Measurement of the Rheological Properties of High Performance Concrete: State of the Art Report. Journal of Research of the National Institute of Standards and Technology. Vol. 104, No. 5, September–October 1999, pp. 461-478.

Ferraris C., F. de Larrard, and N. Martys. 2001. Fresh Concrete Rheology: Recent Developments. Materials Science of Concrete VI, Sidney Mindess and Jan Skalny, eds., The American Ceramic Society, 735 Ceramic Place, Westerville, OH U.S.A. 43081, pp. 215-241.

Ghazvinian, E., M. Perras, M. Diederichs, and D. Labrie. 2012. Formalized Approaches to Defining Damage Thresholds in Brittle Rock: Granite and Limestone. ARMA 12-448. Proceedings of the 46th US Rock Mechanics / Geomechanics Symposium, Chicago, IL, USA, 24-27 June 2012.

Min-Hong Zhang, V., M. Malhotra, and J. Wolsiefer, Sr. 2000. Determination of Free Silicon Content in Silica Fume and Its Effect on Volume of Gas Released from Mortars Incorporating Silica Fume. ACI Materials Journal, no. 97-M66, pp.576-586.

Tinker JA, Cabrera JG. Modeling the thermal conductivity of concrete based on its measured density and porosity. Buildings V. Conference proceedings; 1992; 91-95.

https://www.engineeringtoolbox.com/thermal-conductivity-d_429.html, accessed on October 4, 2021.

GLOSSARY OF TERMINOLOGY AND ABBREVIATIONS

ABM	Asphalt Based Materials
ACI	American Concrete Institute
AECL	Atomic Energy of Canada Limited
ASTM	American Society of Testing and Materials
BDL	below detection limit
CCIL	Canadian Council of Independent Laboratories
CI	crack initiation
CM	cementitious material
CSA	Canadian Standards Association
DGR	Deep Geologic Repository
GU	general use
GUL	general use limestone
HPC	high performance concrete
HS	High-Sulphate resistant
ITLS	Inverse Tangent Lateral Stiffness
K	Hydraulic conductivity
LHHPC	Low Heat High Performance Concrete
LOI	Loss on ignition
MOE	modulus of elasticity (Young’s modulus)
MTO	Ministry of Transportation of Ontario
NA	not applicable
NSC	normal strength concrete
NWMO	Nuclear Waste Management Organization
OHSA	Occupational Health and Safety Act
OPG	Ontario Power Generation
PC	Portland cement
PQP	Project Quality Plan
QA	Quality Assurance
QC	Quality Control
RDL	Reportable Detection Limit
RH	relative humidity
SF	silica fume
SP	superplasticizer

TBD	to be determined
TDS	total dissolved solids
TPS	transient plane source
UCS	unconfined compressive strength
w/cm	water-to-cementitious material ratio
XRD	X-ray diffraction
XRF	X-ray fluorescence

APPENDIX A: GENERAL USE LIMESTONE CEMENT (S198-20)

Votorantim Cimentos

St Marys Cement

Portland Limestone Cement Type GUL- Contempra

Production Period: 12/01/2019 to 12/31/2019

STANDARD REQUIREMENTS

Chemical Data

Item	Spec. Limit	Results
SiO_2 (%)		18.1
Al_2O_3 (%)		4.2
Fe_2O_3 (%)		2.6
CaO (%)		61.0
MgO (%)		3.2
SO_3 (%)*	*3.0 max*	3.42
Loss of ignition (%)	*10.0 max*	6.0
Na_2O (%)		0.23
K_2O (%)		0.53
CO_2 (%)		4.4
Limestone (%)	*5.0 - 15.0*	10.5
CaCO3 in limestone (%)	*75 min*	94.9

Physical Data

Item	Spec. Limit	Results
Retained 325 (%)	*28 max*	2.74
Autoclave expansion (%)	*1.0 max*	0.15
Compressive strength (MPa/psi):		
1 day		14.0 [2035]
3 days	*14.5[2103] min*	23.5 [3401]
7 days	*20.0[2900] min*	29.7 [4311]
28 days *(previous month)*	*26.5[3843] min*	40.0 [5808]
Time of setting (minutes)		
(Vicat) Initial	*45 - 375*	104
(Vicat) Final		243
Mortar Bar Expansion (ASTM C1038) (%)*	*0.02 max*	0.010

ADDITIONAL DATA

Item	Results
Equiv. Alkalies	0.57

Item	Results
Air Content of mortar (volume %)	7
Blaine fineness (m^2/kg)	518
Specific Gravity (g/cm3)	3.16

This cement meets CSA A3001 Specification for Type GUL Portland Limestone Cement. The test methods were performed according to CSA A3003, A3004-A3, A3004-B2, A3004-B5, A3004-C2, A3004-C4, and A3004-C6.

*It is permissible to exceed the max value for SO3 content, provided it is demontrated by C1038 that the cement will not develop expansion exceeding 0.020% in 14 Days

January 13, 2020

St. Marys Cement Co.
St Marys Plant
585 Water Street South
St Marys, ON N4X 1B6
Tel: (519) 284-1020 - Fax: (519) 284-4104

April Innes

April Innes
Lab Supervisor

Table 27: Chemical Composition of GUL Cement (C198-20)

Sample	Votorantim Cimentos (formarly St. Marys Cement) GUL cement	RDL	St. Marys cement GU cement	CRH cement Type GU
Wood Log No.	**C198-20**		**S287-15**	**S306-15**
Element Oxide (%)	(%)	(%)	(%)	(%)
SiO_2	18.40	0.01	18.90	19.0
Al_2O_3	4.32	0.01	4.79	5.11
Fe_2O_3	2.59	0.01	2.98	2.45
MgO	3.32	0.01	3.20	2.51
BaO	0.05	0.01	NA	NA
CaO	62.80	0.01	62.60	62.7
Na_2O	0.19	0.01	0.24	0.22
K_2O	0.45	0.01	0.54	1.07
Na_2O_e	0.49	na	0.60	0.924
TiO_2	0.24	0.01	0.22	0.28
P_2O_5	0.13	0.01	0.14	0.12
MnO	0.07	0.01	0.08	0.06
Cr_2O_3	<0.01	0.01	0.01	0.02
V_2O_5	0.03	0.01	0.03	<0.01
SrO	0.05	0.01	NA	NA
C(t)	1.20	0.01	0.41	0.42
LOI	5.45	0.01	1.46	1.93
S	1.32	0.005	1.41	1.67
SO_3	3.30	-	3.52	4.17
Sum	99.4	0.01	95.3	95.5

The 2020 Votorantim Cimentos (formerly St. Marys Cement) GUL cement is produced in the same Portland cement plant as the GU cement (St. Marys Cement GU). The difference is the 2020 cement is a Portland limestone cement, which has approximately 10% calcium carbonate interground with the cement clinker at the production facility. The GUL cement is slightly lower in total alkali due to the dilution with calcium carbonate, but otherwise very similar to the GU cement. It is likely that the 2020 GUL cement is equal to or slightly lower in heat generation potential than the GU cement.

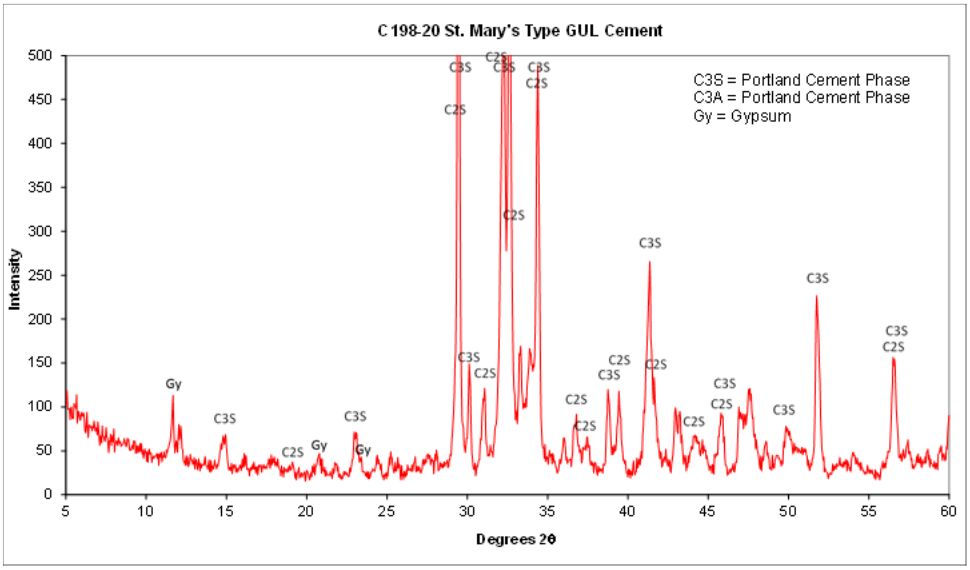

Figure 37: XRD pattern from Votorantim Cimentos (formerly St. Marys Cement) Type GUL

APPENDIX B: SILICA FUME (S070-20)

SILICA FUME
CHEMICAL & PHYSICAL ANALYSIS REPORT

Conforms to ASTM C 1240 & CSA A3001-18 Type SF

CUSTOMER:	Wood PLC		
DESTINATION:	3450 Harvester Road, Suite 100		
	Burlington, Ontario L7N 3W5		
DATE:	1/13/20	SHIPPING #:	Sample
QUANTITY:	217 lbs.	LOT #:	14V27D01-1
BULK:	SUPERSACK:	BAG:	Buckets

CHEMICAL TESTS		ANALYSIS
SiO_2		95.23 %
SO_3		0.22 %
CL^-		0.04 %
Total Alkali		0.34 %
Moisture Content		0.26 %
Loss on Ignition		3.29 %
pH		6.65

PHYSICAL TESTS		ANALYSIS
Oversize - % retained on 45 µm sieve (wet sieved)		2.40 %
Density - (specific gravity)		2.24
Bulk Density - (per ASTM)	726.51 kg/m^3	45.35 lb/ft3
Specific Surface Area (by BET)		23.78 m2/g
Accelerated Pozzolanic Activity Index - with Portland Cement		140.92 %
Autoclave Expansion (per CSA)		-0.08 %
Tendencey to Entrap Air (per CSA)		No visible foam

Prepared by Norchem Inc. QC Department

Form NL 110E Canadian

NORCHEM

www.norchem.com

985 SEAWAY DRIVE, STE A, FORT PIERCE, FL. 34949-2744
TEL. (772) 468-6110 · FAX (888) 617-8520

960 WHEELER ROAD #5537, HAUPPAUGE, N.Y. 11788
TEL. (631) 724-8639 · FAX (888) 617-8520

Table 28: Chemical Composition of Silica Fume (C070-20)

Sample	Silica fume	RDL
Wood Log No.	**C070-20**	
Element Oxide (%)	(%)	(%)
SiO_2	97.0	0.01
Al_2O_3	0.11	0.01
Fe_2O_3	0.03	0.01
MgO	0.21	0.01
BaO	<0.01	0.01
CaO	0.42	0.01
Na_2O	0.01	0.01
K_2O	0.40	0.01
TiO_2	<0.01	0.01
P_2O_5	0.06	0.01
MnO	0.01	0.01
Cr_2O_3	<0.01	0.01
V_2O_5	<0.01	0.01
SrO	<0.01	0.01
C(t)	2.09	0.01
LOI	2.05	0.01
S	0.052	0.005
SO_3	0.130	NA
Sum	100	0.01

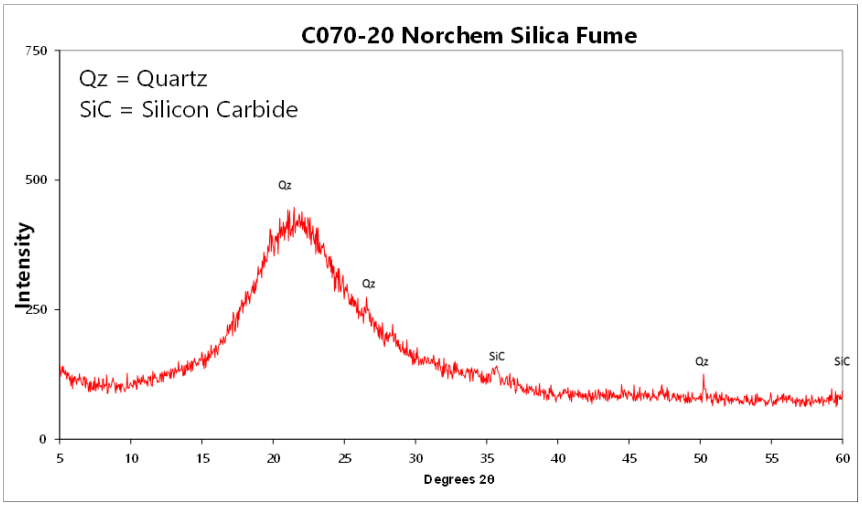

Figure 38: X-ray Diffraction Pattern of Silica Fume (C070-20)

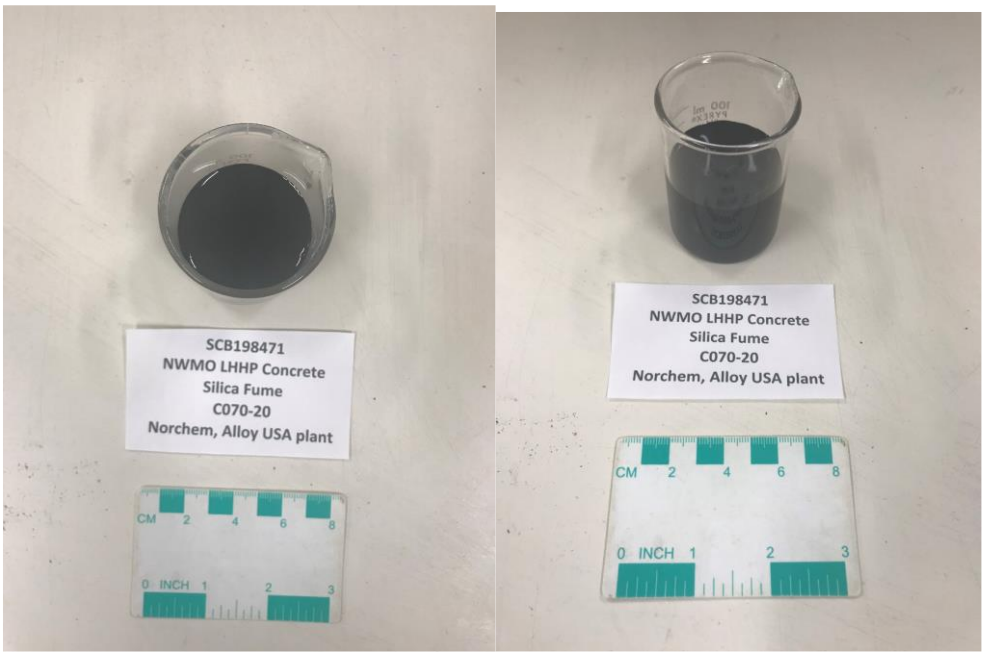

Figure 39: Tendency of Silica Fume to Entrap Air (C070-20)

As per *CSA-A3004-A5 Rapid test method for determining the tendency of silica fume to entrap air in mortar or concrete*: "*If after 20 s no foam exists over the surface of the slurry, the silica fume shall not be likely to entrap significant amounts of air. The presence of a layer of foam over the surface of the slurry after 20 s indicates a susceptibility of the silica fume to entrap air in mortar or concrete, and further testing shall be carried out to determine the suitability of the silica fume for its intended use*." The silica fume sample from Norchem, Alloy plant, USA (C070-20) does not have the tendency to entrap air, as shown in Figure 39.

Potential for hydrogen generation was determined following Min-Hong Zhang et al. (2000). Table 28 gives the free silicon content of the silica fume samples.

Table 29: Free Silicon Content of the Silica Fume Samples (C070-20 and C1104-17)

Wood log No.	Silica Fume Source	Average % Free Silicon (by weight)+	Standard Deviation (%)	Comments
C070-20	Norchem, Alloy plant, USA	0.042%*	0.012%	2020 sample
C1104-17	Norchem, Alloy plant, USA	0.043%**	0.014%	2020 test results for 2017 sample
C1104-17	Norchem, Alloy plant, USA	0.042%***	0.012%	2017 test results for 2017 sample

Notes:
+ Performance target for free silicon (Si) content in silica fume is <0.075% (by mass).
* Average of triplicate determinations.
** Average of five determinations.
*** Average of triplicate determinations for samples from three batches.

Table 30: Calibration Free Silicon Content

Trials year	Al Recovery (%)	Standard Deviation (%)
2020	103.29%*	5.12%
2017	99.69%**	5.63%

Notes:
* Average of four determinations.
** Average of triplicate determinations for each sample.

APPENDIX C: SILICA FLOUR (S158-20)

AGSCO CORPORATION

TECHNICAL DATA

AGSCO SILICA SAND

TYPICAL PHYSICAL PROPERTIES

FUSION POINT	3135 °F
HARDNESS	Knoop - 820; Mohs - 7
GRAIN SHAPE	Spherical
SPECIFIC GRAVITY	2.65 g/cm³
LOOSE PACK BULK DENSITY	1.60 g/cm³ (100 lbs/ft³)
pH	6.8 to 7.2

TYPICAL CHEMICAL PROPERTIES

#10-20 and Coarser Sizes		#12-20 and Finer Sizes	
SiO_2	98.2 %	SiO_2	99.8 %
Fe_2O_3	0.14	Fe_2O_3	0.016
Al_2O_3	0.49	Al_2O_3	0.034
TiO_2	0.02	TiO_2	0.007
CaO	0.02	CaO	0.011
MgO	0.01	MgO	0.007
K_2O	0.21	Loss on Ignition	0.094
Na_2O	0.06		
Loss on Ignition	0.40		

TYPICAL SCREEN ANALYSIS

(Percent Retained)

US SIEVE	#4-8	#8-12	#10-16	#10-20
6	3.4			
7	21.7			
8		6.0	2.8	
10	74.4	54.0	16.6	
12	0.5	35.3	30.7	1.6
14		4.7	32.7	35.3
16		T	13.7	40.4
18			2.4	17.7
20			1.1	4.0
25				0.9
30				
40				
50				
Pan				0.1
	100.0	100.0	100.0	100.0

Effective Size (mm)	2.00	1.70	1.20	1.00

160 West Hintz Road
Wheeling, Ilinois 60090
P: 847-520-4455 • F: 847-520-4970

60 Chapin Road, PO Box 669
Pine Brook, New Jersey 07058
P:973-244-0005 • F:973-244-0091

AGSCO CORPORATION

TECHNICAL DATA

TYPICAL SCREEN ANALYSIS

(Percent Retained)

US SIEVE	12-20	16-30	20-40	(#1) 35-50	(#2) 40-70	50-80	(#7) 70-100	(#10) 100-140	(#110) 140-200	(#16) 140-270
12										
14										
16	70.5									
18	26.0	1.3								
20	1.8	48.2	0.2							
25	0.5	45.4	7.0	0.3						
30	0.3	3.8	20.6	2.0	0.3					
35	0.5	0.9	42.8	20.5	5.2					
40	0.3	0.4	23.3	35.3	16.5	2.7	2.9	1.2	0.3	
50			6.0	32.7	37.0	39.3	17.4	2.9	1.5	
60				4.7	14.2	23.8	---	---	---	
70				2.2	9.3	16.2	39.9	13.2	4.4	
80				2.3	5.5	9.1	---	---	---	
100					4.8	5.4	27.7	41.4	19.8	
120					7.2	3.5	---	---	---	---
140							11.2	36.3	42.8	27.8
170							---	---	---	---
200							0.9	4.8	20.5	50.9
230								---	---	---
270								0.1	8.3	19.3
325/PAN	0.1								2.3	2.0
	100.0	100.0	100.0	100.0	100.0	100.0	100.0	100.0	100.0	100.0

AFS Grain Number	11	15	25	35	47	50	59.6	80.3	111.8	144
Effective Size (mm).	1.0	0.71	0.43	0.30	.15	.15	.11			

SILICA FLOUR

(Typical Percent Retained/Passing)

U.S. Sieve	#70 / 250u	#140 / 106u	#200 / 90u	#230/63u	#270/53u	#325 / 45u
70	3					
100	11	T				
140	8	1	T			
200	14	6	3	1	T	
270	9	10	7	4	3	T
325	5	8	7	5	4	2
Passing 325	50	75	83	90	93	98
Totals	100	100	100	100	100	100

160 West Hintz Road
Wheeling, Ilinois 60090
P: 847-520-4455 • F: 847-520-4970

60 Chapin Road, PO Box 669
Pine Brook, New Jersey 07058
P:973-244-0005 • F:973-244-0091

Table 31: Chemical Composition of Silica Flour (C158-20)

Sample	**Silica flour***	**RDL**
Wood Log No.	**C158-20**	
Element Oxide (%)	(%)	(%)
SiO_2	100	0.01
Al_2O_3	0.16	0.01
Fe_2O_3	0.03	0.01
MgO	0.02	0.01
BaO	<0.01	0.01
CaO	0.02	0.01
Na_2O	0.01	0.01
K_2O	0.01	0.01
TiO_2	<0.01	0.01
P_2O_5	<0.01	0.01
MnO	<0.01	0.01
Cr_2O_3	<0.01	0.01
V_2O_5	<0.01	0.01
SrO	<0.01	0.01
C(t)	<0.01	0.01
LOI	0.11	0.01
S	<0.05	0.005
SO_3	<0.1	NA
Sum	100	0.01

Note: Source AGSCO, product #270/53u.

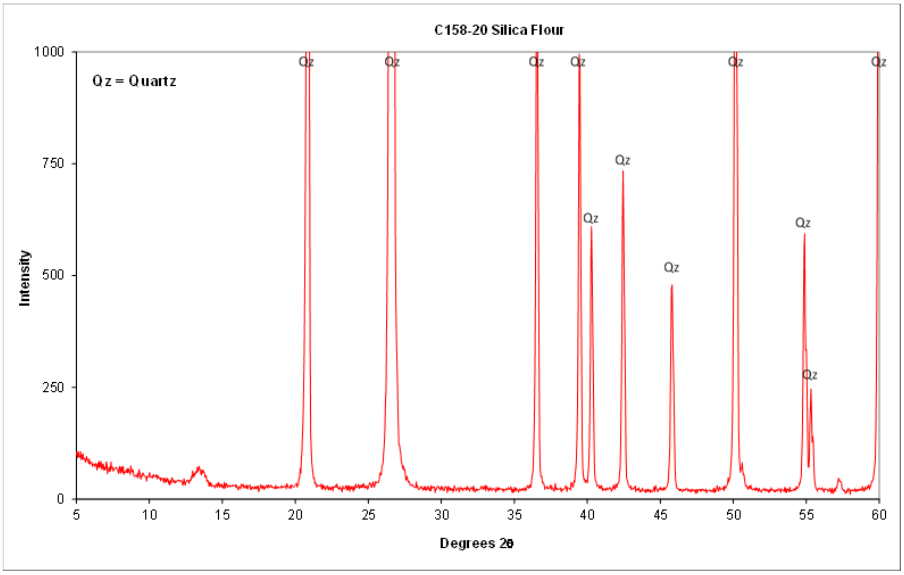

Figure 40: XRD Pattern Silica Flour (C158-20)

APPENDIX D: SAND (S027-20)

Specific gravity : 2.771
Absorption: 0.89

Table 32: Chemical Composition of Natural Silica Sand (S027-20)

Sample	**Lafarge Cambridge Natural concrete sand**	**RDL**
Wood Log No.	**S027-20**	
Element Oxide (%)	(%)	(%)
SiO_2	26.6	0.01
Al_2O_3	3.36	0.01
Fe_2O_3	1.33	0.01
MgO	11.2	0.01
BaO	<0.01	0.01
CaO	24.9	0.01
Na_2O	0.68	0.01
K_2O	0.75	0.01
TiO_2	0.16	0.01
P_2O_5	0.05	0.01
MnO	0.07	0.01
Cr_2O_3	<0.01	0.01
V_2O_5	<0.01	0.01
SrO	0.03	0.01
C(t)	8.04	0.01
LOI	30.6	0.01
S	0.011	0.005
SO_3	0.028	NA
Sum	99.70	0.01

wood.

SIEVE ANALYSIS OF FINE AND COARSE AGGREGATE
ASTM C136

Report Date: 4 March 2020
Project No.: SCB198471

Client: NWMO
Sample Source: Lafarge - Cambridge Pit
Date Sampled: 4 February 2020
Sampled by: A representative of Lafarge
Sample Type: Fine Aggregate
Specification: ASTM C 33/C 33M - 18, 6.1 Fine Aggregate Grading Natural Sand

Lab No: S027-20
Date Received: 05 February 2020
Date Tested: 04 March 2020
Lab Technician: KH
Fineness Modulus: 2.9

SIEVE SIZES (mm)	100	90.0	75.0	63	50	37.5	25.0	19	12.5	9.5	4.75	2.36	1.18	0.600	0.300	0.150	0.075
SPECIFICATIONS	-	-	-	-	-	-	-	-	-	100.0	95-100	80-100	50-85	25-60	5-30	0-10	0-3
% PASSING	-	-	-	-	-	-	-	-	-	100.0	99.2	84.6	63.3	38.7	16.1	6.6	2.2

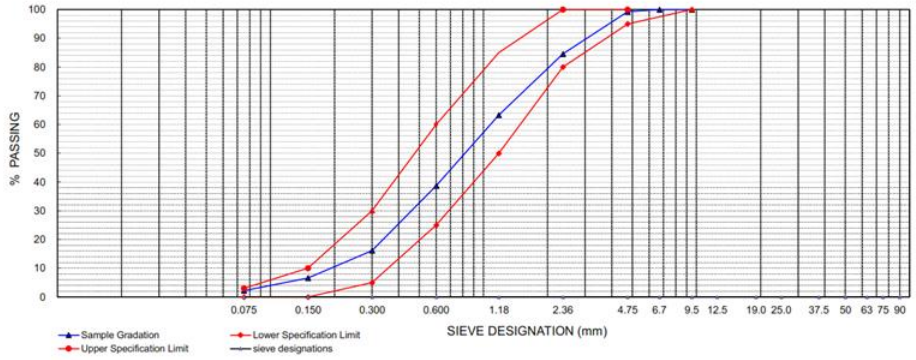

Wood Environment & Infrastructure Solutions 3450 Harvester Rd., Suite 100, Burlington, ON, L7N 3W5

HA-TEM-MAT-1000C-01

Figure 41: Natural Silica Sand Particle Size Distribution (S027-20)

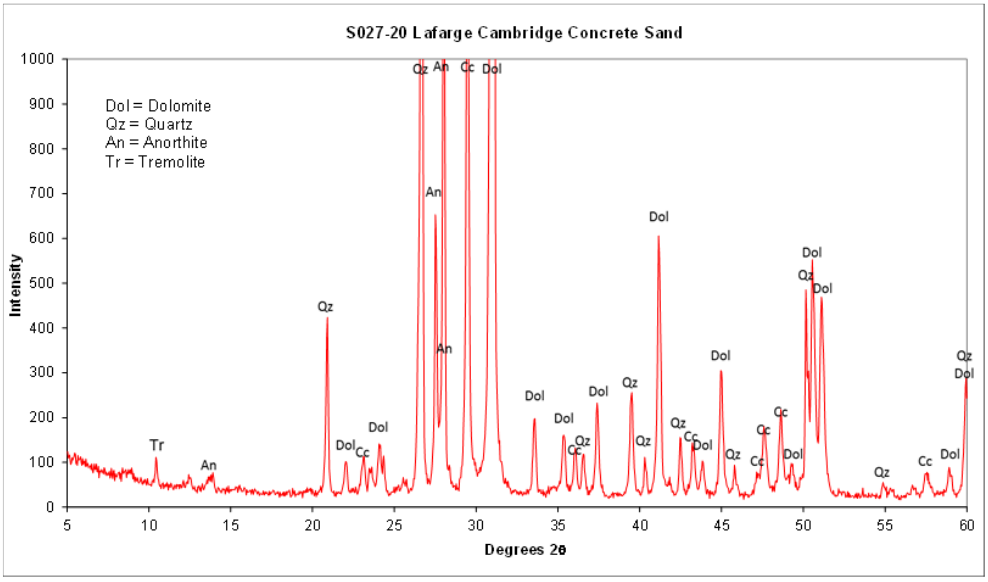

Figure 42: Natural Silica Sand XRD Pattern (S027-20)

APPENDIX E: COARSE AGGREGATE (S028-20 & S029-20)

Specific gravity: 2.787
Absorption : 0.92

Table 33: Chemical Composition of Coarse Aggregate (S028-20 & S029-20)

Sample	**Lafarge Cambridge, ON Coarse aggregate**	**RDL**
Wood Log No.	**S028-20 & S029-20**	
Element Oxide (%)	(%)	(%)
SiO_2	8.87	0.01
Al_2O_3	1.36	0.01
Fe_2O_3	0.89	0.01
MgO	17.3	0.01
BaO	<0.01	0.01
CaO	29.0	0.01
Na_2O	0.20	0.01
K_2O	0.30	0.01
TiO_2	0.10	0.01
P_2O_5	0.02	0.01
MnO	0.06	0.01
Cr_2O_3	<0.01	0.01
V_2O_5	<0.01	0.01
SrO	0.01	0.01
C(t)	10.9	0.01
LOI	40.9	0.01
S	<0.005	0.005
SO_3	<0.01	NA
Sum	99.0	0.01

wood.

SIEVE ANALYSIS OF FINE AND COARSE AGGREGATE
ASTM C136

Report Date: 17 March 2020
Project No.: SCB198471

Client: NWMO
Sample Source: Lafarge - Cambridge Pit
Date Sampled: 4 February 2020
Sampled by: A representative of Lafarge
Sample Type: 19 to 4.75 mm
Specification: ASTM C 33/C 33M - 18, Size No. 67
Table 3 Grading Requirements for Coarse Aggregates

Lab No: S028 & S029 Blend
Date Received: 05 February 2020
Date Tested: 16 March 2020
Lab Technician: KH

SIEVE SIZES (mm)	100	90.0	75.0	63	50	37.5	25.0	19	12.5	9.5	4.75	2.36	1.18	0.600	0.300	0.150	0.075
SPECIFICATIONS	-	-	-	-	-	-	100.0	90-100	-	20-55	0-10	0-5	-	-	-	-	-
% PASSING	0.0	100.0	100.0	100.0	100.0	100.0	100.0	97.3	44.6	27.8	3.2	1.2	0.9	0.8	0.7	0.7	0.6

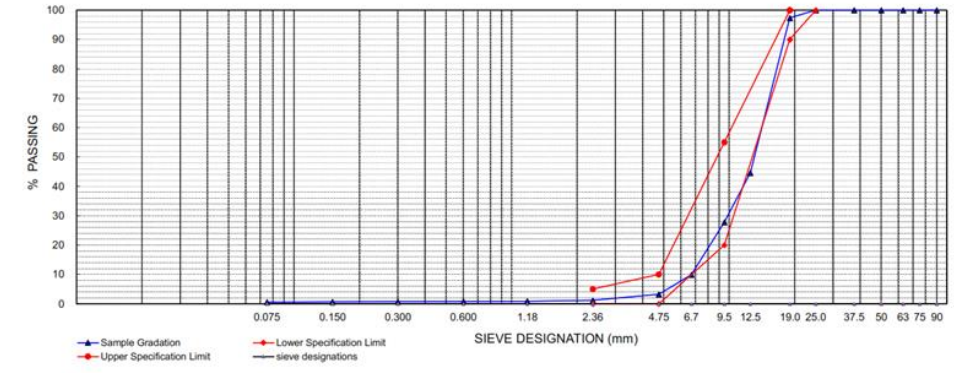

Figure 43: Coarse aggregate particle size distribution (S028-20 & S029-20)

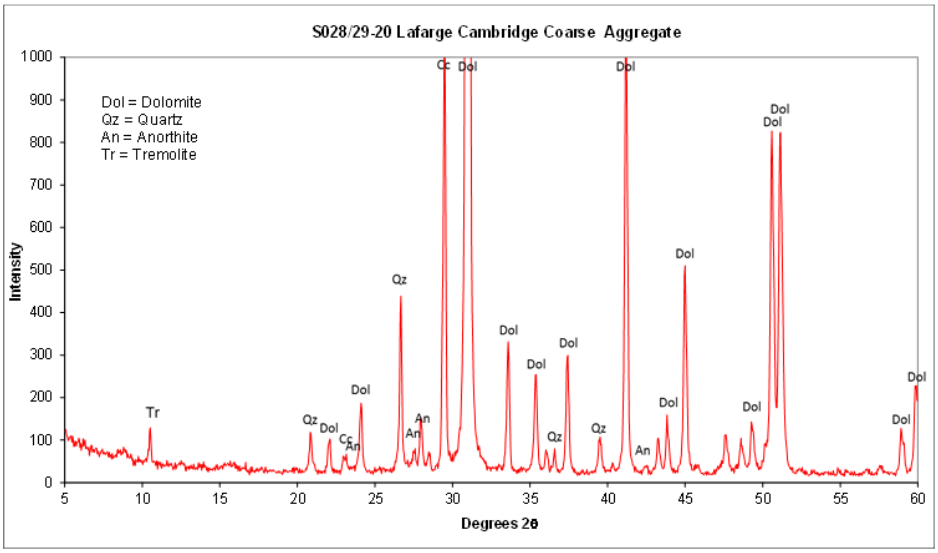

Figure 44: Coarse Aggregate XRD Pattern (S028-20 & S029-20)

APPENDIX F: SUPER PLASTICIZER (C115-20)

MASTER® BUILDERS SOLUTIONS | BASF We create chemistry

3	03 30 00	Cast-in-Place Concrete
	03 40 00	Precast Concrete
	03 70 00	Mass Concrete
4	04 05 16	Masonry Grouting

MasterGlenium® 7500

Full-Range Water-Reducing Admixture

Description

MasterGlenium 7500 full-range water-reducing admixture is very effective in producing concrete mixtures with different levels of workability including applications that require self-consolidating concrete (SCC). MasterGlenium 7500 admixture meets ASTM C 494/C 494M compliance requirements for Type A, water-reducing, and Type F, high-range water-reducing, admixtures.

Applications

Recommended for use in:

- Concrete with varying water reduction requirements (5-40%)
- Concrete where control of workability and setting time is critical
- Concrete where high flowability, increased stability, high-early and ultimate strengths, and improved durability are needed
- Producing self-consolidating concrete (SCC)
- Strength-on-demand concrete, such as 4x4™ Concrete
- Pervious concrete

Features

MasterGlenium 7500 full-range water-reducing admixture is based on the next generation of polycarboxylate technology found in all of the MasterGlenium 7000 series products. This technology combines state-of-the-art molecular engineering with a precise understanding of regional cements to provide specific and exceptional value to all phases of the concrete construction process.

- Dosage flexibility for normal, mid-range and high-range applications
- Excellent early strength development
- Controls setting characteristics
- Optimizes slump retention/setting relationship
- Consistent air entrainment

Benefits

- Faster turnover of forms due to accelerated early strength development
- Reduces finishing labor costs due to optimized set times
- Use in fast track construction
- Minimizes the need for slump adjustments at the jobsite
- Less jobsite QC support required
- Fewer rejected loads
- Optimizes concrete mixture costs

Performance Characteristics

Concrete produced with MasterGlenium 7500 admixture achieves significantly higher early age strength than first generation polycarboxylate high-range water-reducing admixtures. MasterGlenium 7500 admixture also strikes the perfect balance between workability retention and setting characteristics in order to provide efficiency in placing and finishing concrete. The dosage flexibility of MasterGlenium 7500 allows it to be used as a normal, mid-range, and high-range water reducer.

Guidelines for Use

Dosage: MasterGlenium 7500 admixture has a recommended dosage range of 2-15 fl oz/cwt (130-975 mL/100 kg) of cementitious materials. For most mid- to high-range applications, dosages in the range of 5-8 fl oz/cwt (325-520 mL/100 kg) will provide excellent performance. For high performance and producing self-consolidating concrete mixtures, dosages of up to 12 fl oz/cwt (780 mL/100 kg) of cementitious materials can be utilized. Because of variations in concrete materials, jobsite conditions and/or applications, dosages outside of the recommended range may be required. In such cases, contact your local sales representative.

Mixing: MasterGlenium 7500 admixture can be added with the initial batch water or as a delayed addition. However, optimum water reduction is generally obtained with a delayed addition.

Product Notes

Corrosivity – Non-Chloride, Non-Corrosive: MasterGlenium 7500 admixture will neither initiate nor promote corrosion of reinforcing steel embedded in concrete, prestressing steel or of galvanized steel floor and roof systems. Neither calcium chloride nor other chloride-based ingredients are used in the manufacture of MasterGlenium 7500 admixture.

Compatibility: MasterGlenium 7500 admixture is compatible with most admixtures used in the production of quality concrete, including normal, mid-range and high-range water-reducing admixtures, air-entrainers, accelerators, retarders, extended set control admixtures, corrosion inhibitors, and shrinkage reducers.

Do not use MasterGlenium 7500 admixture with admixtures containing beta-naphthalene sulfonate. Erratic behaviors in slump, workability retention and pumpability may be experienced.

Storage and Handling

Storage Temperature: MasterGlenium 7500 admixture must be stored at temperatures above 40 °F (5 °C). If MasterGlenium 7500 admixture freezes, thaw and reconstitute by mechanical agitation.

Shelf Life: MasterGlenium 7500 admixture has a minimum shelf life of 9 months. Depending on storage conditions, the shelf life may be greater than stated. Please contact your local sales representative regarding suitability for use and dosage recommendations if the shelf life of MasterGlenium 7500 admixture has been exceeded.

Packaging

MasterGlenium 7500 admixture is supplied in 55 gal (208 L) drums, 275 gal (1040 L) totes and by bulk delivery.

Related Documents

Safety Data Sheets: MasterGlenium 7500 admixture

Additional Information

For additional information on MasterGlenium 7500 admixture or on its use in developing concrete mixtures with special performance characteristics, contact your local sales representative.

The Admixture Systems business of BASF's Construction Chemicals division is the leading provider of solutions that improve placement, pumping, finishing, appearance and performance characteristics of specialty concrete used in the ready-mixed, precast, manufactured concrete products, underground construction and paving markets. For over 100 years we have offered reliable products and innovative technologies, and through the Master Builders Solutions brand, we are connected globally with experts from many fields to provide sustainable solutions for the construction industry.

Limited Warranty Notice

BASF warrants this product to be free from manufacturing defects and to meet the technical properties on the current Technical Data Guide, if used as directed within shelf life. Satisfactory results depend not only on quality products but also upon many factors beyond our control. BASF MAKES NO OTHER WARRANTY OR GUARANTEE, EXPRESS OR IMPLIED, INCLUDING WARRANTIES OF MERCHANTABILITY OR FITNESS FOR A PARTICULAR PURPOSE WITH RESPECT TO ITS PRODUCTS. The sole and exclusive remedy of Purchaser for any claim concerning this product, including but not limited to, claims alleging breach of warranty, negligence, strict liability or otherwise, is shipment to purchaser of product equal to the amount of product that fails to meet this warranty or refund of the original purchase price of product that fails to meet this warranty, at the sole option of BASF. Any claims concerning this product must be received in writing within one (1) year from the date of shipment and any claims not presented within that period are waived by Purchaser. BASF WILL NOT BE RESPONSIBLE FOR ANY SPECIAL, INCIDENTAL, CONSEQUENTIAL (INCLUDING LOST PROFITS) OR PUNITIVE DAMAGES OF ANY KIND.

Purchaser must determine the suitability of the products for the intended use and assumes all risks and liabilities in connection therewith. This information and all further technical advice are based on BASF's present knowledge and experience. However, BASF assumes no liability for providing such information and advice including the extent to which such information and advice may relate to existing third party intellectual property rights, especially patent rights, nor shall any legal relationship be created by or arise from the provision of such information and advice. BASF reserves the right to make any changes according to technological progress or further developments. The Purchaser of the Product(s) must test the product(s) for suitability for the intended application and purpose before proceeding with a full application of the product(s). Performance of the product described herein should be verified by testing and carried out by qualified experts.

BASF Corporation
Admixture Systems
www.master-builders-solutions.basf.us

United States
23700 Chagrin Boulevard
Cleveland, Ohio 44122-5544
Tel: 800 628-9990 ▪ Fax: 216 839-8821

Canada
1800 Clark Boulevard
Brampton, Ontario L6T 4M7
Tel: 800 387-5882 ▪ Fax: 905 792-0651

APPENDIX G: CANMETMINING TEST REPORT

Natural Resources Canada
CanmetMINING
555 Booth Street
Ottawa, Canada K1A 0G1

Ressources naturelles Canada
CanmetMINES
555, rue Booth
Ottawa, Canada K1A 0G1

CanmetMINING File Number: P-002797.004
Final (R0)

October 21, 2021

Corina-Maria Aldea, Ph.D., P.Eng.
Senior Associate Materials Engineer
Wood PLC
3450 Harvester Road, Suite 100
Burlington, ON
L7N 3W5

RE: Mechanical Testing of High Performance Concrete Core Samples (LHHPC)

Dear Dr. Aldea:

The following report briefly summarizes the methodology and results of the mechanical testing program completed on behalf of Wood PLC (Wood) at CanmetMINING's Rock Mechanics Laboratory in Ottawa, Ontario. This work has been completed under CanmetMINING Project No. P-002797.004, in accordance with the agreed upon scope of work summarized in the CanmetMINING Service Offer.

The testing program described herein included the following: sample preparation, measurement of intact physical properties, and determination of mechanical properties (strength, Young's modulus and crack initiation) of the core specimens by uniaxial compression strength (UCS) tests. All work was completed in conformity with client Test Plans, and accordance with internal standard operating procedures and applicable ASTM Standards. Key personnel involved in this testing program include the following:

- Steve Gaines, Rock Mechanics Engineer – *Project Lead*
- Ted Anderson, Senior Technologist – *Laboratory testing*
- Gilles Brisson, Technician – *Sample preparation and dimensioning*

1.0 Sample Preparation and Physical Properties

Concrete core samples were received from the client in cylindrical moulds with unique sample identifiers. Samples were stored in their individual sealed mould to cure until the predefined testing date (cure time) in an environmental chamber at 21 degrees Celsius and 90% relative humidity. Samples were removed from the moulds for preparation approximately 24 hours prior to testing.

The general procedure for sample preparation consisted of the following steps:

- Specimens were carefully removed from their mould.
- Sample ends were polished to ensure that flatness and parallelism met ASTM D4543-19 standards. Grinding was completed using fresh water.
- Measurements of diameter, length and mass were recorded for each specimen.
- Ultrasonic pulse velocities (P- and S-wave velocities) were measured in accordance with ASTM D2845-08. *It should be noted that this ASTM has been withdrawn without a replacement; however, this method is still considered valid for measurement of pulse velocities and calculation of the dynamic elastic constants*.
- Following preparation, specimens were wrapped in a clean, moist towel and placed in the environmental chamber (21ºC, 90% RH).
- The morning of testing, samples were removed from the chamber and strain gauges installed on sample surface (two lateral/horizontal and two vertical strain gauges).
- Specimens were allowed to sit for a minimum of one hour prior to testing to allow the epoxy to set.

Sample specifications and physical properties are summarized in Table A.1, Attachment A.

2.0 Unconfined Compression Strength Testing

Unconfined compression strength (UCS) tests were completed on a total of 18 specimens. Each target test age, based on the casting date supplied by the client, consisted of three samples. Therefore, testing was completed over six testing dates between September 10, 2020 and May 11, 2021.

Compression tests were completed in accordance with internal standard operating procedures (SOP-T 2122) and standard test methods, specifically ASTM C39/C39M-18 and C469/C469M-14. All tests were completed with the MTS 815 load frame using an axial load rate of 1.96 kN/s (~ 0.025 MPa/s). Axial and lateral displacements were measured using mechanical gauges in addition to the strain gauges. A series of three linear variable displacement transducers (LVDTs), spaced 120º apart were used to monitor axial displacement, and a chain extensometer, placed at sample mid-height, was used to record circumferential (lateral) strain. Core samples were wrapped in polyethylene heat shrink tubing prior testing to prevent damage to instrumentation resulting from brittle failure of the samples.

Peak strength was recorded as the maximum load/stress sustained by the sample at failure. Elastic properties (Young's modulus and Poisson's ratio) were determined using the axial stress and strain relationships over the range of 50 microstrain (με) to 40% of the peak strength.

The crack initiation (CI) threshold was interpreted using the Inverse Tangent Lateral Strain (ITLS) approach, as summarized in Ghazvinian et al. (2012). This approach uses raw strain data collected during the compression tests to identify the onset of non-linear lateral strain and does not depend on the calculated values of Young's modulus and Poisson's ratio. Unless otherwise specified, mechanical axial and lateral strain data was used for this interpretation. Although electrical strain gauges provide very precise and useful data, the reported strain can be influenced by the location of the strain gauge on the surface of the

core sample relative to aggregate or pore space, which may localize stress concentrations and result in anomalous, or 'noisy', strain output. Conversely, the mechanical data provides full sample strain and is considered more representative of the bulk sample behaviour for a porous, heterogeneous material such as concrete.

Compression test results are summarized in Table A.2, Attachment A. Test data, including stress-strain plots and sample photographs before and after failure are included in Attachment B. The interpreted CI threshold is shown on the ITLS versus axial stress plots, presented in Attachment C.

3.0 Closure

The report will be held confidential for a period of ten (10) years. At the end of the confidentiality period, except as permitted by the Contract or the scope of work, CanmetMINING shall not publish or use in any manner whatsoever any data, samples or information provided by CLIENT or generated in the course of the work without the prior written consent of the CLIENT's ultimate client (NWMO).

Should you have any questions regarding the data report and/or the work carried out, please do not hesitate to contact me at 613-947-2170, or email at steven.gaines@canada.ca.

Regards,

_____

Steven Gaines, M.A.Sc., P.Eng., P.Geo.

Senior Rock Mechanics Engineer
CanmetMINING, Strategic Mining Technologies and Industry Support

Reviewed by: KT

Attachments (3):

Attachment A – Summary Tables
Attachment B – Compression Test Data
Attachment C – CI Interpretation

CC. Contracts Officer (CMIN-BA)

References:

ASTM C39 / C39M-18, Standard Test Method for Compressive Strength of Cylindrical Concrete Specimens, ASTM International, West Conshohocken, PA (USA), 2018.

ASTM C469 / C469M-14e1, Standard Test Method for Static Modulus of Elasticity and Poisson's Ratio of Concrete in Compression, ASTM International, West Conshohocken, PA (USA), 2014.

ASTM D2845-08, Standard Test Method for Laboratory Determination of Pulse Velocities and Ultrasonic Elastic Constants of Rock, ASTM International, West Conshohocken, PA (USA), 2008.

ASTM D4543-19, Standard Practices for Preparing Rock Core as Cylindrical Test Specimens and Verifying Conformance to Dimensional and Shape Tolerances, ASTM International, West Conshohocken, PA (USA), 2019.

Ghazvinian, E., *et al.* 2012. Formalized approaches to defining damage thresholds in brittle rock: Granite and Limestone. *Proceedings 46th US Rock Mechanics/Geomechanics Symposium*, Chicago, IL, USA, June.

Notes:

(1) Revision history:

- Draft: 19-May-21
- Final (R0): 21-Oct-21

(2) Test results apply only to tested rock specimens. CanmetMINING makes no representation or warranty respecting the results arising therefrom, either expressly or implied by law or otherwise, including but not limited to implied warranties or conditions of merchantability or fitness for a particular purpose.

(3) Elastic properties (Young's modulus and Poisson's ratio) are calculated using mechanical strain gauges, within a window comprised between 50 microstrain (axial strain gauges) and 40% of the peak strength, unless otherwise noted.

(4) The test program was carried out at CanmetMINING's Rock Mechanics Testing Laboratory located in Ottawa, Ontario. The address of the laboratory is:

Natural Resources Canada
CanmetMINING – Transformative Technologies and Ground Control Specialized Services
Bells Corners Complex, Building 10
1 Haanel Drive
Ottawa, Ontario
Canada K1A 1M1

Attachment A – Summary Tables

Table A.1 - Dimensions and Dynamic Moduli

Specimen Identification					Specifications (prepared)						Ultrasonic Velocities and Dynamic Moduli				
Specimen ID	Batch Date	Prepared Date	Test Date	Nominal Age (days)	Diameter (mm)	Length (mm)	L : D	Volume (cm^3)	Mass (g)	Bulk Density (g/cm^3)	P-wave Velocity (km/s)	S-wave Velocity (km/s)	Young's Modulus (GPa)	Shear Modulus (GPa)	Poisson's Ratio
C2000-20D	03-Sep-20	09-Sep-20	10-Sep-20	7	101.32	198.58	1.96	1600.98	3996.64	2.50	4.58	2.40	37.6	14.4	0.31
C2000-20E	03-Sep-20	09-Sep-20	10-Sep-20	7	101.61	198.59	1.95	1610.24	4014.49	2.49	4.62	2.47	39.5	15.2	0.30
C2000-20F	03-Sep-20	09-Sep-20	10-Sep-20	7	101.77	198.58	1.95	1615.34	4007.91	2.48	4.62	2.46	39.0	15.0	0.30
C2000-20G	03-Sep-20	30-Sep-20	01-Oct-20	28	101.96	198.74	1.95	1622.58	4008.22	2.47	4.69	2.52	40.7	15.7	0.30
C2000-20H	03-Sep-20	30-Sep-20	01-Oct-20	28	102.21	198.73	1.94	1630.46	3994.28	2.45	4.73	2.51	40.2	15.4	0.30
C2000-20I	03-Sep-20	30-Sep-20	01-Oct-20	28	101.92	198.73	1.95	1621.33	4002.84	2.47	4.75	2.51	40.6	15.5	0.31
C2000-20J	03-Sep-20	30-Oct-20	02-Nov-20	56	101.80	198.64	1.95	1616.68	4001.38	2.48	4.66	2.51	40.4	15.6	0.30
C2000-20K	03-Sep-20	30-Oct-20	02-Nov-20	56	101.77	198.72	1.95	1616.48	4016.34	2.48	4.69	2.50	40.3	15.5	0.30
C2000-20L	03-Sep-20	30-Oct-20	02-Nov-20	56	101.92	198.72	1.95	1621.25	3998.96	2.47	4.75	2.53	41.2	15.8	0.30
C1074-20D	12-Aug-20	09-Nov-20	10-Nov-20	90	101.55	197.99	1.95	1603.59	3969.77	2.48	4.74	2.51	40.8	15.6	0.30
C1074-20E	12-Aug-20	09-Nov-20	10-Nov-20	90	101.80	197.99	1.94	1611.49	3982.56	2.47	4.69	2.53	40.9	15.8	0.30
C1074-20F	12-Aug-20	09-Nov-20	10-Nov-20	90	102.02	197.99	1.94	1618.57	3979.29	2.46	4.69	2.50	40.0	15.4	0.30
C1074-20G	12-Aug-20	08-Feb-21	09-Feb-21	180	101.24	198.49	1.96	1597.73	3983.48	2.49	4.68	2.56	42.0	16.3	0.29
C1074-20H	12-Aug-20	08-Feb-21	09-Feb-21	180	101.59	198.49	1.95	1608.90	3969.99	2.47	4.66	2.53	40.8	15.8	0.29
C1074-20I	12-Aug-20	08-Feb-21	09-Feb-21	180	101.82	198.50	1.95	1616.17	3965.84	2.45	4.66	2.49	39.5	15.2	0.30
C1074-20J	12-Aug-20	10-May-21	11-May-21	270	101.74	198.74	1.95	1615.58	3963.51	2.45	4.60	2.52	40.0	15.5	0.29
C1074-20K	12-Aug-20	10-May-21	11-May-21	270	101.77	198.73	1.95	1616.56	3998.89	2.47	4.60	2.52	40.3	15.7	0.29
C1074-20L	12-Aug-20	10-May-21	11-May-21	270	101.74	198.73	1.95	1615.50	3970.12	2.46	4.71	2.53	40.8	15.7	0.30

Notes:

- Samples stored in a controlled environmental chamber (21^{o}C, 90% relative humidity) prior to sample preparation and testing
- Specimen preparation in accordance with ASTM D4345-19
- Ultrasonic pulse velocities collected in accordance with ASTM D2845-08

Table A.2 - Compression Test Results

Specimen Identification					Strength and Elastic Properties					Description of Failure Mode
Specimen ID	Batch Date	Prepared Date	Test Date	Nominal Age (days)	Peak Strength (MPa)	Young's Modulus (GPa)	Poisson's Ratio	CI (MPa)	CI / Peak (%)	
C2000-20D	03-Sep-20	09-Sep-20	10-Sep-20	7	30.7	25.5	0.22	13.2	43%	- axial splitting, shear
C2000-20E	03-Sep-20	09-Sep-20	10-Sep-20	7	30.4	25.6	0.17	12.5	41%	- axial splitting, shear
C2000-20F	03-Sep-20	09-Sep-20	10-Sep-20	7	30.5	25.0	0.24	13.3	44%	- axial splitting, shear
C2000-20G	03-Sep-20	30-Sep-20	01-Oct-20	28	64.1	31.4	0.32	28.6	45%	- axial splitting
C2000-20H	03-Sep-20	30-Sep-20	01-Oct-20	28	62.6	31.0	0.25	29.5	47%	- axial splitting
C2000-20I	03-Sep-20	30-Sep-20	01-Oct-20	28	62.3	31.8	0.29	29.1	47%	- axial splitting
C2000-20J	03-Sep-20	30-Oct-20	02-Nov-20	56	75.2	34.1	0.25	43.8	58%	- axial splitting
C2000-20K	03-Sep-20	30-Oct-20	02-Nov-20	56	76.5	34.3	0.29	26.9*	35%	- axial splitting
C2000-20L	03-Sep-20	30-Oct-20	02-Nov-20	56	74.0	31.2	0.17	44.1	60%	- axial splitting
C1074-20D	12-Aug-20	09-Nov-20	10-Nov-20	90	73.4	33.0	0.25	38.6*	53%	- axial splitting, Y-type failure
C1074-20E	12-Aug-20	09-Nov-20	10-Nov-20	90	71.4	31.6	0.26	38.7	54%	- axial splitting, shear
C1074-20F	12-Aug-20	09-Nov-20	10-Nov-20	90	69.4	32.9	0.23	34.5	50%	- axial splitting, shear
C1074-20G	12-Aug-20	08-Feb-21	09-Feb-21	180	80.1	33.7	0.25	35.7	45%	- axial splitting, Y-type failure
C1074-20H	12-Aug-20	08-Feb-21	09-Feb-21	180	78.6	33.6	0.21	37.6	48%	- axial splitting, shear
C1074-20I	12-Aug-20	08-Feb-21	09-Feb-21	180	78.4	34.7	0.24	35.8	46%	- axial splitting, shear
C1074-20J	12-Aug-20	10-May-21	11-May-21	270	76.7	33.3	0.11	39.4*	51%	- axial splitting, shear
C1074-20K	12-Aug-20	10-May-21	11-May-21	270	79.6	33.8	0.08	39.2	49%	- axial splitting, shear
C1074-20L	12-Aug-20	10-May-21	11-May-21	270	80.7	33.9	0.12	36.9*	46%	- axial splitting, shear

Notes:

- Testing and interpretation completed in accordance with ASTM C39/C39M-18 and C469/C469M-14, using the MTS 815 load frame (axial load control @ 1.96 kN/s, ~ 0.025 MPa/s)
- Samples stored in a controlled environmental chamber (21^{o}C, 90% relative humidity) and wraped in a moist towel following sample preparation and prior to testing
- Elastic properties calculated using electric strain gauge data, between 50 microstrain (axial) and 40 % of peak strength.
- Crack initiation (CI) threshold determined by the Inverse Tangent Lateral Stiffness (ITLS) method, using mechanical strain gauge data unless otherwise specified (Ghazvinian et al., 2012).
-* anomolous chain extensometer data, therefore strain gauge data used to estimate CI

Attachment B – Test Data

Specimen ID: **C2000-20D**
Test: **UCS**

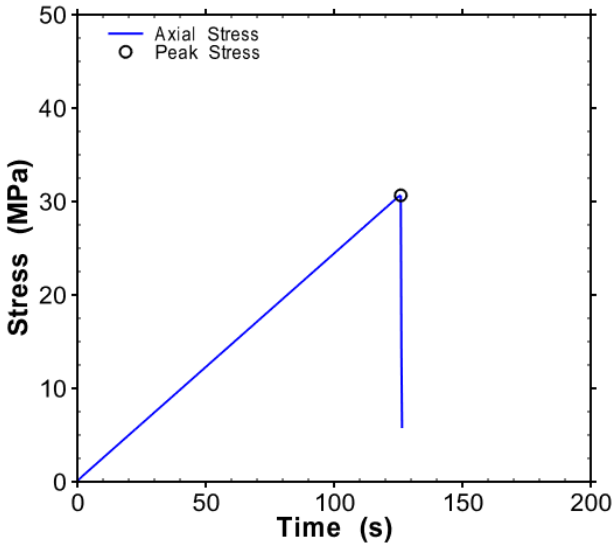

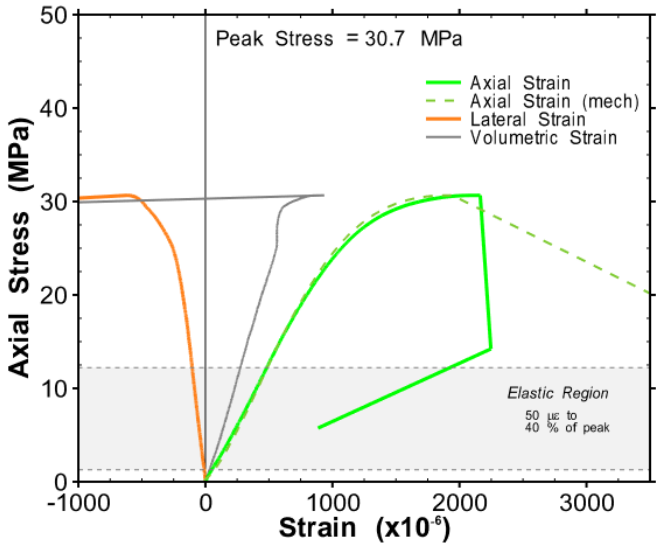

Test Information:

Load Control = 1.96 kN/s
Time to Failure = 2.1 min

Specimen Dimensions:

Length = 198.58 mm
Diameter = 101.32 mm

Electrical Gauges:

Young's modulus = 25.5 GPa
Poisson's ratio = 0.22

C2000-20D.dat

P-002797.004_UCS_R0.mView

Failure Description: axial splitting, shear

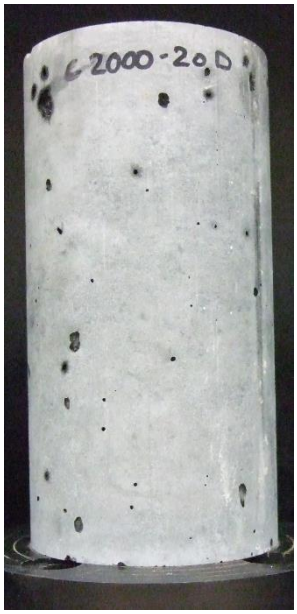

Pre-Test

Post-Test

Specimen ID: **C2000-20E**
Test: **UCS**

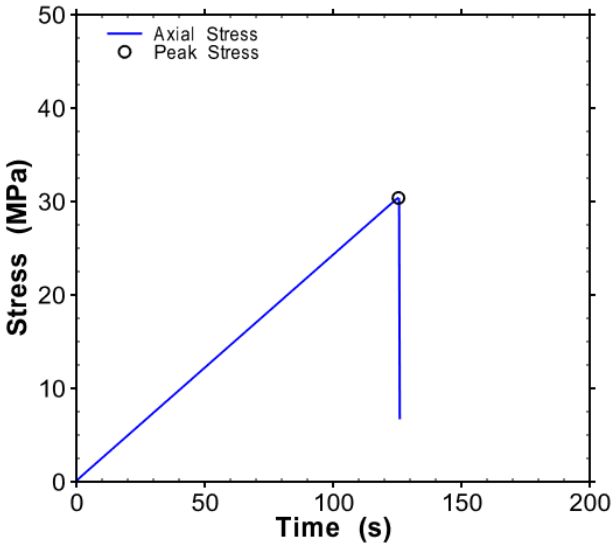

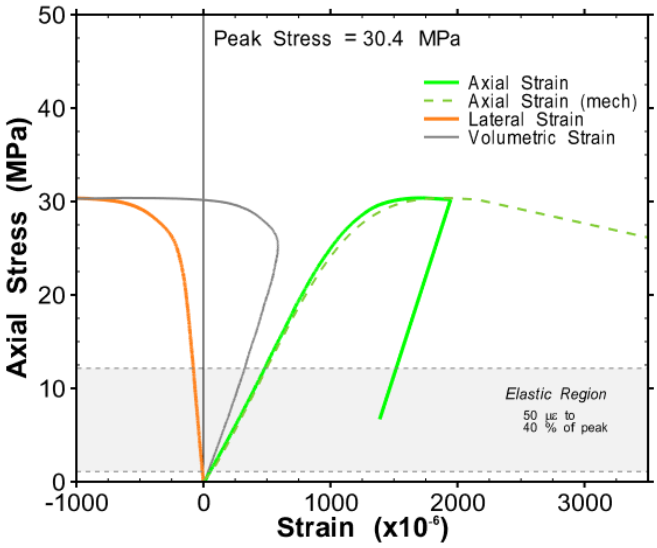

Test Information:

Load Control = 1.96 kN/s
Time to Failure = 2.1 min

Specimen Dimensions:

Length = 198.59 mm
Diameter = 101.61 mm

Electrical Gauges:

Young's modulus = 25.6 GPa
Poisson's ratio = 0.17

C2000-20E.dat

P-002797.004_UCS_Batch 1_R0.mView

Failure Description: axial splitting, shear

Pre-Test

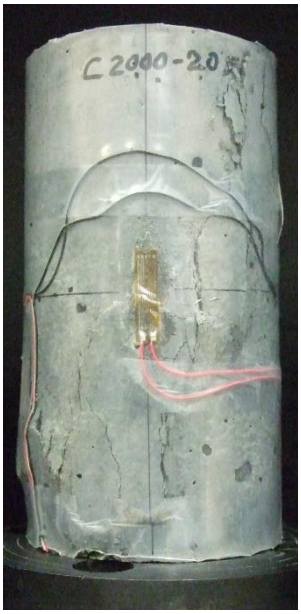

Post-Test

Specimen ID: **C2000-20F**
Test: **UCS**

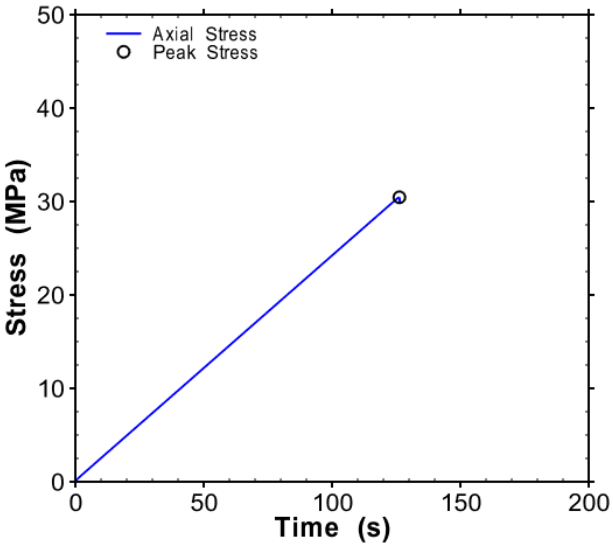

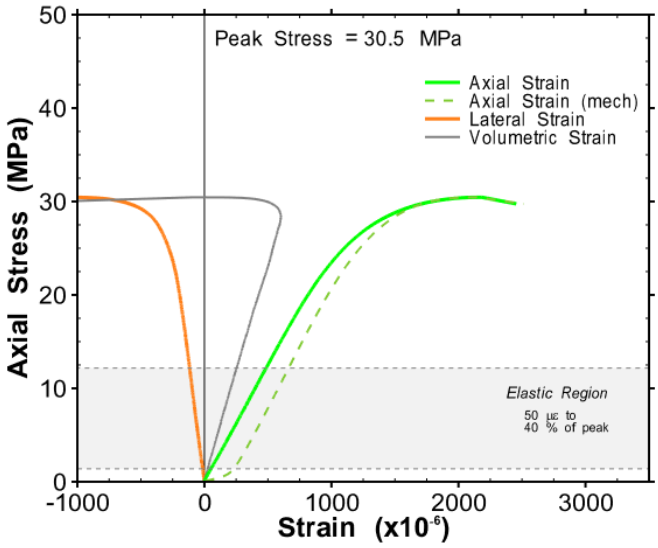

Test Information:

Load Control = 1.96 kN/s
Time to Failure = 2.1 min

Specimen Dimensions:

Length = 198.58 mm
Diameter = 101.77 mm

Electrical Gauges:

Young's modulus = 25.0 GPa
Poisson's ratio = 0.24

C2000-20F.dat

P-002797.004_UCS_Batch 1_R0.mView

Failure Description: axial splitting, shear

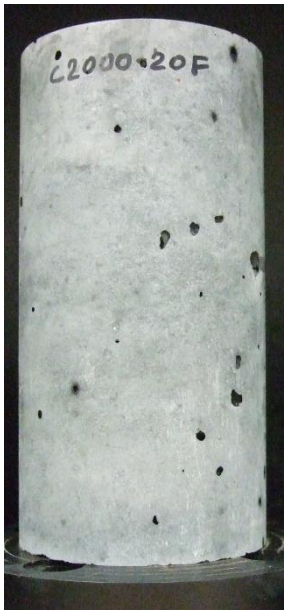

Pre-Test

Post-Test

Specimen ID: **C2000-20G**
Test: **UCS**

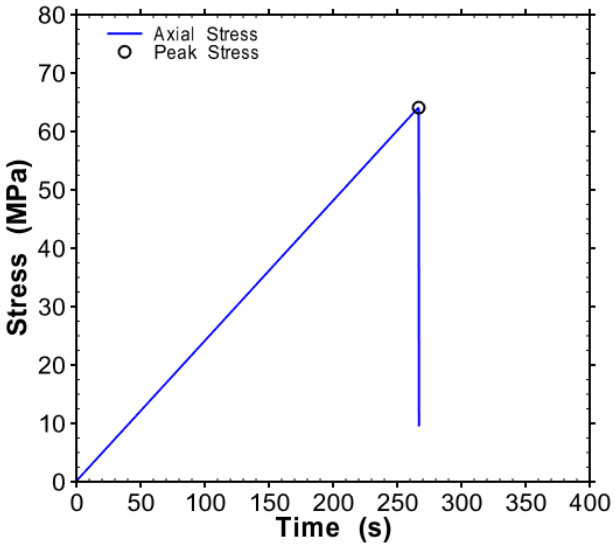

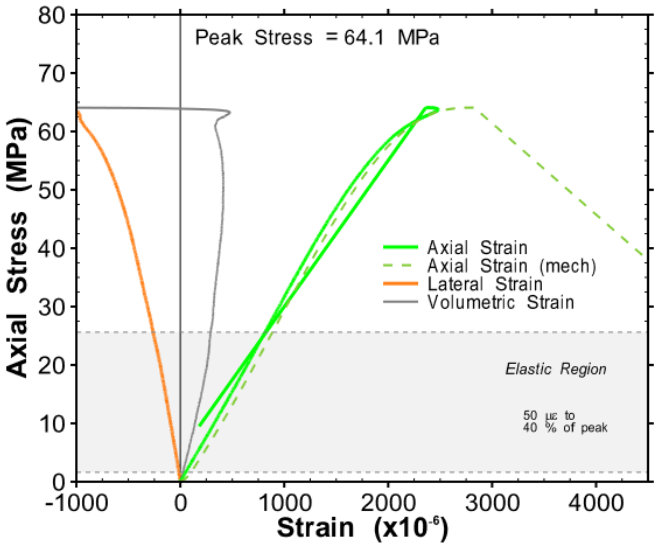

Test Information:

Load Control = 1.96 kN/s
Time to Failure = 4.4 min

Specimen Dimensions:

Length = 198.74 mm
Diameter = 101.96 mm

Electrical Gauges:

Young's modulus = 31.4 GPa
Poisson's ratio = 0.32

C2000-20G.dat

P-002797.004_UCS_Batch 2_R0.mView

Failure Description: axial splitting

Pre-Test

Post-Test

Specimen ID: **C2000-20H**
Test: **UCS**

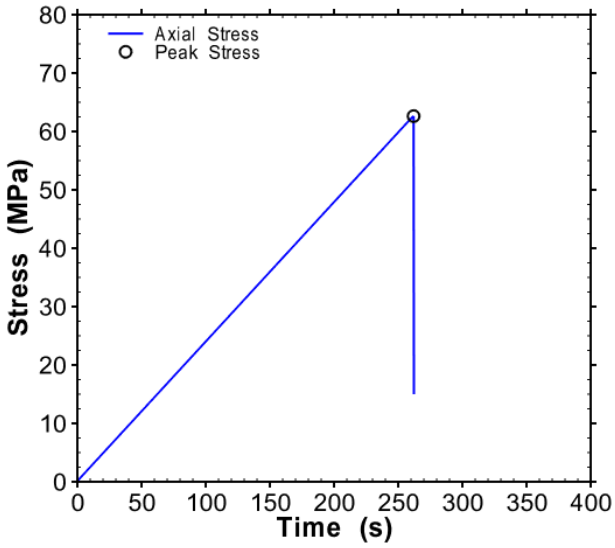

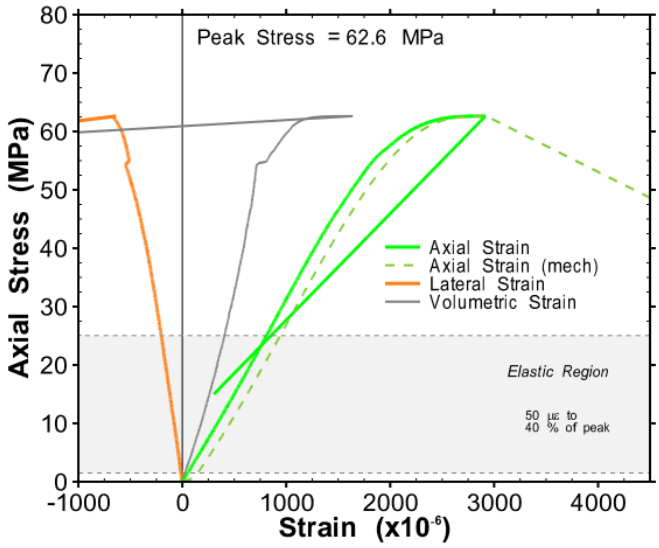

Test Information:

Load Control = 1.96 kN/s
Time to Failure = 4.4 min

Specimen Dimensions:

Length = 198.73 mm
Diameter = 102.21 mm

Electrical Gauges:

Young's modulus = 31.0 GPa
Poisson's ratio = 0.25

C2000-20H.dat

P-002797.004_UCS_Batch 2_R0.mView

Failure Description: axial splitting

Pre-Test

Post-Test

Specimen ID: **C2000-20I**
Test: **UCS**

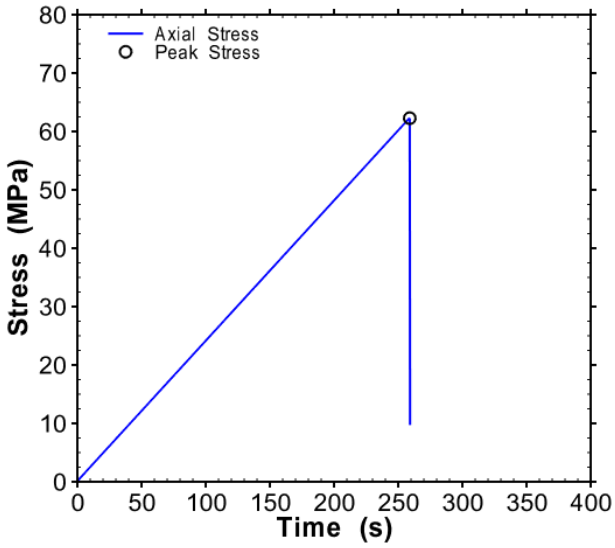

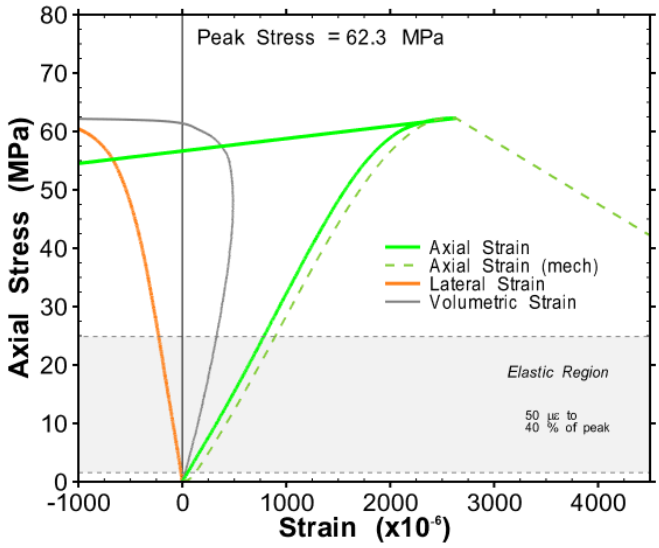

Test Information:

Load Control = 1.96 kN/s
Time to Failure = 4.3 min

Specimen Dimensions:

Length = 198.73 mm
Diameter = 101.92 mm

Electrical Gauges:

Young's modulus = 31.8 GPa
Poisson's ratio = 0.29

C2000-20I.dat

P-002797.004_UCS_Batch 2_R0.mView

Failure Description: axial splitting

Pre-Test

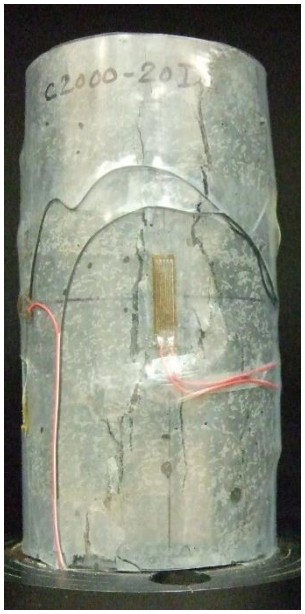

Post-Test

Specimen ID: **C2000-20J**
Test: **UCS**

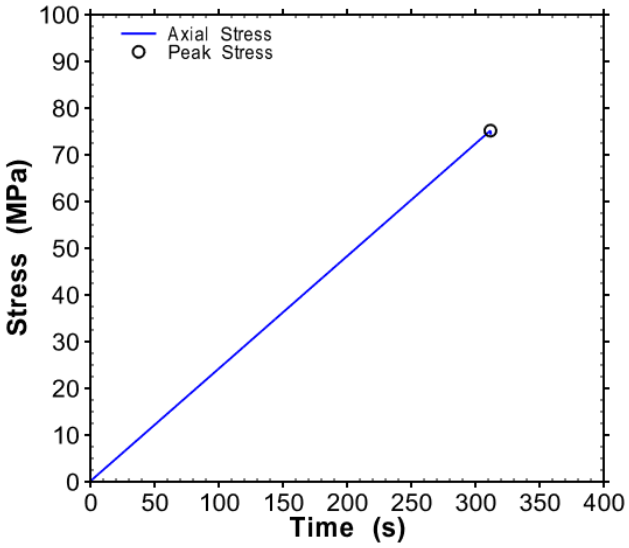

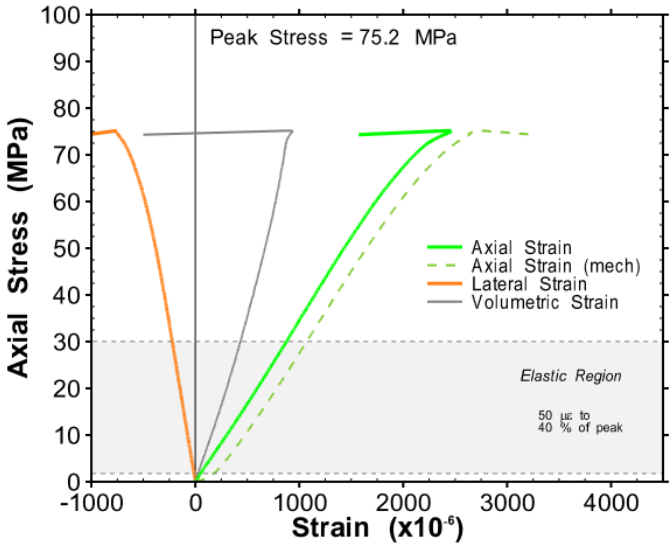

Test Information:

Load Control = 1.96 kN/s
Time to Failure = 5.2 min

Specimen Dimensions:

Length = 198.64 mm
Diameter = 101.80 mm

Electrical Gauges:

Young's modulus = 34.1 GPa
Poisson's ratio = 0.25

C2000-20J.dat

P-002797.004_UCS_Batch 3_R0.mView

Failure Description: axial splitting

Pre-Test

Post-Test

Specimen ID: **C2000-20K**
Test: **UCS**

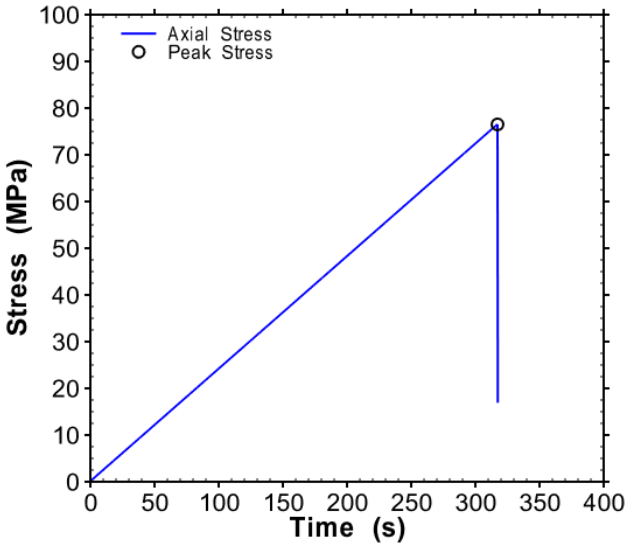

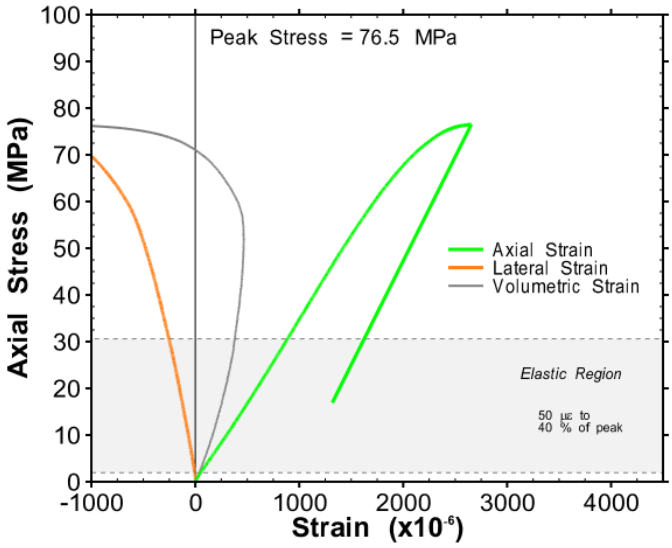

Test Information:

Load Control = 1.96 kN/s
Time to Failure = 5.3 min

Specimen Dimensions:

Length = 198.72 mm
Diameter = 101.77 mm

Electrical Gauges:

Young's modulus = 34.3 GPa
Poisson's ratio = 0.30

C2000-20K.dat

P-002797.004_UCS_Batch 3_R0.mView

Failure Description: axial splitting

Pre-Test

Post-Test

Specimen ID: **C2000-20L**
Test: **UCS**

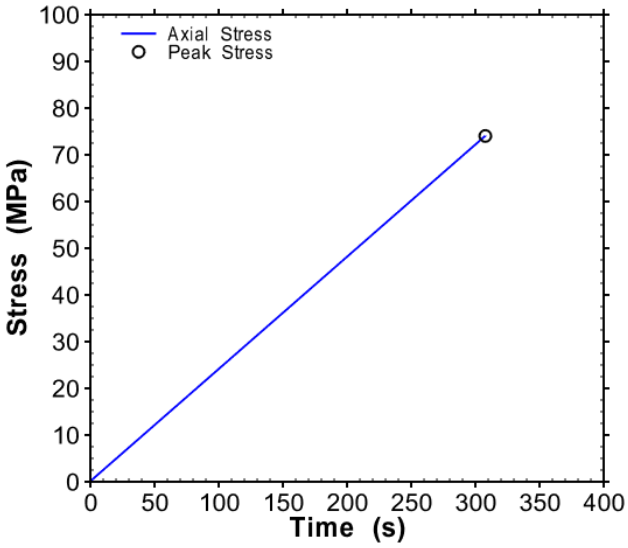

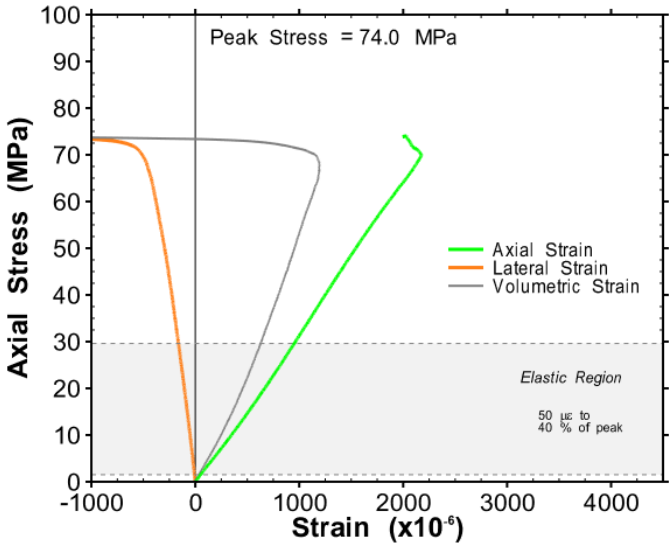

Test Information:

Load Control = 1.96 kN/s
Time to Failure = 5.1 min

Specimen Dimensions:

Length = 198.72 mm
Diameter = 101.92 mm

Electrical Gauges:

Young's modulus = 31.2 GPa
Poisson's ratio = 0.17

C2000-20L.dat

P-002797.004_UCS_Batch 3_R0.mView

Failure Description: axial splitting

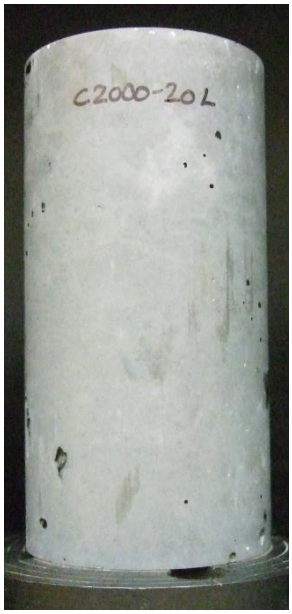

Pre-Test

Post-Test

Specimen ID: **C1074-20D**
Test: **UCS**

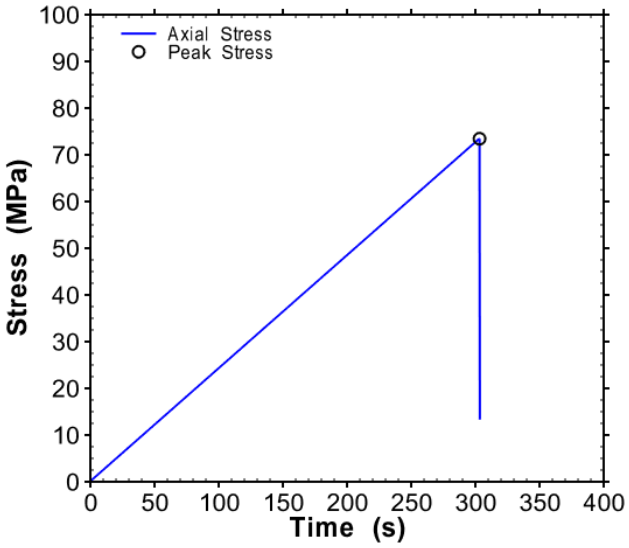

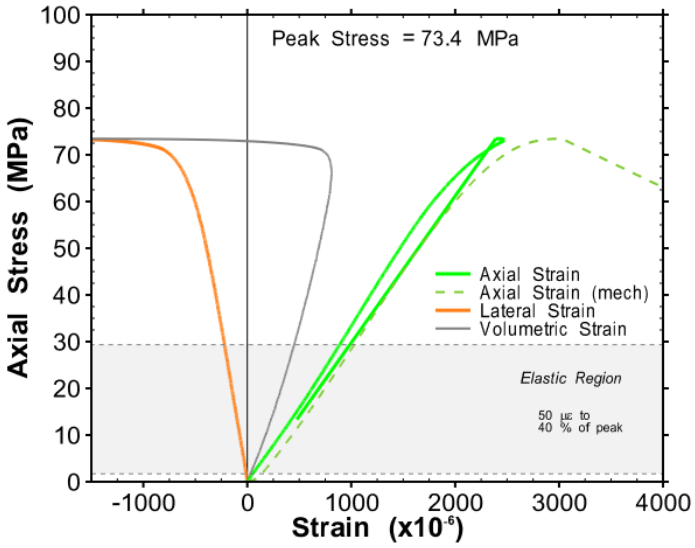

Test Information:

Load Control = 1.96 kN/s
Time to Failure = 5.0 min

Specimen Dimensions:

Length = 197.99 mm
Diameter = 101.55 mm

Electrical Gauges:

Young's modulus = 33.0 GPa
Poisson's ratio = 0.25

C1074-20D.dat

P-002797.004_UCS_Batch 4_R0.mView

Failure Description: axial splitting, Y-type failure

Pre-Test

Post-Test

Specimen ID: **C1074-20E**
Test: **UCS**

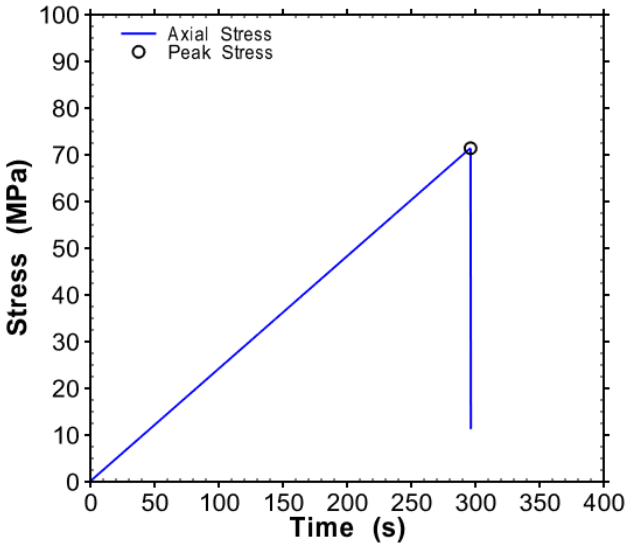

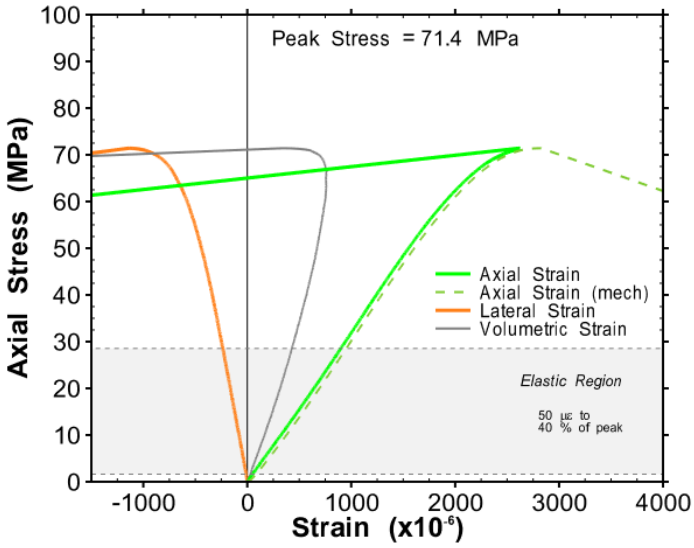

Test Information:

Load Control = 1.96 kN/s
Time to Failure = 4.9 min

Specimen Dimensions:

Length = 197.99 mm
Diameter = 101.80 mm

Electrical Gauges:

Young's modulus = 31.6 GPa
Poisson's ratio = 0.26

C1074-20E.dat

P-002797.004_UCS_Batch 4_R0.mView

Failure Description: axial splitting, shear

Pre-Test

Post-Test

Specimen ID: **C1074-20F**
Test: **UCS**

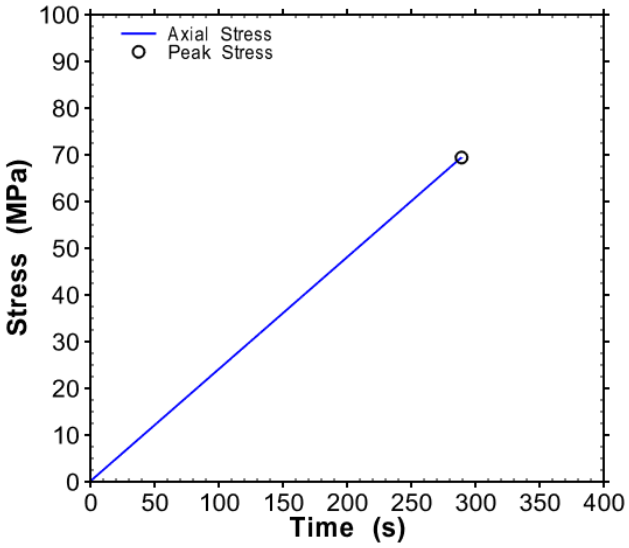

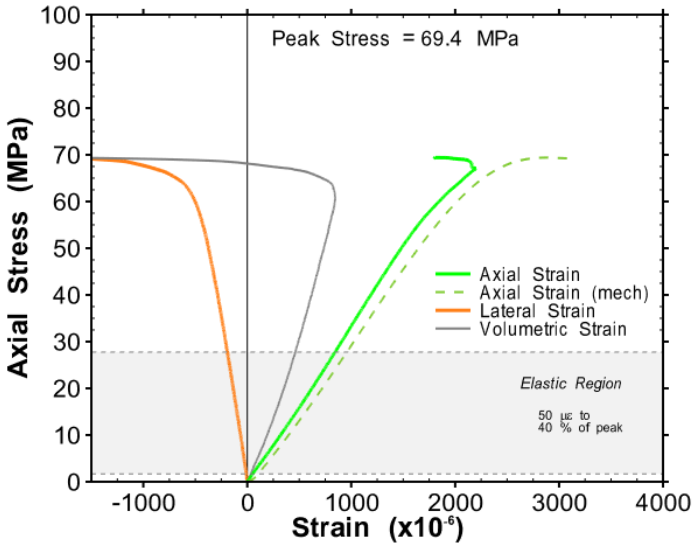

Test Information:

Load Control = 1.96 kN/s
Time to Failure = 4.8 min

Specimen Dimensions:

Length = 197.99 mm
Diameter = 102.02 mm

Electrical Gauges:

Young's modulus = 32.9 GPa
Poisson's ratio = 0.23

C1074-20F.dat

P-002797.004_UCS_Batch 4_R0.mView

Failure Description: axial splitting, shear

Pre-Test

Post-Test

Specimen ID: **C1074-20G**
Test: **UCS**

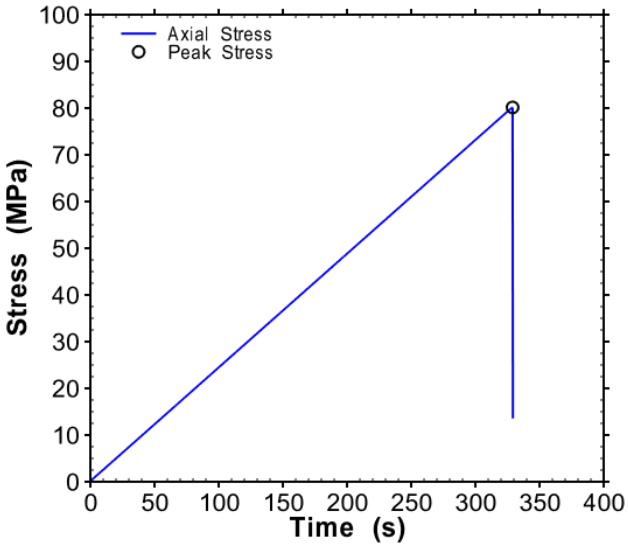

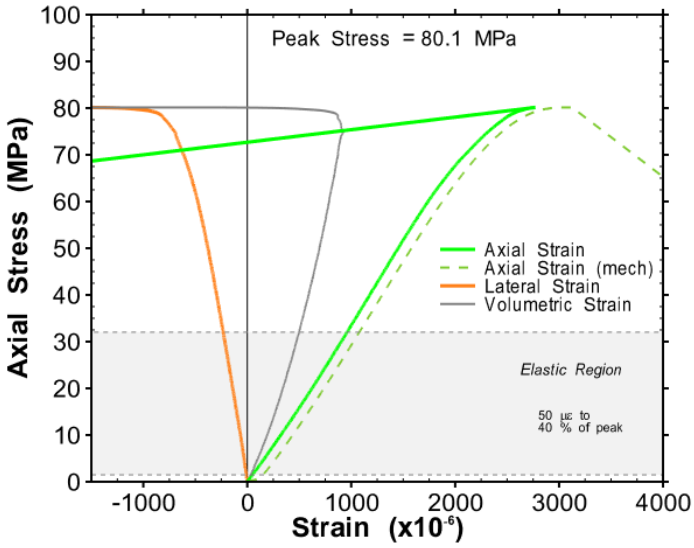

Test Information:

Load Control = 1.96 kN/s
Time to Failure = 5.5 min

Specimen Dimensions:

Length = 198.49 mm
Diameter = 101.24 mm

Electrical Gauges:

Young's modulus = 33.7 GPa
Poisson's ratio = 0.25

C1074-20G.dat

P-002797.004_UCS_Batch 5_R0.mView

Failure Description: axial splitting, Y-type failure

Pre-Test

Post-Test

Specimen ID: **C1074-20H**
Test: **UCS**

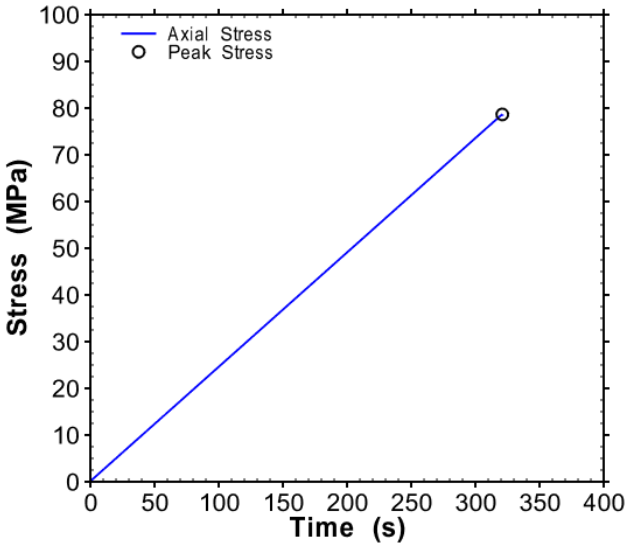

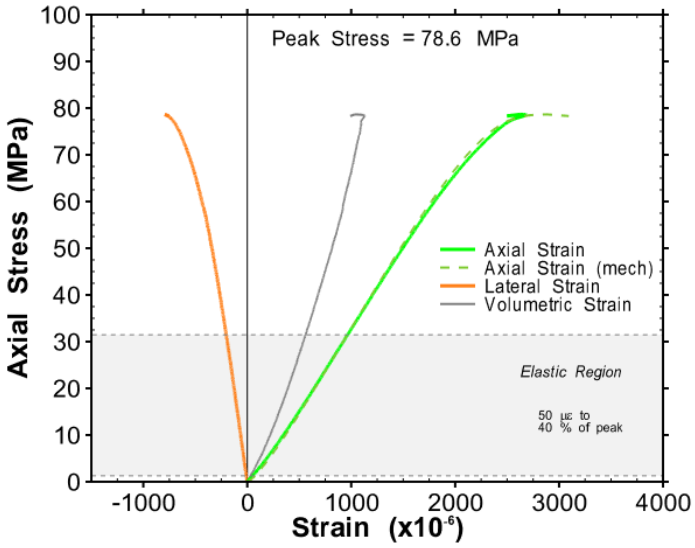

Test Information:

Load Control = 1.96 kN/s
Time to Failure = 5.3 min

Specimen Dimensions:

Length = 198.49 mm
Diameter = 101.59 mm

Electrical Gauges:

Young's modulus = 33.6 GPa
Poisson's ratio = 0.21

C1074-20H-B.dat

P-002797.004_UCS_Batch 5_R0.mView

Failure Description: shear and axial splitting

Pre-Test

Post-Test

Specimen ID: **C1074-20I**
Test: **UCS**

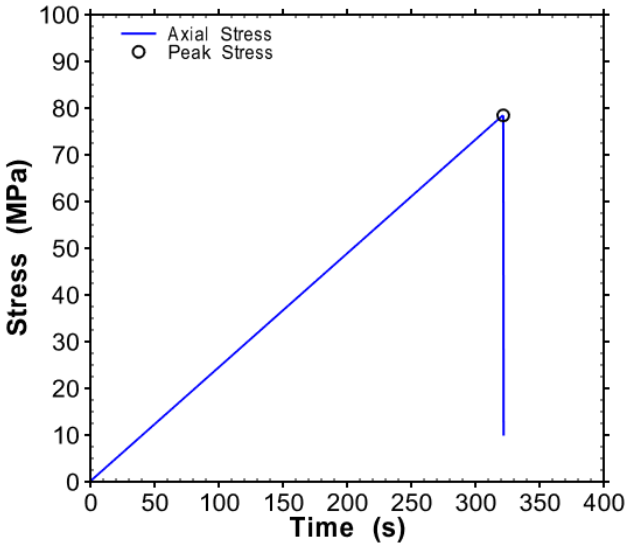

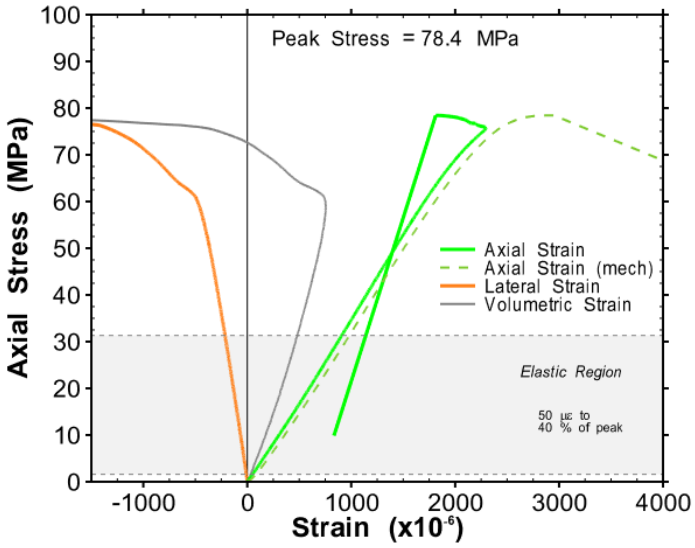

Test Information:

Load Control = 1.96 kN/s
Time to Failure = 5.4 min

Specimen Dimensions:

Length = 198.50 mm
Diameter = 101.82 mm

Electrical Gauges:

Young's modulus = 34.7 GPa
Poisson's ratio = 0.24

C1074-20I.dat

P-002797.004_UCS_Batch 5_R0.mView

Failure Description: axial splitting, shear

Pre-Test

Post-Test

Specimen ID: **C1074-20J**
Test: **UCS**

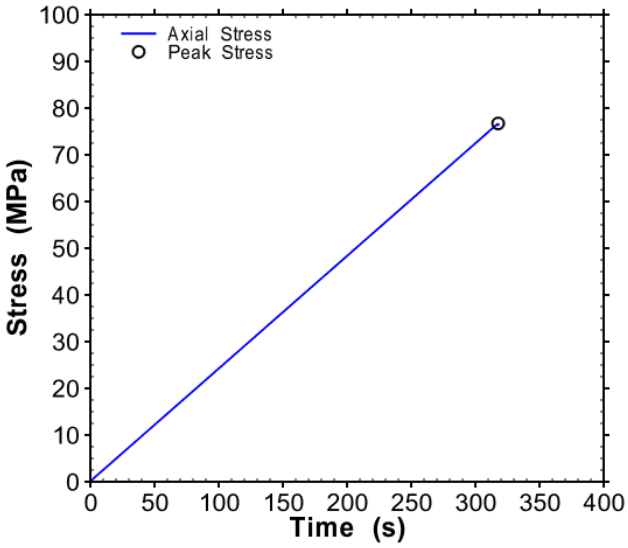

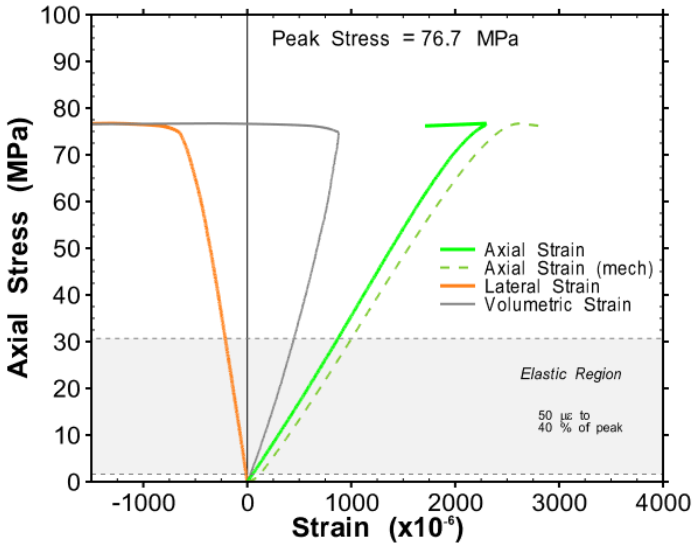

Test Information:

Load Control = 1.96 kN/s
Time to Failure = 5.3 min

Specimen Dimensions:

Length = 198.74 mm
Diameter = 101.74 mm

Electrical Gauges:

Young's modulus = 35.4 GPa
Poisson's ratio = 0.25

C1074-20J.dat

P-002797.004_UCS_Batch 6_R0.mView

Failure Description: axial splitting, shear

Pre-Test

Post-Test

Specimen ID: **C1074-20K**
Test: **UCS**

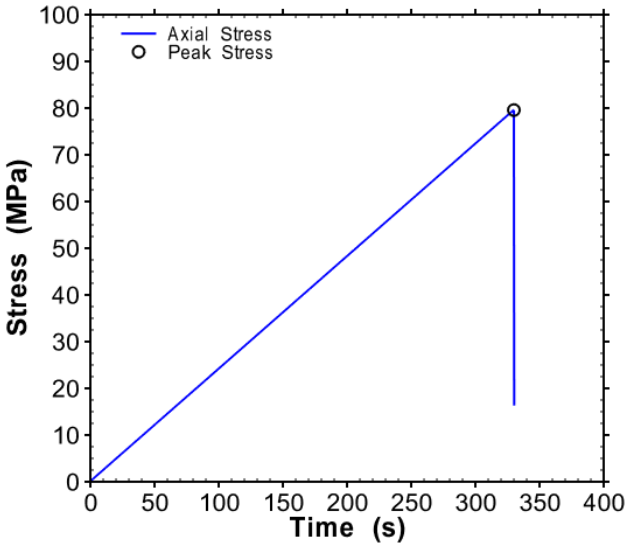

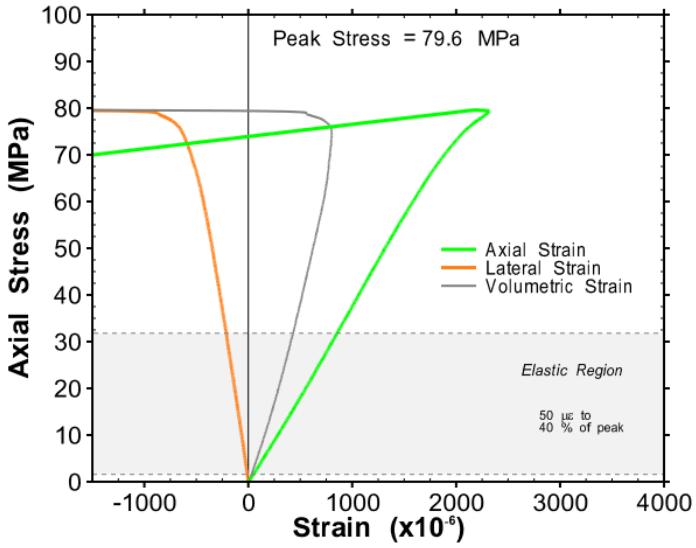

Test Information:

Load Control = 1.96 kN/s
Time to Failure = 5.5 min

Specimen Dimensions:

Length = 198.73 mm
Diameter = 101.77 mm

Electrical Gauges:

Young's modulus = 37.6 GPa
Poisson's ratio = 0.25

C1074-20K.dat

P-002797.004_UCS_Batch 6_R0.mView

Failure Description: axial splitting, shear

Pre-Test

Post-Test

Specimen ID: **C1074-20L**
Test: **UCS**

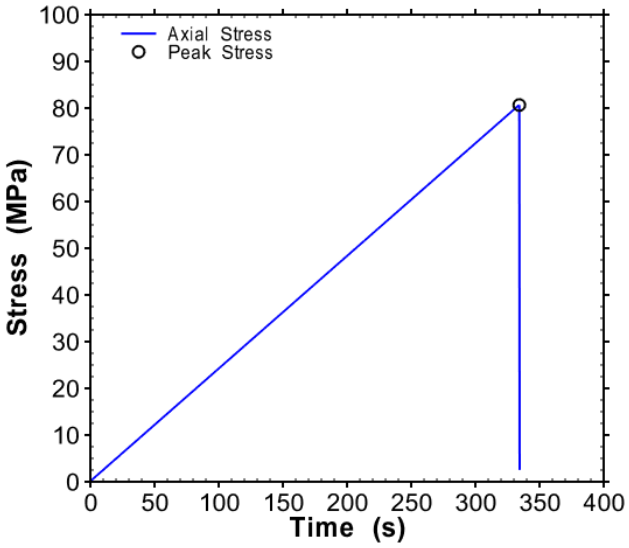

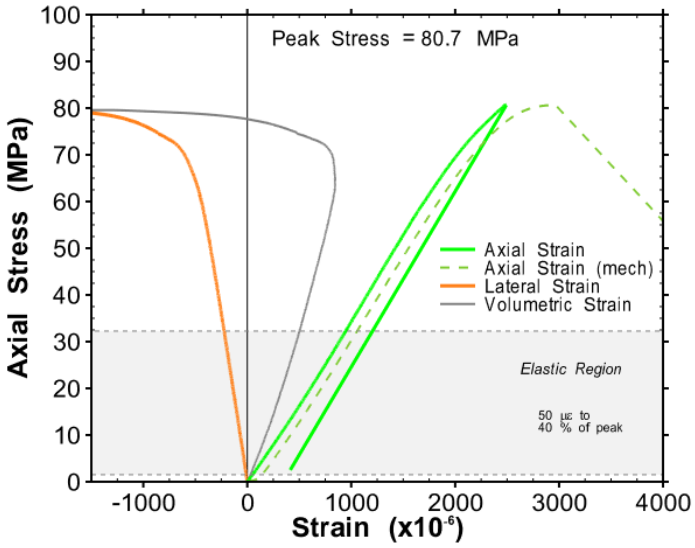

Test Information:

Load Control = 1.96 kN/s
Time to Failure = 5.6 min

Specimen Dimensions:

Length = 198.73 mm
Diameter = 101.74 mm

Electrical Gauges:

Young's modulus = 34.3 GPa
Poisson's ratio = 0.24

C1074-20L.dat

P-002797.004_UCS_Batch 6_R0.mView

Failure Description: axial splitting, shear

Pre-Test

Post-Test

Attachment C – CI Interpretation

Specimen ID: **C2000-20D**

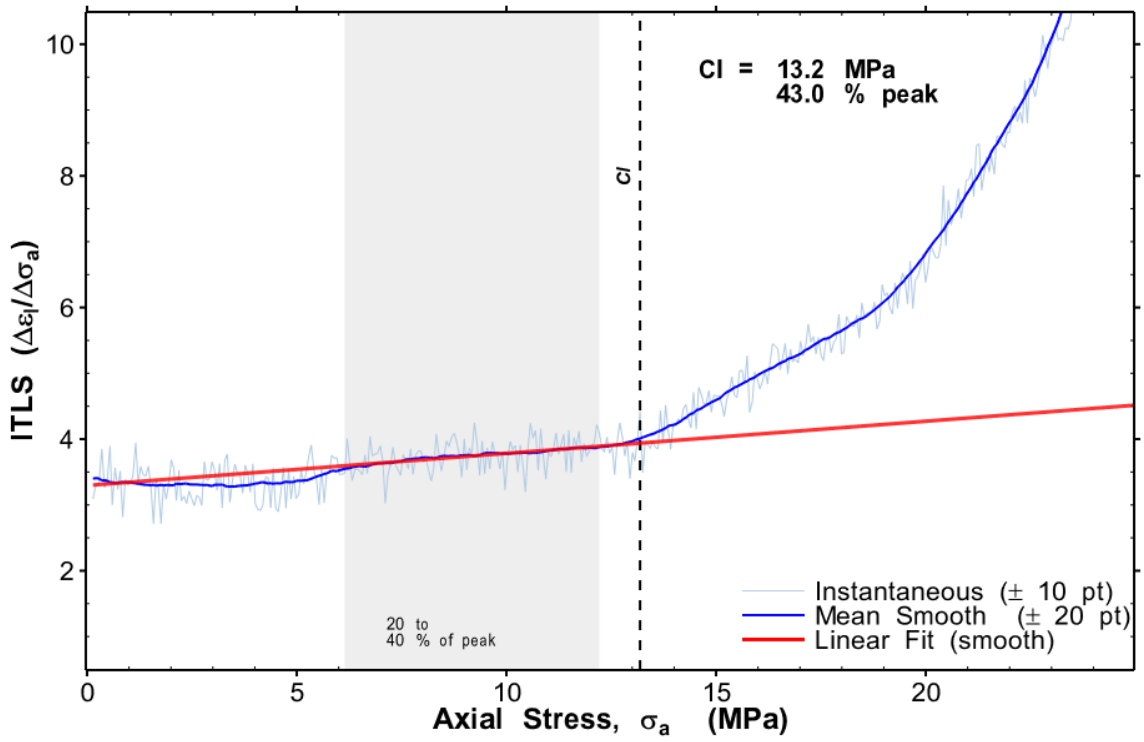

C2000-20D.dat

P-002797.004_UCS_Batch 1_R0.mView

Specimen ID: **C2000-20E**

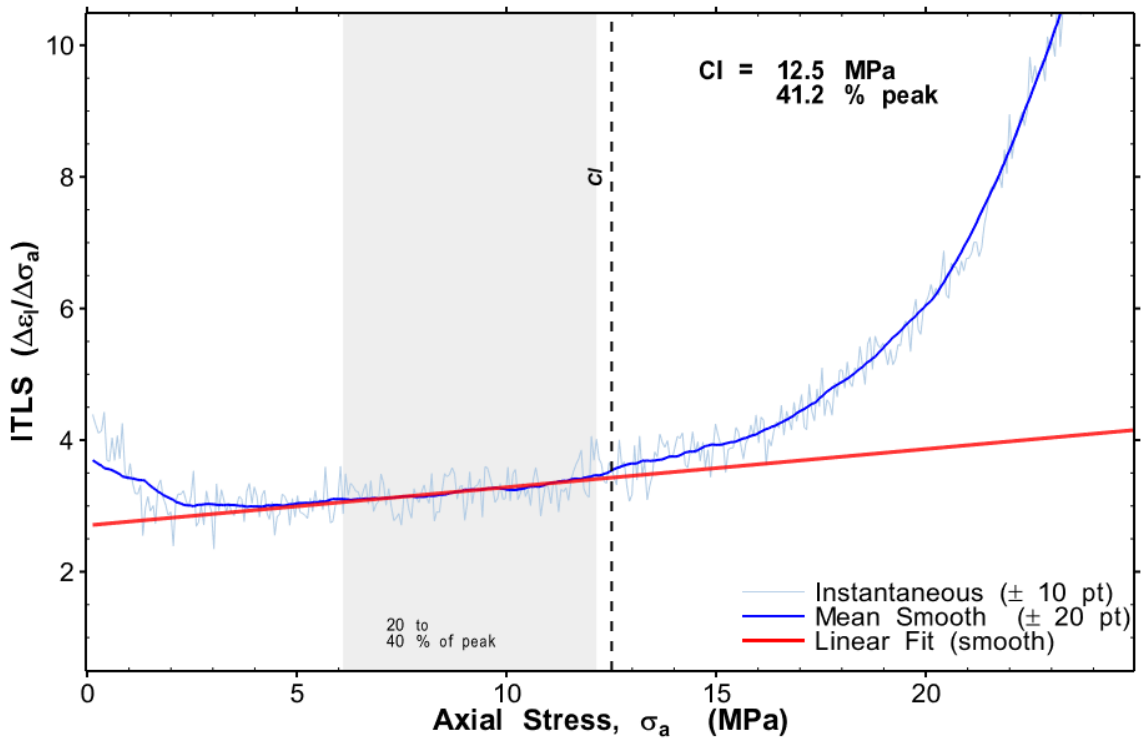

C2000-20E.dat

P-002797.004_UCS_Batch 1_R0.mView

Specimen ID: **C2000-20F**

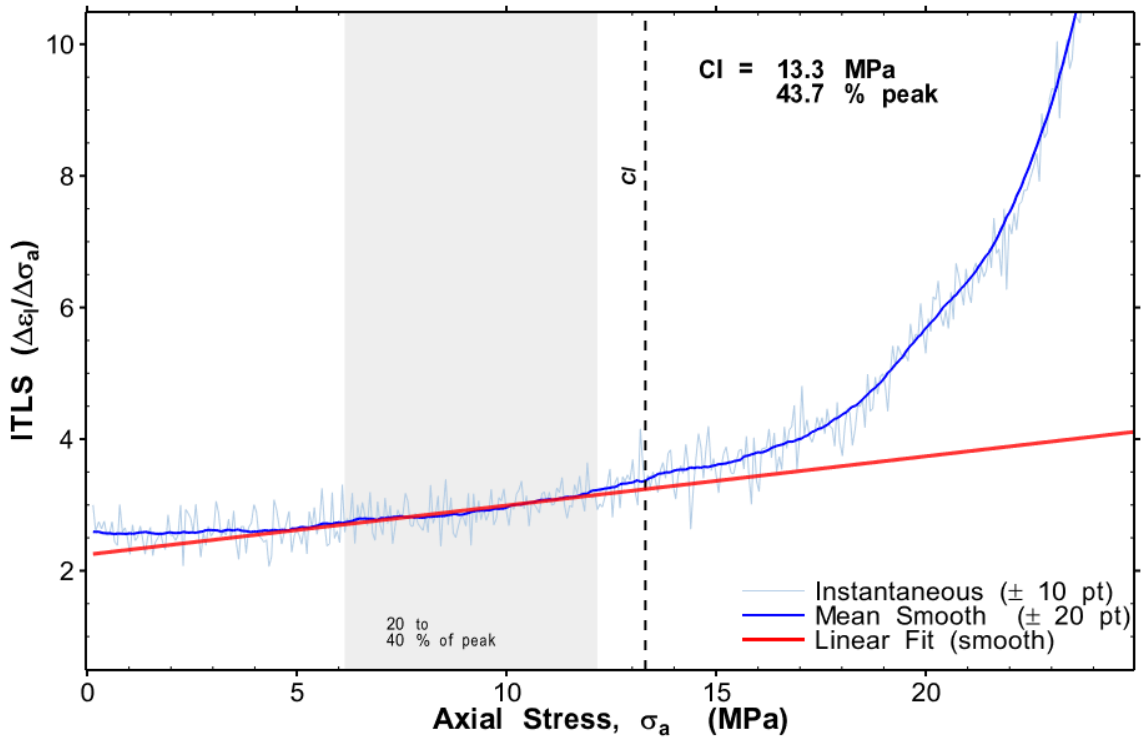

C2000-20F.dat

P-002797.004_UCS_Batch 1_R0.mView

Specimen ID: **C2000-20G**

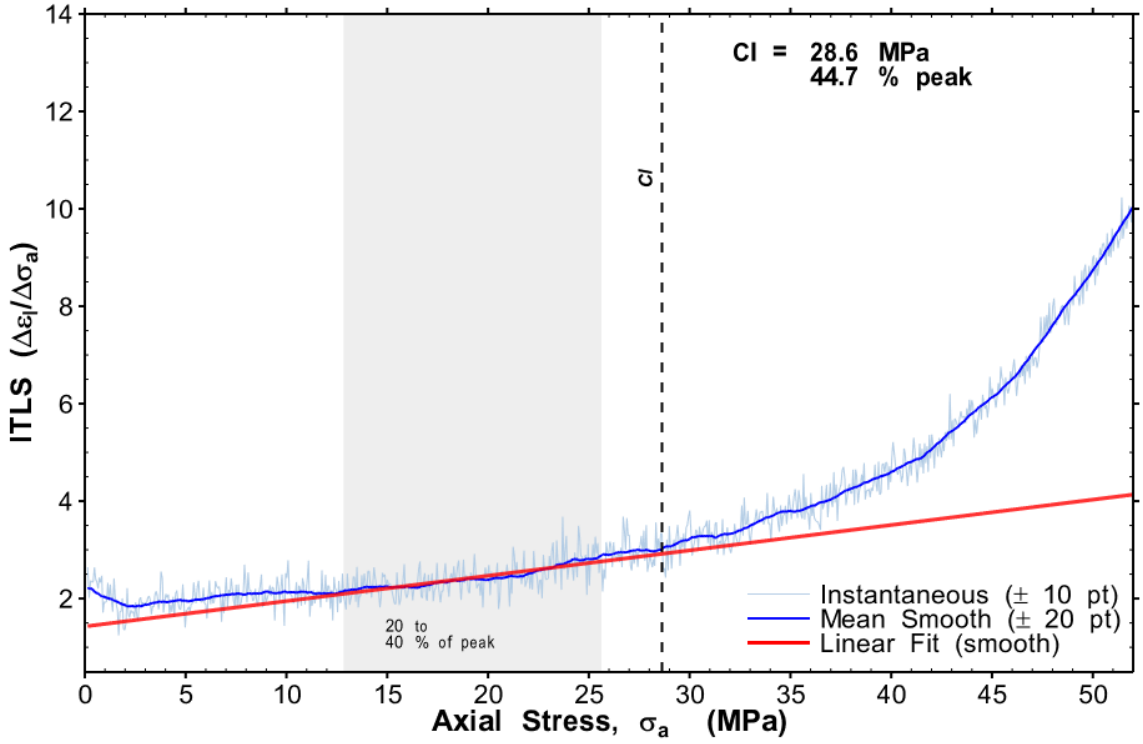

C2000-20G.dat

P-002797.004_UCS_Batch 2_R0.mView

Specimen ID: **C2000-20H**

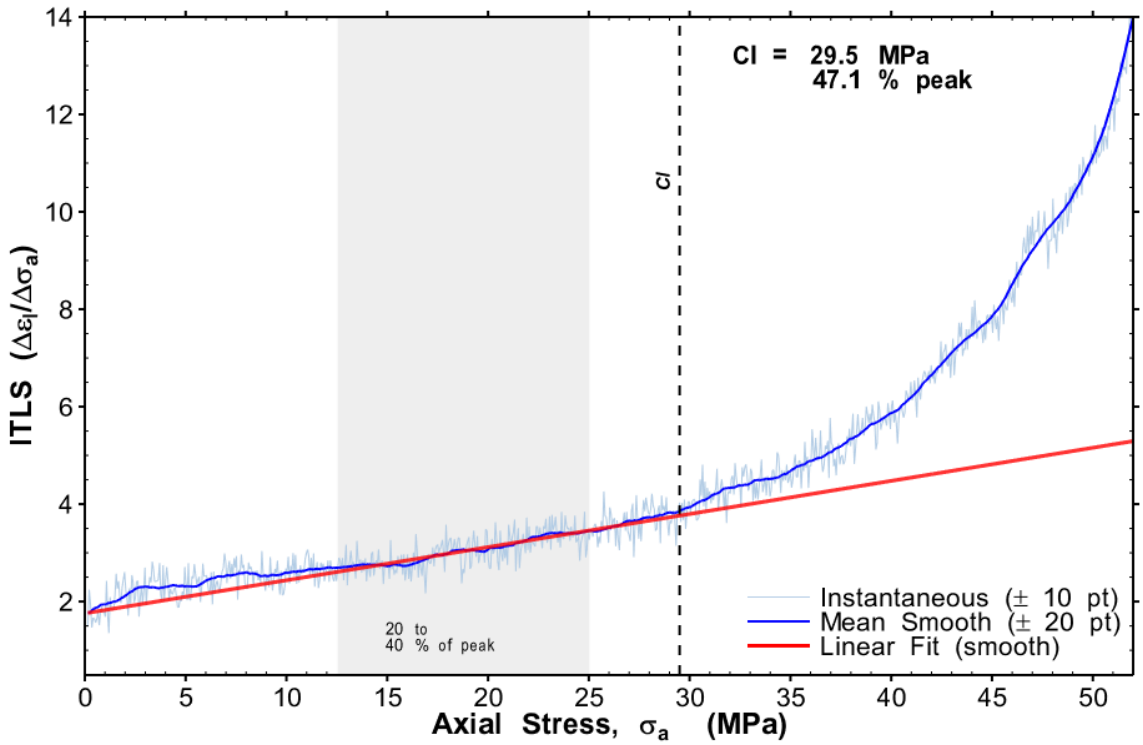

C2000-20H.dat

P-002797.004_UCS_Batch 2_R0.mView

Specimen ID: **C2000-20I**

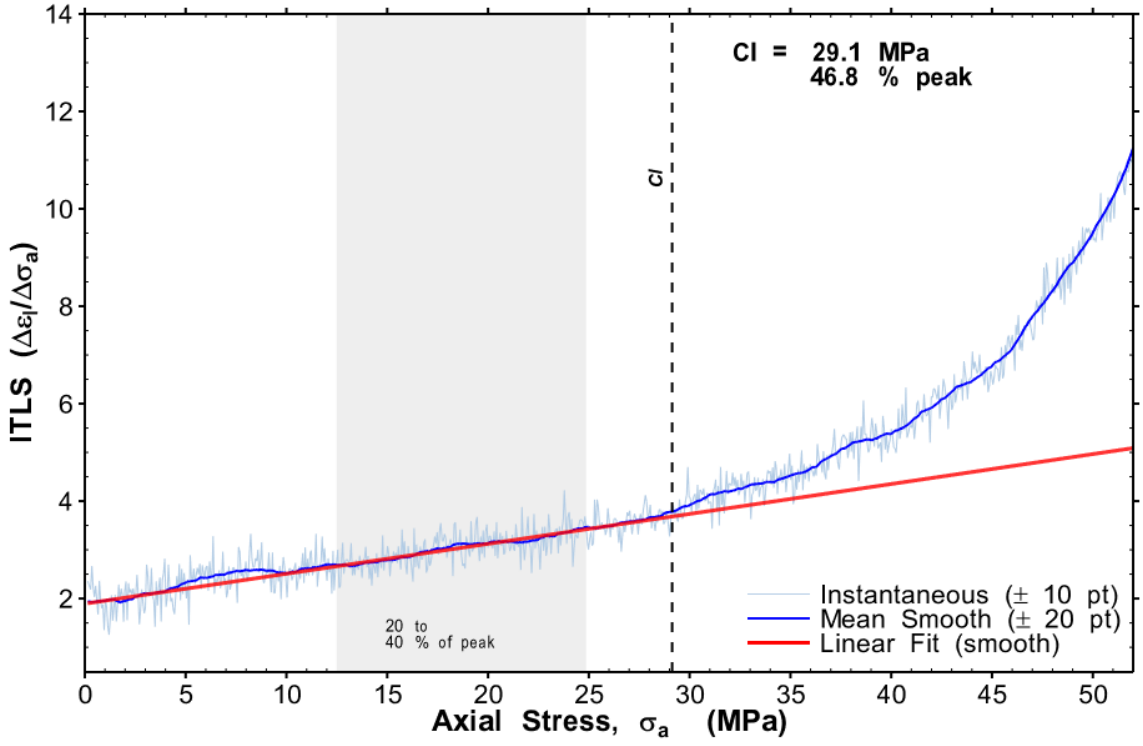

C2000-20I.dat

P-002797.004_UCS_Batch 2_R0.mView

Specimen ID: **C2000-20J**

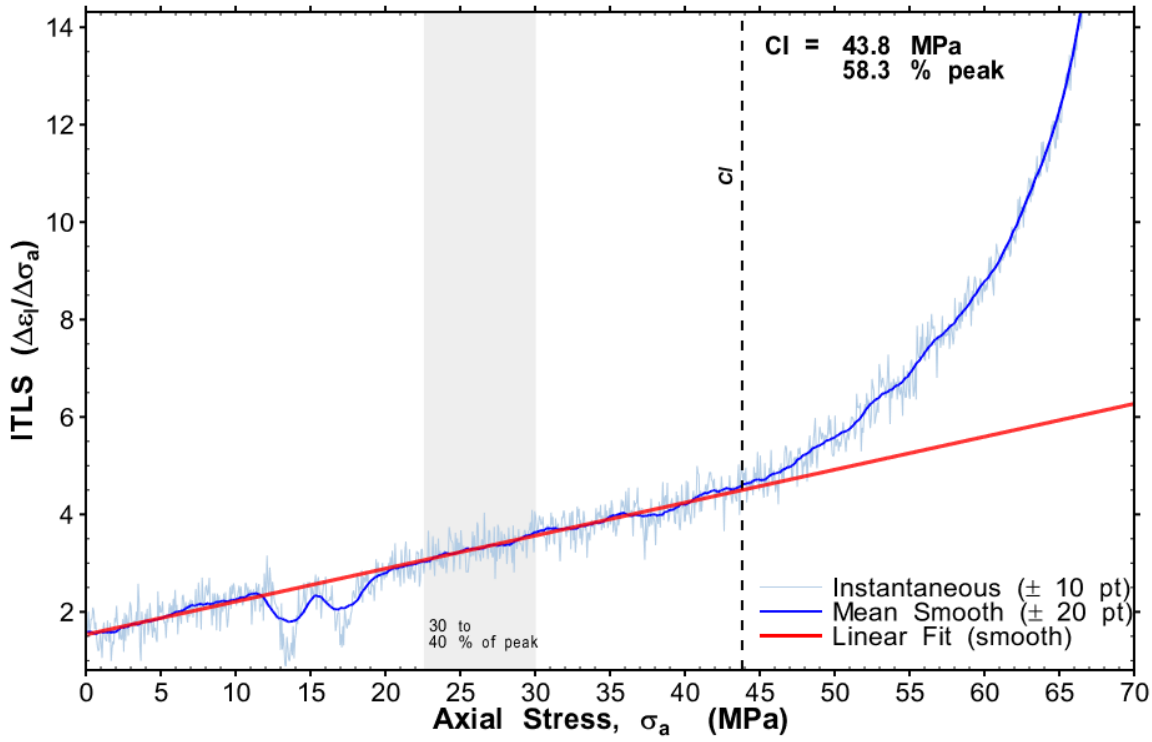

C2000-20J.dat

P-002797.004_UCS_Batch 3_R0.mView

Specimen ID: **C2000-20K**

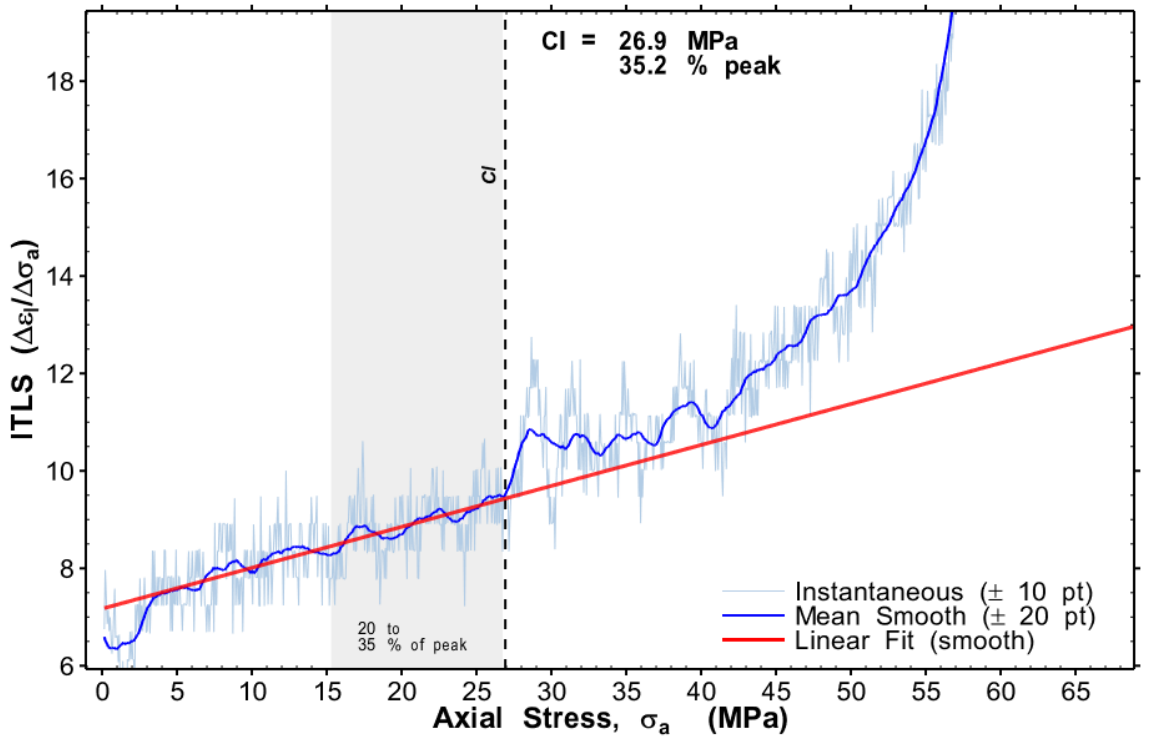

C2000-20K.dat

P-002797.004_UCS_Batch 3_R0.mView

Specimen ID: **C2000-20L**

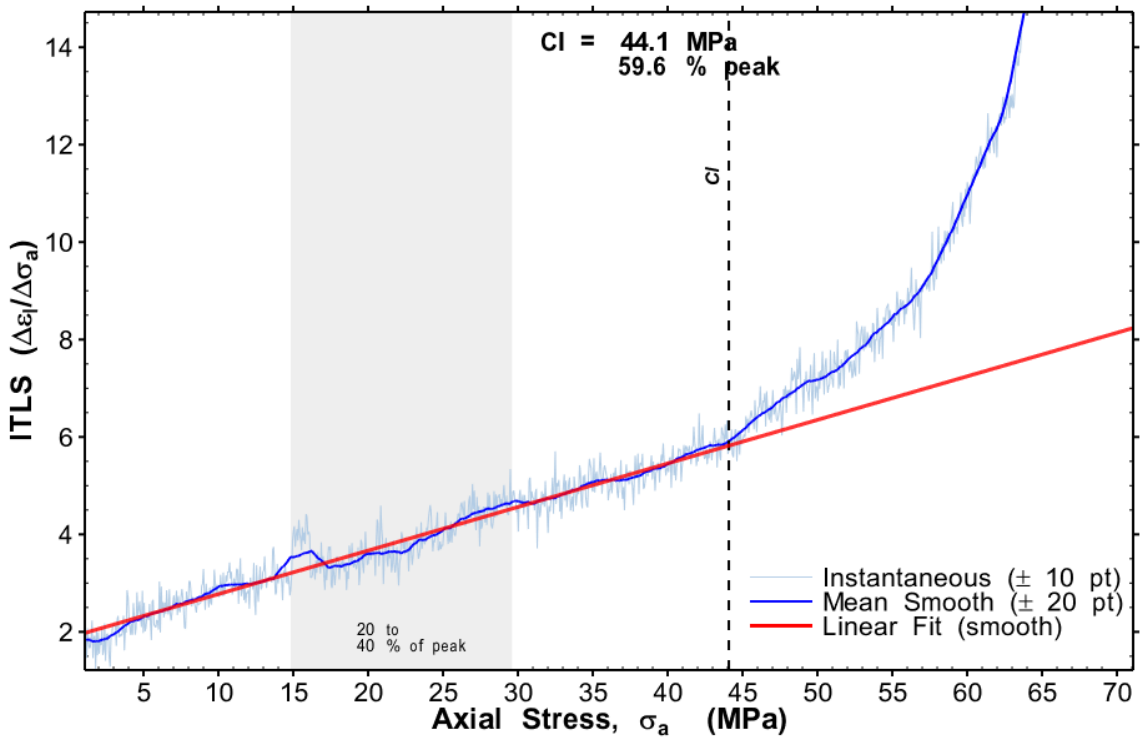

C2000-20L.dat

P-002797.004_UCS_Batch 3_R0.mView

Specimen ID: **C1074-20D**

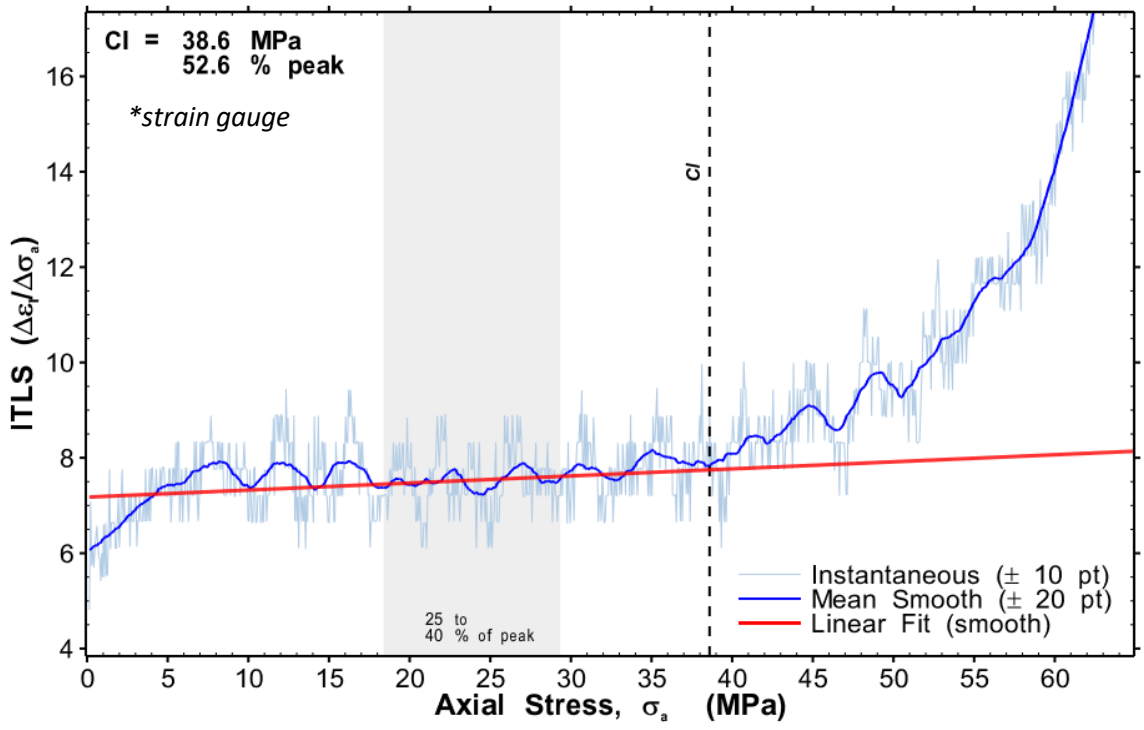

C1074-20D.dat

P-002797.004_UCS_Batch 4_R0.mView

Specimen ID: **C1074-20E**

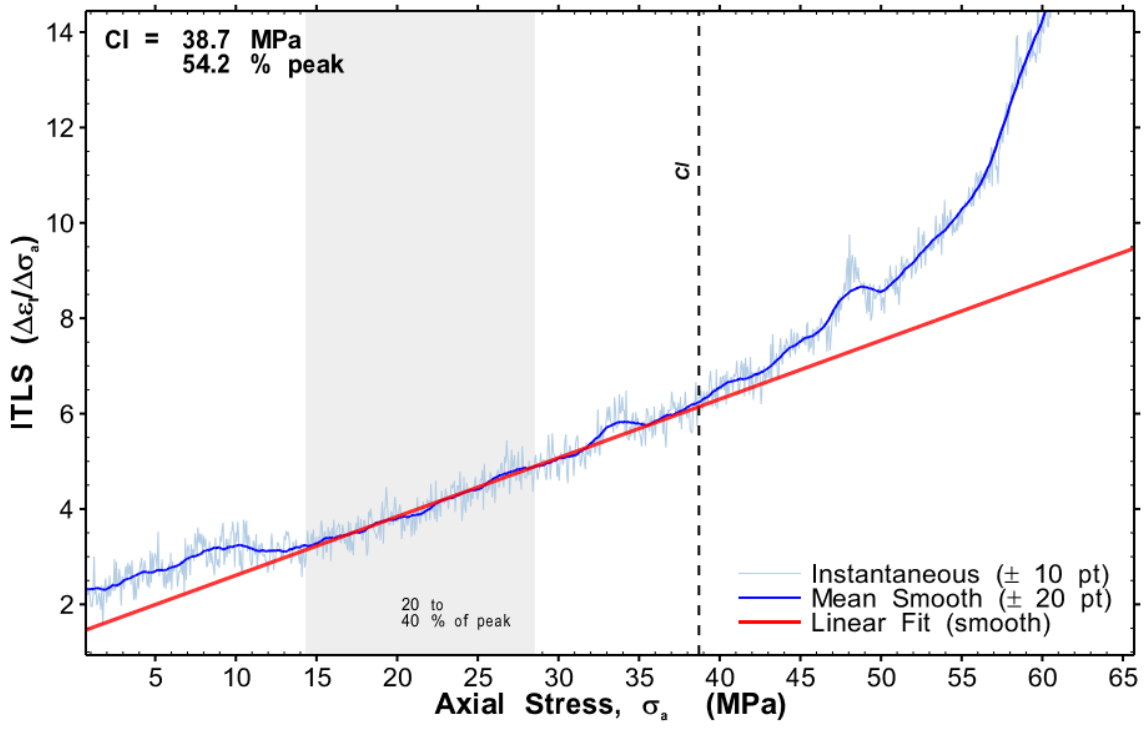

C1074-20E.dat

P-002797.004_UCS_Batch 4_R0.mView

Specimen ID: **C1074-20F**

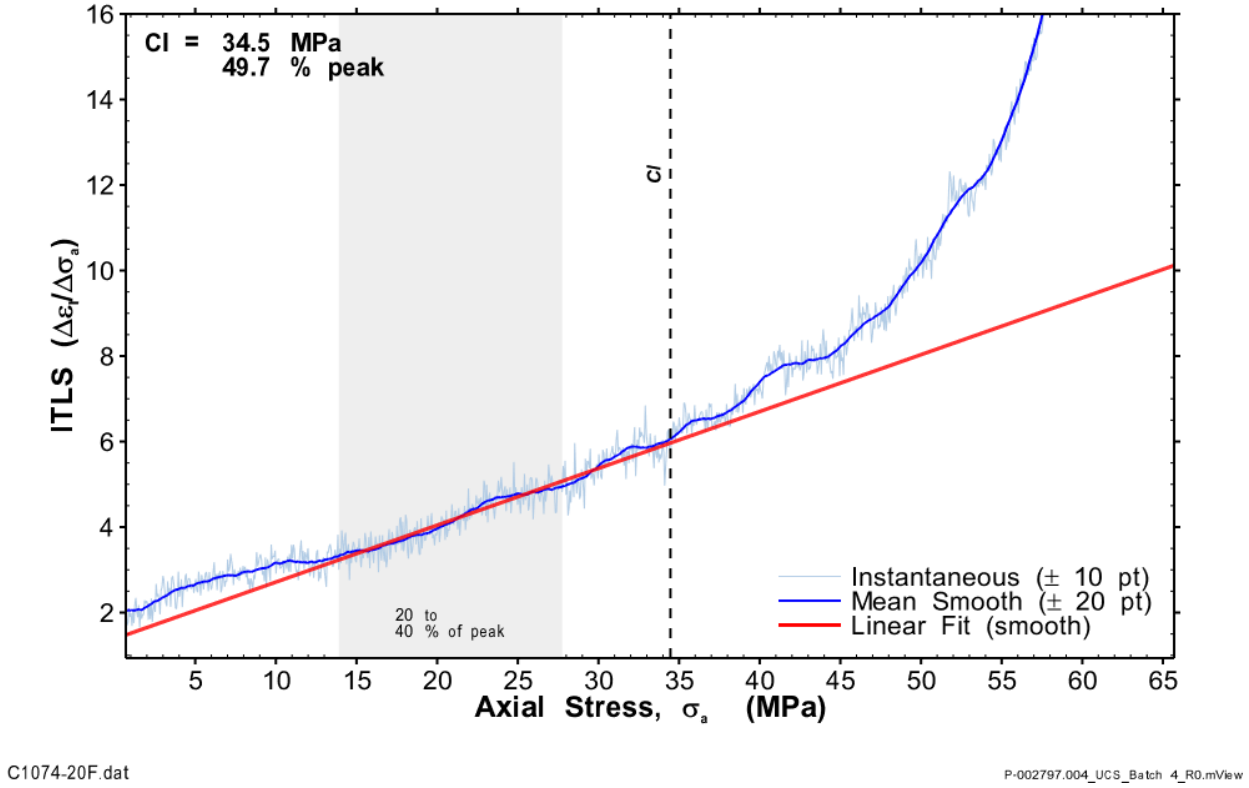

Specimen ID: **C1074-20G**

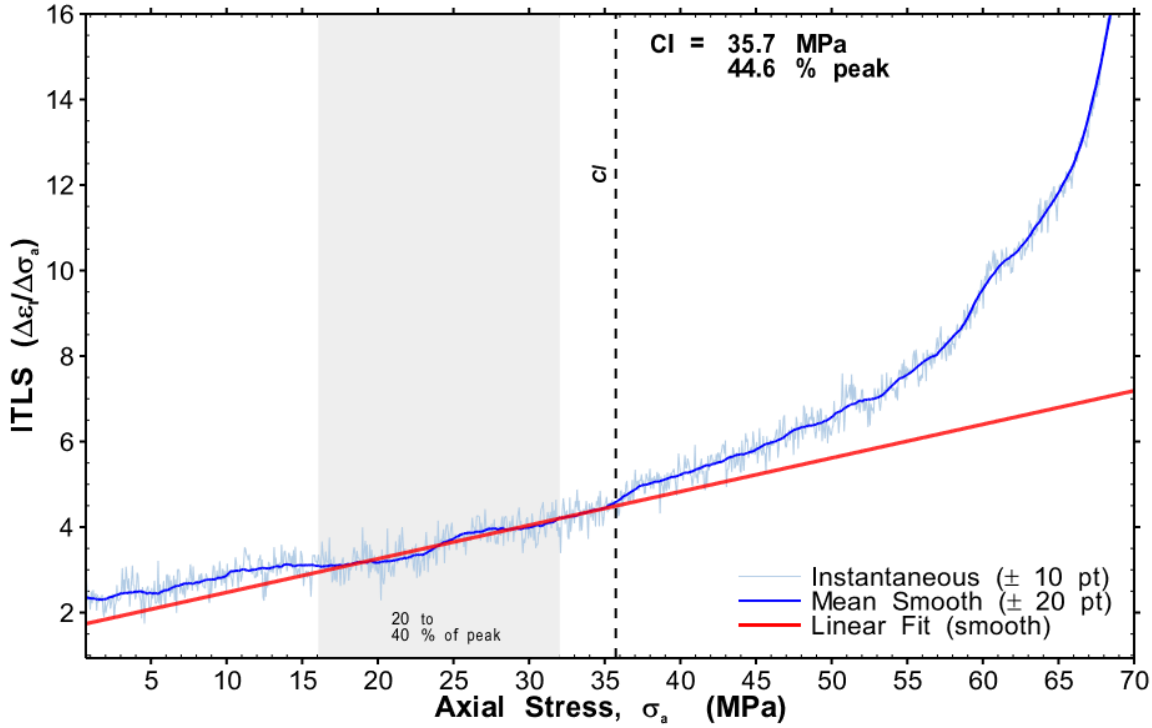

C1074-20G.dat

P-002797.004_UCS_Batch 5_R0.mView

Specimen ID: **C1074-20H**

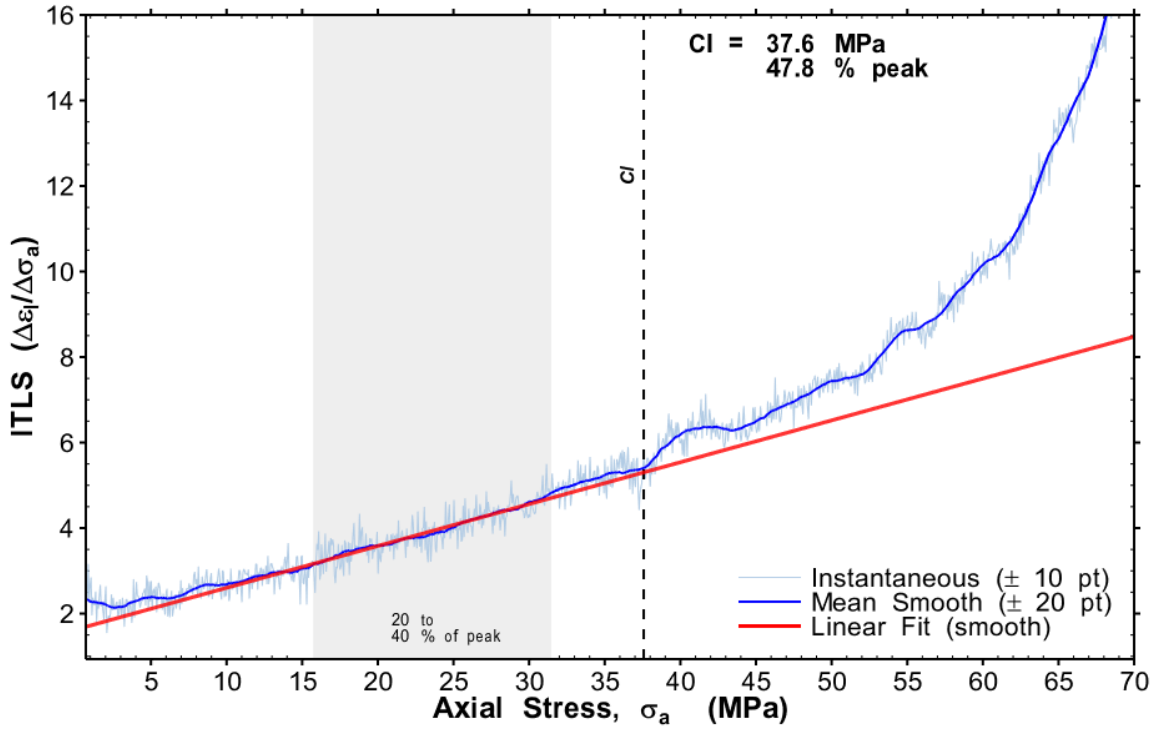

C1074-20H-B.dat

P-002797.004_UCS_Batch 5_R0.mView

Specimen ID: **C1074-20I**

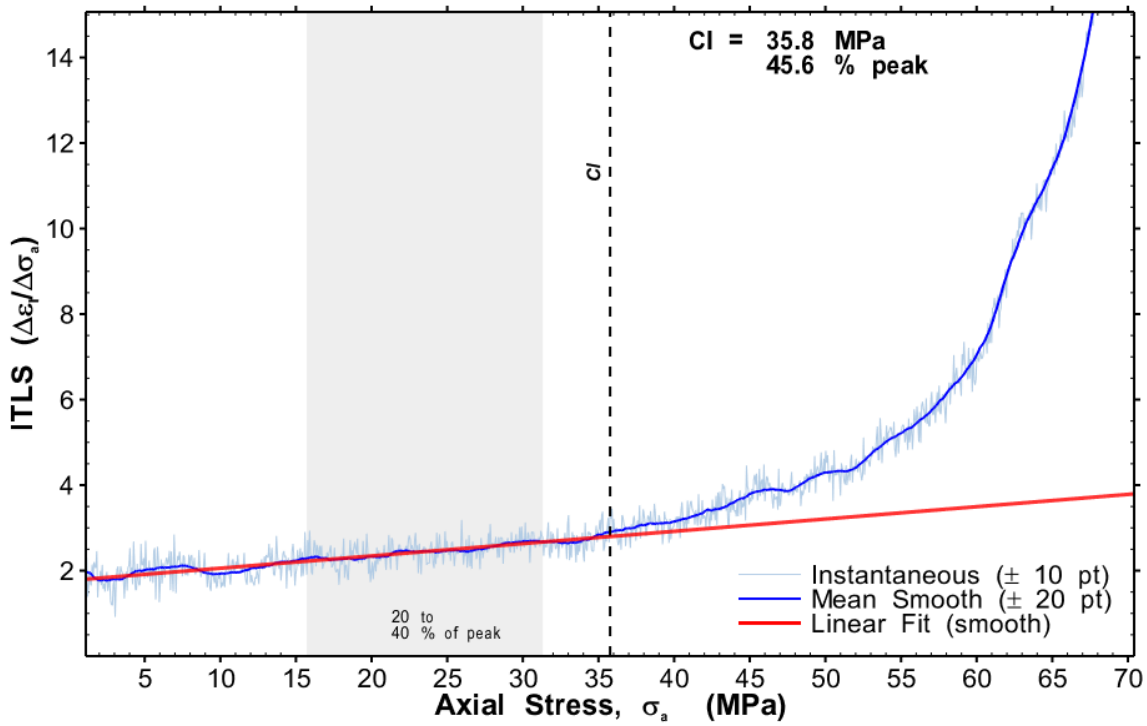

C1074-20I.dat

P-002797.004_UCS_Batch 5_R0.mView

Specimen ID: **C1074-20J**

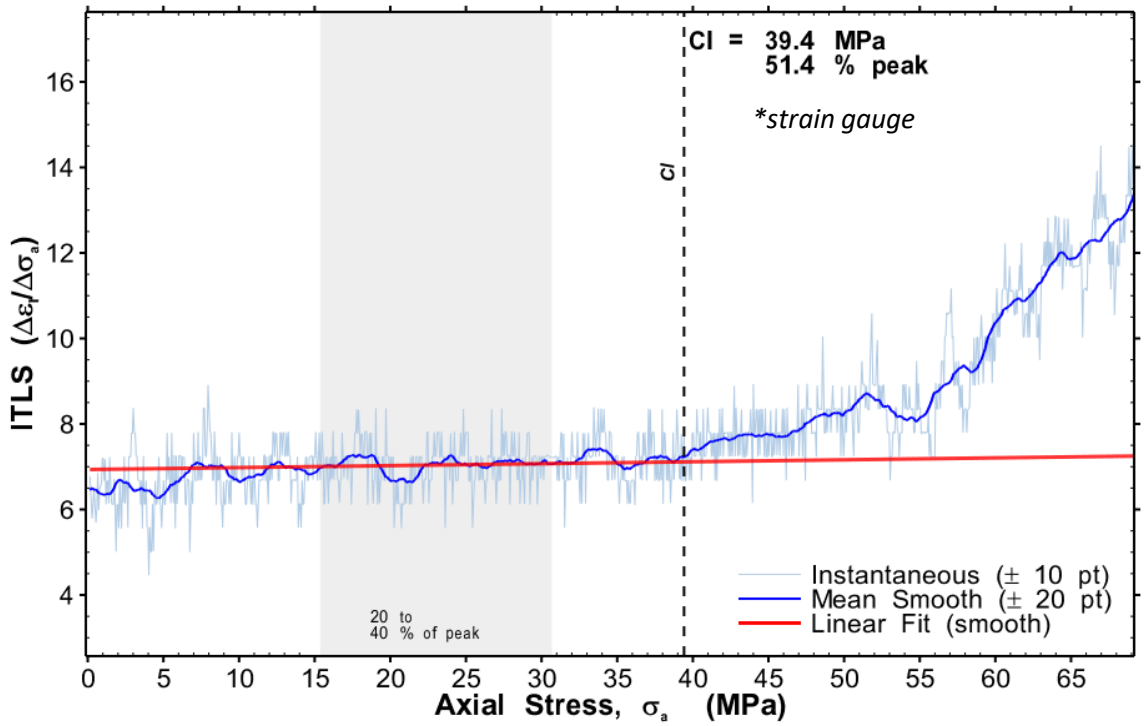

Specimen ID: **C1074-20K**

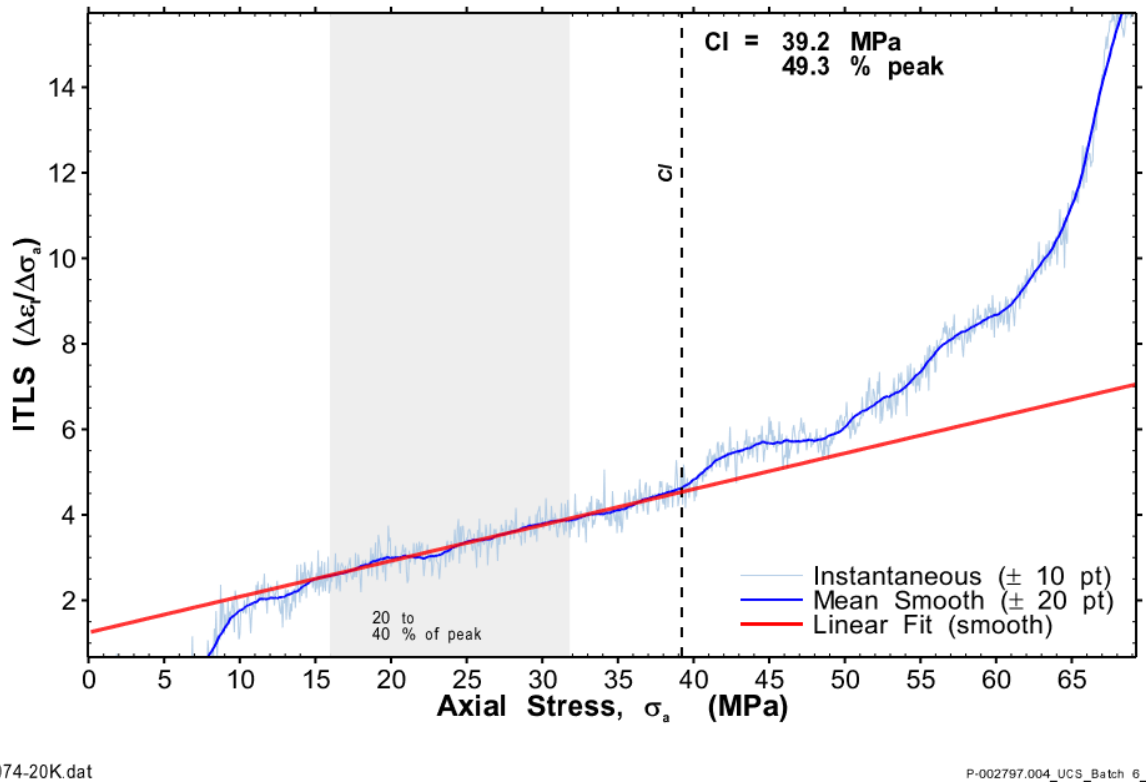

Specimen ID: **C1074-20L**

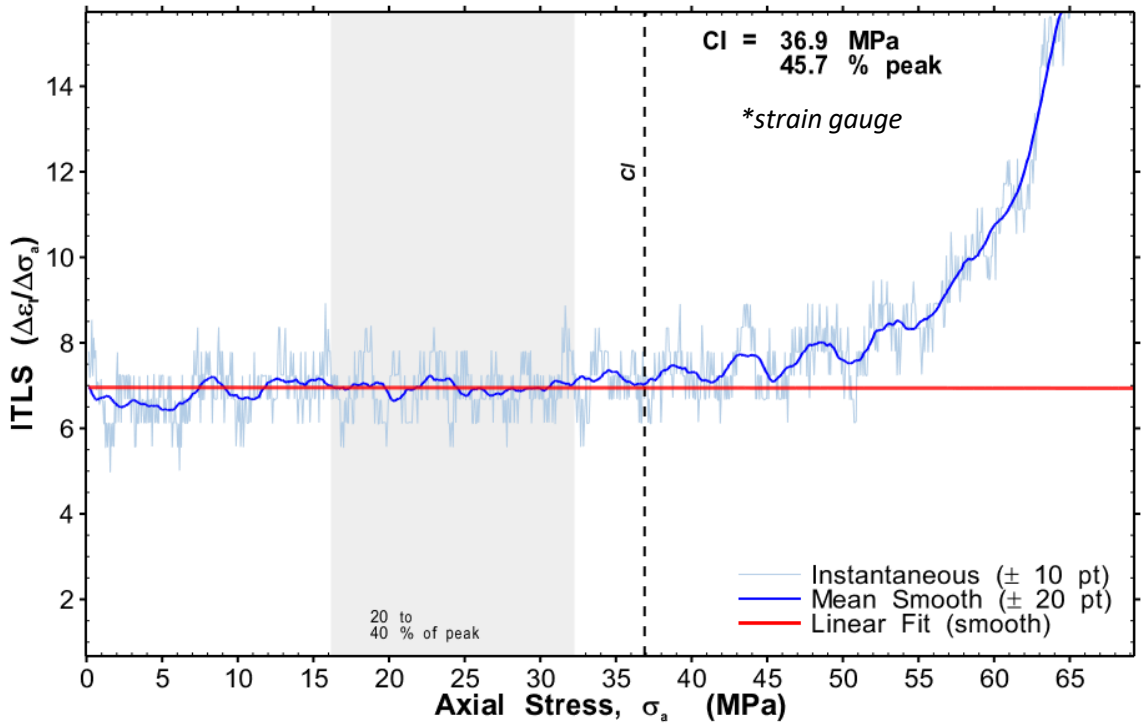

C1074-20L.dat

P-002797.004_UCS_Batch 6_R0.mView